Università degli Studi di Parma
Facoltà di Medicina e Chirurgia
Dipartimento di Neuroscienze
Sezione di Fisiologia Umana

DOTTORATO DI RICERCA IN NEUROSCIENZE

XIX CICLO

ARCHITECTONICS AND CORTICAL CONNECTIONS OF THE VENTRAL PREMOTOR AREA F5 OF THE MACAQUE

PhD THESIS OF ABDELOUAHED BELMALIH

COORDINATOR

PROF. VITTORIO GALLESE

TUTOR

PROF. GIUSEPPE LUPPINO

To my parents, my sisters and brothers

To my wife and my sweet Yasmine

This study was supported by MIUR (PRIN-2004057380_002). A. Belmalih is supported by a fellowship from EU (Marie Curie, Early stage training program "Sensoprim" MEST-CT-2004-007825). The 3D reconstruction software was developed by CRS4, Pula, Cagliari, Italy.

Abstract

The rostral part of the macaque ventral premotor cortex (PMv), corresponding to the histochemical area F5, is a functionally heterogeneous cortical sector. Two main populations of visuomotor neurons were electrophysiologically identified in this premotor sector : “Mirror neurons” and “Canonical neurons”. “Mirror neurons” were mostly found in the F5 sector extending on the lateral convexity while “Canonical neurons” were found in the F5 sector located in the posterior bank of the inferior arcuate sulcus (IAS). In the present study, we aimed to verify whether there is an anatomical counterpart underlying this differential distribution of F5 visuomotor neurons using both, architectonic and hodological approaches. The results showed that the rostral PMv hosts three architectonically distinct areas, which occupy different parts of F5. One area, referred to as “convexity” (F5c) F5, extends on most of the postarcuate convexity cortex adjacent to the IAS. The other two areas, referred to as “posterior” (F5p) and “anterior” (F5a) F5, lie within the postarcuate bank at different antero-posterior levels. This subdivision was strongly supported by our hodological data showing that the three architectonically defined PMv areas are characterized by different connectional patterns. F5p was strongly connected with the hand field of F1, with the arm-related premotor fields of F4, F2vr, F6 and F3 and with the cingulate areas 24d and 24c. Parietal afferents originated from areas PF, PFG, AIP, PEip and SII region. Weak connections with the prefrontal cortex involved the caudal sector of area 46v. Finally, F5p was a source of corticospinal projections. F5c was strongly connected with face/mouth fields of F4 and F3 and weakly with F1. Cingulate connections involved areas 24c and 24a. Strong connections were observed with caudal frontal opercular areas. Parietal afferents mostly originated from PF, SII and PV (mostly face/mouth representations), but also from AIP and PFG. Connections with the prefrontal cortex involved a more rostral sector of area 46v and area 12r. F5a lacked connections with F1 and displayed connections with F4, F6 and cingulate areas, 24c, 24d and 24a. Strong connections were observed with rostral frontal opercular areas. Parietal afferents originated mostly from PF, PFG, AIP and from the hand representations of PV and SII. Relatively robust prefrontal connections were observed with rostral area 46v and areas 12r and 12l. The present data, together with functional data available in the literature, suggest that the three rostral PMv areas F5p, F5a

and F5c correspond to functionally distinct cortical entities. Thus, the current study provides a new anatomical frame of reference of the macaque PMv that appears to be very promising for gaining new insight into the possible role of this premotor sector in different aspects of motor control and cognitive motor functions.

Keywords: architecture, hodology, area F5, monkey, visuomotor, frontal lobe, parietal lobe , mirror neurons, canonical neurons.

Table of contents

Abbreviations list

ABC	*avidin-biotin complex*
AIP	*anterior intraparietal area*
ANOVA	*analysis of variance between groups*
BDA	*biotinylated dextran amine*
C	*central sulcus*
CB	*calcium binding protein*
Cg	*cingulated sulcus*
CTB-A	*cholera toxin sub-unit B conjugated with alexa*
C4-C5, C7-C8	*spinal cervical segments*
DAB	*diaminobenzedine*
DO	*dorsal opercular area*
dPCD	*dorsal precentral dimple*
DY	*diamino yellow*
FB	*fast blue*
FIA	*fundal inferior arcuate area*
FR	*fluororuby*
F1	*agranular frontal area F1*
F2vr	*ventral rostral sector of the agranular frontal area F2*
F3	*agranular frontal area F3*
F4	*agranular frontal area F4*
F5	*agranular frontal area F5*
F6	*agranular frontal area F6*
F5a	*anterior agranular frontal area F5*
F5ab	*F5 sector located within the bank of the inferior arcuate sulcus*
F5c	*agranular frontal area F5 convexity*
F5p	*posterior agranular frontal area F5*
GrF	*granular frontal area*
HRP	*horseradish peroxidase*
IAS	*inferior arcuate sulcus*
IB	*Inner band of Baillarger*
IP	*intraparietal sulcus*
IPL	*inferior parietal lobule*
ir	*immunoreactivity*
L, LF	*lateral fissure*
LBLF	*lower bank of the lateral fissure*
LO	*lateral orbital sulcus*
Lu	*lunate sulcus*
MO	*medial orbital sulcus*
MR	*microruby*
OB	*outer band of Baillarger*
Opt	*part of caudal inferior parietal convexity caudal to PG*
P	*principal sulcus*
PBS	*phosphate buffer saline*
PE	*cytoarchitectonic area of superior parietal lobule*
PEip	*cytoarchitectonic area of intraparietal sulcus*
PF	*part of rostral inferior parietal convexity*
PFG	*part of rostral inferior parietal convexity caudal to PF*
PG	*part of caudal inferior parietal convexity caudal to PFG*
PMV	*ventral premotor area*
PrCO	*precentral opercular area*
PV	*parietal ventral area*
SII	*second somatosensory area*
SAS	*superior arcuate sulcus*
SMI-32	*non-phosphorylated neurofilaments antibody*
UBLF	*upper bank of the lateral fissure*
vPCD	*ventral precentral dimple*
WGA-HRP	*wheat germ agglutinin conjugated to HRP*

A-Introduction

A. Introduction

1. Architectonic organization of the monkey ventral premotor cortex

The primates agranular frontal cortex has been subdivided by Brodmann (1909) into two cytoarchitectonically distinct areas: area 4 located in the precentral gyrus and area 6 located rostrally to area 4. This simple cytoarchitectonic map corresponded to an equally simple view of a functional organization: the “primary motor cortex”, corresponding to area 4, the “supplementary motor area” in the mesial surface (Penfield and Welch, 1951; Woolsey et al. 1952) and the “premotor area” on the lateral convexity (Fulton 1935), which correspond to Brodmann’s area 6.

All of the subsequent architectonic, connectional and functional studies agreed that area 6 is made up of many structural and functional fields, each of which processes different aspects of the motor behaviour.

Area 6 was subdivided into three main regions: 1) the supplementary motor area “SMA proper” and area “pre-SMA” on the mesial surface, 2) the dorsal premotor cortex (PMd) on the dorsolateral convexity, and 3) the ventral premotor cortex (PMv) on the ventrolateral convexity. Moreover, the PMv resulted anatomically not homogeneous as well (Vogt and Vogt, 1919; Bonin and Bailey 1947; Matelli et al., 1985; Barbas and Pandya, 1987; Preuss and Goldmann-Rakic, 1991), (Fig. 1).

Architectonic investigations provided variable maps of the PMv, which differ in terms of number, location and extent of the areas. Two cytoarchitectonic areas were defined by Bonin and Bailey (1947) within the PMv: area FBA located caudally and area FCBm extending rostrally (Fig. 1). Other architectonic studies of the PMv have resulted in markedly different parcellation schemes. For example, Barbas and Pandya (1987), similarly to Vogt and Vogt (1919), have subdivided the PMv into a dorsal, an intermediate and ventral area, designated as 4C, 6Va and 6Vb, respectively (Fig. 1). A dorsoventral subdivision of the PMv based on cyto- and myloarchitectonic criteria, but in two areas only, 6Va and 6Vb, has been proposed by Preuss and Goldman-Rakic, (1991).

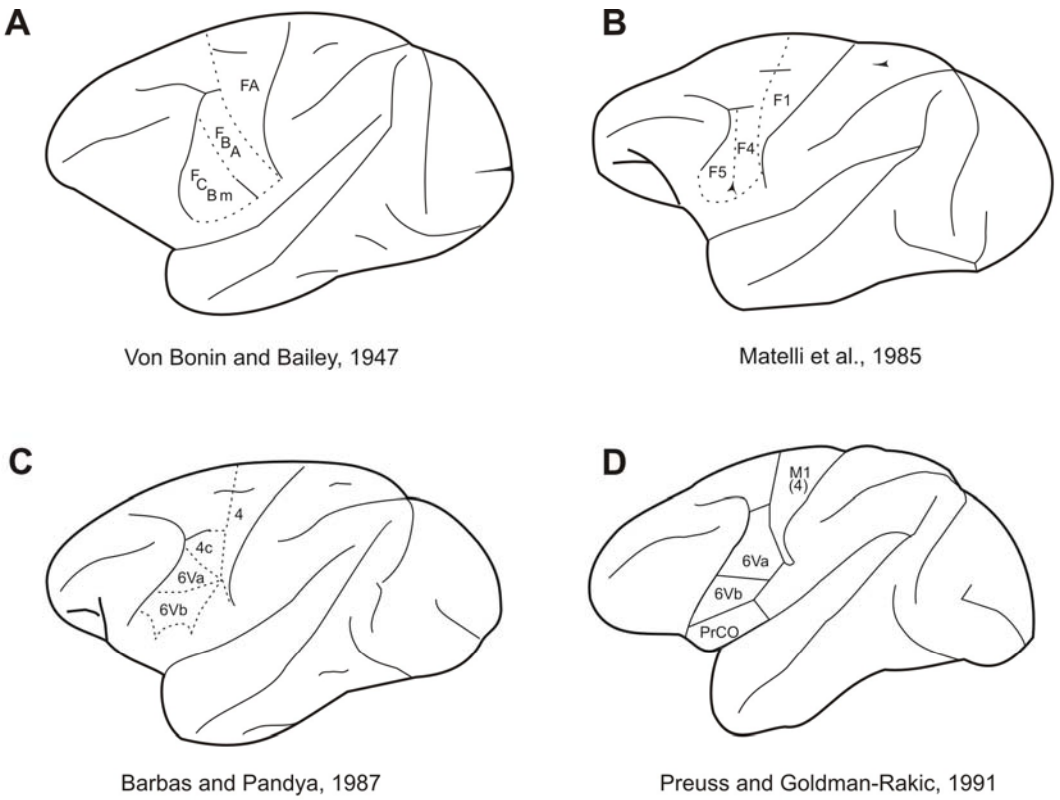

Fig. 1. Parcellation of the PMv of the macaque monkey according to four different architectonic maps published in previous studies. Architectonic subdivisions defined by (A) Von Bonin and Bailey, (1947), (B) Matelli et al, (1985), (C) Barbas and Pandya, (1987) and (D) Preuss and Goldman-Rakic, (1991).

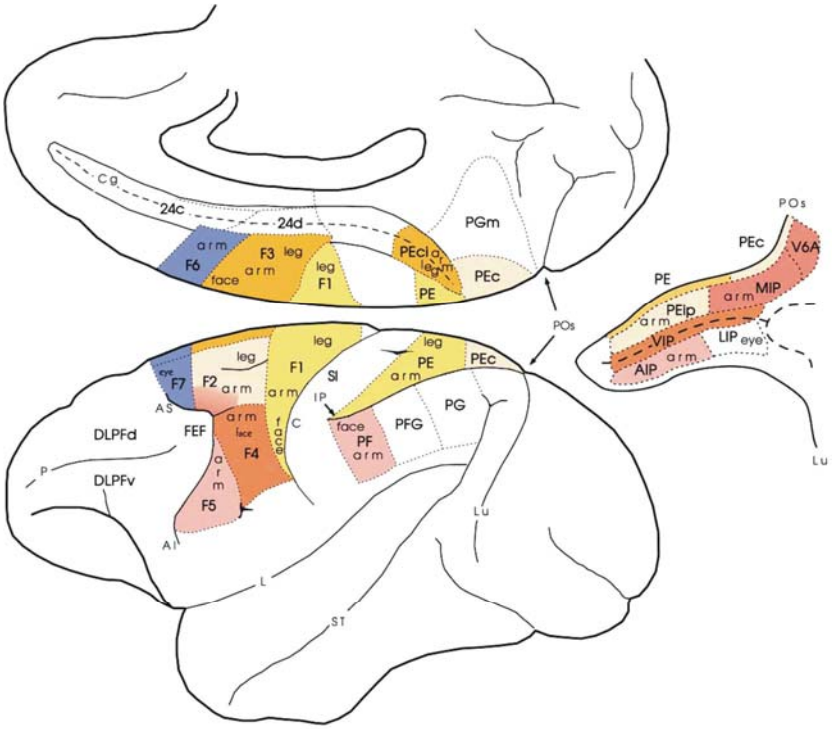

Fig. 2. Mesial and lateral views of the monkey brain showing the parcellation of the motor cortex, posterior parietal and cingulate cortices. The areas locatded within the intraparietal sulcus are shown in an unfolded view of the sulcus in the right part of the figure For *Abbreviations see the list*. (*Rizzolatti and Luppino, 2001*)

The laminar pattern of cytochrome oxidase activity was studied in the agranular frontal cortex of the macaque monkey by Matelli and co-workers (1985). This study provided a new detailed parcellation of the agranular frontal cortex and distinguished two histochemically different areas in the PMv: area F4 which lies on the precentral gyrus, just rostral to the precentral area F1 (area 4) and area F5 which lies rostrally to F4 on the lateral cortical convexity and extends in the posterior bank of the inferior limb of the arcuate sulcus (IAS), (Figs. 1 and 2).

More recently, Petrides and Pandya, (1994; 2002) analyzing sections cut orthogonally to the IAS, have defined an area -area 44- mostly located in the anterior part of the postarcuate bank that, according to Petrides et al. (2005), represents an architectonic and functional distinct cortical entity.

2. Connections of the ventral premotor area F5

Recently, the monkey premotor area F5 has received strong interest from the anatomical and functional investigations of the last two decades. Connectional studies have shown that area F5 is connected with the primary motor cortex (area F1), particularly with hand and face/mouth fields (Pandya and vignolo, 1971; Matelli et al.,1987; Lu et al., 1994; Dum and Strick, 2005). Other hodological investigations have shown that area F5 is connected with the supplementary motor areas F3 (SMA-proper) and F6 (pre-SMA), (Luppino et al., 1993). Area F5 displays connections also with the dorsal premotor area F2 (Marconi et al., 2001) and with the adjacent premotor area F4 (Godschalk et al., 1984, Matelli et al.,1986).

Other connectional studies which targeted the prefrontal cortex, showed that the rostral PMv sector (corresponding to area F5) is consistently connected with area 12 (Carmichael and price, 1995) and with area 46v (Preuss and Goldman-Rakic, 1989).

Several connectional investigations carried out on the parietal cortex have demonstrated that area F5 receives strong projections from the posterior parietal areas. Its major connections arise from the inferior parietal lobule (IPL) areas, PF, PFG and PG and from the intraparietal areas AIP and PEip (Cavada and Goldman-Rakic, 1989; Rozzi et al., 2006; Borra et al., 2007). In another study conducted by Disbrow et al, (2003) in which electrophysiologically controlled tracer injections were

made in the PV/SII complex, demonstrated that the rostral PMv sector displays connections with this somatosensory complex.

Finally, a series of hodological studies made by Strick and co-workers (1991, 1993), in which the topographic organization of corticospinal neurons in the frontal lobe was examined by injecting neural tracers in different segmental levels of the spinal cord, showed that the only ventral premotor area sending projections to the spinal cord is the rostral part of the PMv, in particular, its sector located in the posterior part of the bank of the IAS (Dum and Strick, 1991; He et al., 1993).

It is noteworthy that the previous anatomical and functional studies carried out on area F5 considered this area as one entity.

3. Functional properties of the ventral premotor area F5

3.1. General properties of F5 neurons

Single neurons recordings during the execution of active movements and intracortical microstimulation of area F5 have shown that this area contains a representation of hand and mouth movements (Okano and Tanji, 1987; Rizzolatti et al., 1988; Gentilucci et al., 1988; Hepp-Reymond et al., 1994; Ferrari et al 2003a; Raos et al 2006).

The great majority of F5 ‘hand’ neurons discharge during goal-directed actions such as grasping, manipulating, tearing and holding (Rizzolatti et. al., 1988). The mostly represented F5 neurons are ‘grasping neurons’. These neurons typically begin to discharge before the contact between the hand and the object. Some neurons are more active during the opening of the fingers that precedes the closure phase, some discharge during finger closure and some others discharge during the whole movement, from the beginning of fingers opening until their contact with the object (Fadiga et al., 2000). This temporal relation between grasping movement and neuron discharge varies from neuron to neuron (Fadiga et al., 2000). Furthermore, many grasping neurons discharge in association with a particular type of grip. Most of them are selective for one of the three most common grip types of the monkey: precision grip, finger prehension and whole hand prehension.

Another population of F5 neurons has been described by Ferrari et al. (2003a). These neurons are related to the mouth actions such as grasping, sucking and breaking food.

on the basis of the functional properties of F5 neurons, it has been suggested that area F5 stores a set of motor schemata (Arbib, 1981), or a 'vocabulary' of motor acts (Rizzolatti and Gentilucci, 1988). Populations of neurons constitute the 'words' composing this vocabulary. Some of them indicate the general category of an action (hold, grasp, tear, manipulate). Finally, other neurons are concerned with the temporal segmentation of the actions (hand opening, fingers closure, object holding).

Beside the motor properties of F5 neurons, visual stimuli have been shown to be able to trigger F5 neurons activity (Murata et al., 1997; Rizzolatti et al., 1988; Raos et al., 2006). Two completely different categories of F5 visuomotor neurons have been identified: neurons of the first category discharge when the monkey observes graspable objects 'canonical' F5 neurons, (Murata et al., 1997; Rizzolatti and Fadiga, 1998), (Fig. 3A). Neurons of the second category, 'mirror neurons', discharge when the monkey observes another individual making an action in front of it (Di Pellegrino et al., 1992; Gallese et al., 1996; Rizzolatti et al., 1996), (Fig. 3B).

It is noteworthy that the two categories of F5 neurons are located in two different sectors of area F5: 'canonical neurons' were mostly found in F5 sector buried within the arcuate sulcus, whereas 'mirror neurons' were almost exclusively found in the cortical convexity of F5.

3.2. Visuomotor transformations for grasping execution

3.2.1. Canonical neurons

In the typical course of daily events, we make a variety of body movements on the basis of what we interact manually with objects in our environment. Usually, we gaze at an object, reach toward it and grasp it.

As described some years ago, in single neuron recording experiments in which a monkey was required to grasp food and other objects, many F5 neurons fired also in response to food or object presentation (Rizzolatti et al., 1988).

More recently, the visual responses of F5 neurons were re-examined using a formal behavioural paradigm, which allowed to separately test the response related to object presentation, during the

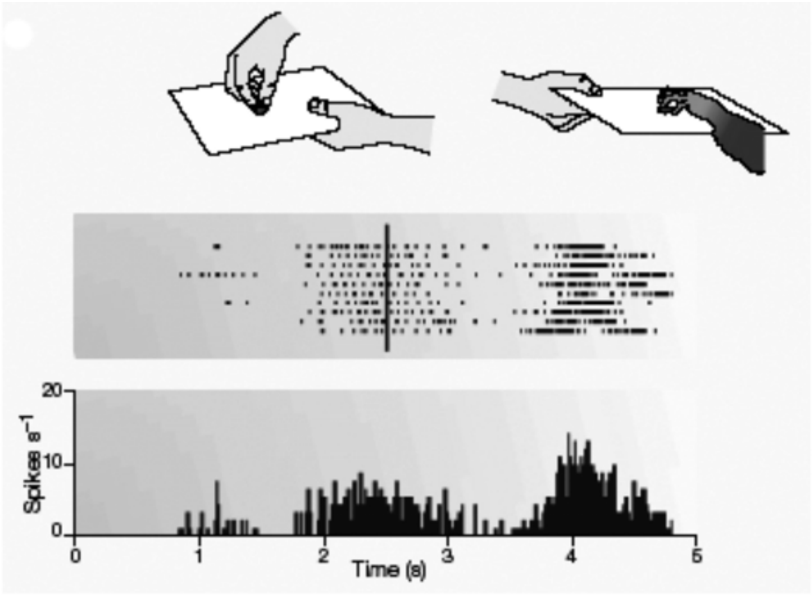

Fig. 3. A- Visual and motor responses of a Mirror neuron in area F5 (*Rizzolatti et al., 2001*)

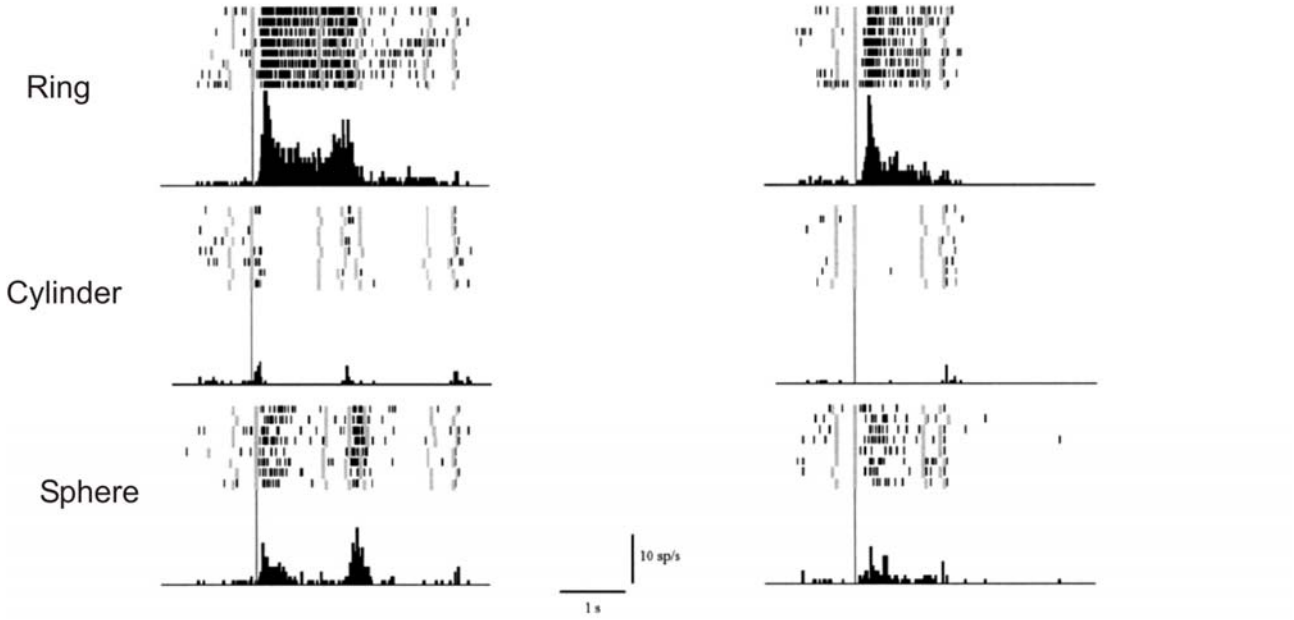

Fig. 3. B- Example of a selective F5 'canonical' visuomotor neuron. Panels show neural activity recorded during 'grasping in light' and 'object fixation' tasks with three objects (*Murata et al., 1997*).

Waiting phase between object presentation and movement's onset, and during movement execution.

The results showed that a high percentage of the tested neurons, in addition to the motor response, responded also to visual presentation of three-dimensional graspable object (Murata et al., 1997). Among these visuomotor neurons, two-thirds were selective to one or a few specific objects (Fig. 3B). Very often there is a strict relationship between the type of prehension coded by a neuron and the physical characteristics of the stimulus effective in triggering response (Rizzolatti et al., 1988). In congruence with this data, Raos et al. (2006) showed that F5 grasping neurons displayed a preference for grasping of an object or a set of objects. This preference was also maintained when grasping was performed in the dark in the absence of any visual feedback. Often the object that evoked the strongest activity during grasping also evoked optimal activity during its observation.

3.2.2. Parieto-frontal circuit for visuomotor transformations for grasping

'Canonical neurons' neurons are mostly located in the posterior part of the inferior postarcuate bank (F5 of the arcuate bank -F5ab- in Rizzolatti and Luppino, 2001), which is reciprocally connected with the intraparietal area AIP. Extensive studies made by Sakata and collaborators (Taira et al., 1990; Sakata et al., 1995; Murata et al., 2000) showed that the properties of AIP neurons are strikingly similar to those of F5 'canonical neurons': visual responses in area AIP are determined by the shape and orientation of objects, while the motor responses are triggered in relation to specific hand movements. It has been suggested that F5 'canonical neurons' receive visual information about the object features from area AIP (Luppino et al., 1999; Borra et al., 2007). Area F5 in turn 'translates' these object features into a potential action, with which the individual may act on the object. Thus, Jeannerod et al. (1995) suggested that the AIP-F5 circuit seems to be involved in transforming intrinsic object properties into the appropriate hand movements. This hypothesis is supported by reversible inactivation studies performed both, in area F5 (Gallese et al., 1994) and in area AIP (Fogassi et al., 2001). In both areas the inactivation caused very similar deficits: awkward object grasping or even a complete grasping failure. According to Sakata and co-workers (1995), the motor activity in AIP reflects a corollary discharge

originating in area F5ab. Its function is to create reverberatory activity that keeps AIP neurones active during action (Murata et al., 1996). The activity of F5 'canonical neurons' represents the step that transforms the object representations coded in the AIP into a format suitable to active area F1 motor neurons plus a series of subcortical centres among which are the basal ganglia and cerebellum (Jeannerod et al., 1995).

3.3. Mirror neurons system

A category of stimuli of great importance for primates is that formed by actions done by the other individuals. In the daily life, we must understand the actions of the others because without action understanding, social organization becomes impossible (Rizzolatti and Graighero, 2004). Recently, Rizzolatti and colleagues proposed a neurophysiological mechanism -the mirror neurons mechanism- that appears to play a fundamental role in both action understanding and imitation. Now, there is a wide consensus that the activation of the motor system, particularly the ventral premotor area F5 is a necessary requisite for these cognitive abilities.

3.3.1. Mirror neurons properties

Single-neuron recording experiments in monkeys have shown that area F5 contains a population of visuomotor neurons, 'mirror neurons' which are endowed with an intriguing visual property: these neurons become active not only when the monkey does a particular action (like grasping an object) but also when it observes another individual (Monkey or human) doing the same action (Fig. 3A), (Gallese et al., 1996).

Early studies on mirror neurons concerned essentially the upper sector of F5 where hand actions are mostly represented (Di Pellegrino et al., 1992; Gallese et al., 1996). Recently, in order to investigate the functional properties of F5 neurons located in its lateral sector -where neuron activity is mostly related to mouth actions- Ferrari et al. (2003a) have demonstrated that about one third of mouth motor neurons discharge also when the monkey observes another individual performing mouth actions. The majority of these 'mouth mirror neurons' become active during the execution and observation of mouth actions related to ingestive functions such as grasping, sucking or breaking food, but the most effective visual stimuli in triggering them are communicative

mouth gestures (e.g. lips macking). These findings extend the notion of mirror neurons system from hand to mouth action.

In order to be triggered by visual stimuli, the 'mirror neurons' require an interaction between a biological effector (hand or mouth) and an object. The sight of an object alone, of an agent mimicking an action, or of an individual making intransive (non object directed) gestures are all ineffective. The object significance for the monkey has no obvious influence on the mirror neuron response. Grasping a piece of food or geometric solid produces responses of the same intensity (Rizzolatti and Graighero, 2004).

An important functional aspect of mirror neurons is the relation between their visual and motor properties. Virtually all mirror neurons show congruence between the visual actions they respond to and the motor responses they code. According to the type of congruence they exhibit, mirror neurons have been subdivided into 'strictly congruent' and 'broadly congruent' neurons (Gallese et al., 1996).

3.3.2. Mirror neurons circuit

Neurons responding to the observation of actions done by others are present not only in area F5 but also in the superior temporal sulcus (STS), (Perrett et al., 1989; Jellema et al., 2002). A set of neurons in the STS have been shown to respond to the action observation. Movements effective in eliciting neuron responses in the STS are walking, turning the head, bending the torso, and moving the arms. A small set of STS neurons discharge also during the observation of goal-directed hand movements (Perrett et al., 1990).

Another cortical area where there are neurons that respond to the observation of actions done by other individuals, is area 7b or PF/PFG complex in the IPL (Fogassi et al., 1998; Gallese et al., 2002; Fogassi et al., 2005). This area receives inputs from the STS and sends an important output to the PMv including area F5 (Rozzi et al., 2006). PF/PFG neurons are functionally heterogeneous. Most of them respond to sensory stimuli, but about 50% of them have motor properties discharging when the monkey performs specific movements or actions (Fogassi et al 2005; Gallese et al., 2002; Hyvarinen, 1982). PF/PFG neurons responding to sensory stimuli have been subdivided into: somatosensory neurons, visual neurons, and bimodal (somatosensory and visual) neurons.

Visually responsive neurons in area PF/PFG respond specifically to action observation, most of them have mirror properties (Gallese et al., 2002; Fogassi et al., 2005).

In conclusion, the cortical mirror-neuron circuit is formed by two main regions: the rostral part of the inferior parietal lobule and the rostral ventral premotor cortex. The STS is strictly related to it but, lacking the motor properties, cannot be considered part of it (Rizzolatti and Graighero, 2004).

3.3.3. Functions of the mirror neuron system: action understanding

One of the hypotheses which have been advanced on what the functional role of mirror neurons was that these neurons could be at the basis of action understanding. A mechanism was proposed by Rizzolatti and co-workers explaining how the mirror neurons mediate understanding of actions done by the others. Following these authors, each time an individual sees an action done by another individual, neurons that represent that action are activated in the observer's premotor cortex. This automatically induced, motor representation of the observed action corresponds to that to which is spontaneously generated during active action and whose outcome is known to the acting individual (Rizzolatti et al., 2001).

4. Objective

On the basis of the functional data focused on the rostral PMv, we hypothesized that area F5 -considered histochemically as a unique area- could be formed by a complex of anatomically and functionally distinct entitites, possibly corresponding to F5ab, F5c (Rizzolatti and Luppino, 2001) and to area 44 (Petrides and Pandya, 1994, 2002; Petrides et al., 2005). To resolve this question, two different, but complementary studies were undertaken:

a-The first study was focused on the analysis of the architectonic organization of area F5, and the adjacent areas. For this purpose, we used a qualitative multimodal histological approach combining cyto- and myeloarchitectonics with SMI-32 and calcium binding protein (CB) immunohistochemistry, along with a quantitative analysis of SMI-32-ir and CB-ir cells within each architectonically defined sector of area F5, area F4 and area F1.

b-The second study consisted in the analysis of the connectional pattern of each F5 architectonically defined sector, to seek for an eventual differential connectivity of the different F5 sectors, which could enable us to confirm the data from the architectonic study. For this purpose,

retrograde, anterograde and retro-anterograde neuronal tracers were injected in each architectonically defined sector of F5 and the distribution of labeled neurons and terminals were analysed in the cerebral cortex, in parallel with the examination of the cortico-spinal projections, mainly in the upper and lower cervical segments of the spinal cord.

Preliminary data have been presented previously (Luppino et al., 2005; Nelissen et al., 2005; Belmalih et al., 2007).

B-Materials and methods

B. Materials and methods

Animal care and all experimental procedures were performed according to protocols approved by the Veterinarian Animal Care and Use Committee of the University of Parma and complied with the European law on the care and use of laboratory animals.

1. Architectonics

19 adult macaque monkeys (11 *Macaca nemestrina*, 6 *Macaca fascicularis* and 2 *Macaca mulatta*) of both sexes weighing between 5 and 8 kg were used in the present study. We didn't observe any architectonic differences consistently related to either the species or the gender. Brains from 6 monkeys (PR11, PR17, PR18, PR19, PR20 and CNR-29) were used exclusively for the purposes of architectonic studies. M3 and M4 have been used as subjects in fMRI experiments as well (Nelissen et al., 2005). The remaining monkeys have been used in tract-tracing studies in which neural tracers were injected in different frontal or posterior parietal areas (see, e.g., Galletti et al., 2001; Luppino et al., 2001; Rozzi et al., 2006).

1.1. Surgical and histological procedures

Each animal was anesthetized with ketamine hydrochloride and subsequently received an i.v. lethal injection of sodium thiopental. Intracardial perfusion was initiated through the left cardiac ventricle with saline solution, followed by 3.5-4% paraformaldehyde. In all animals, except for cases PR18 and PR19, the perfusion was continued with 5% glycerol. All solutions were prepared in phosphate buffer 0.1M, pH 7.4. The brain was then exposed, eventually blocked on a stereotaxic apparatus, removed from the skull and photographed. All brains, but cases PR18 and PR19, were placed in 10% (three days) and then in 20% (three days) buffered glycerol for cryoprotection. The right hemisphere of case PR18 and the left hemisphere of case PR19 were embedded in celloidin and cut tangentially to the IAS and parasagittally, respectively, at 50 µm. All the other brains were cut frozen, at 60 µm, for a total number of 16 hemispheres coronally, 10 parasagittally, 1 perpendicularly to the IAS and 1 tangential to IAS. Table 1 summarizes the cases used for this study.

The parasagittal, tangential and perpendicular to the IAS planes of sectioning were used in order to obtain optimal and complementary views of the architecture of the postarcuate bank and

TABLE 1**.** Summary of cases studied

Case	Species	Hemisphere	Cut	Staining *
PR17	*Nemestrina*	Right	Perpendicular to IAS	Nissl, Myelin (120), SMI-32 (60), CB (60)
PR18	*Nemestrina*	Right	Tangential to IAS	Nissl (celloidin)
PR19	*Nemestrina*	Left	Parasagittal	Nissl (celloidin)
PR11	*Nemestrina*	Left	Parasagittal	Nissl, SMI-32 (60)
PR20	*Nemestrina*	Right	Parasagittal	Nissl, Myelin (120), SMI-32 (60), CB (60)
M4	*Mulatta*	Left	Parasagittal	Nissl, Myelin (60), SMI-32 (60)
		Right	Parasagittal	Nissl, Myelin (60), SMI-32 (60)
M3	*Mulatta*	Right	Parasagittal	Nissl, Myelin (120), SMI-32 (60), CB (60)
		Left	Coronal	Nissl, Myelin (120), SMI-32 (60), CB (60)
MEF16	*Fascicularis*	Right	Parasagittal	Nissl, SMI-32 (120), CB (60)
		Left	Parasagittal	Nissl, SMI-32 (120), CB (60)
MEF17	*Fascicularis*	Left	Parasagittal	Nissl, SMI-32 (60)
CNR-29	*Fascicularis*	Left	Parasagittal	Nissl, SMI-32 (60)
Case 12	*Nemestrina*	Right	Coronal	Nissl, Myelin (120), SMI-32 (120), CB (60)
Case 24	*Nemestrina*	Right	Coronal	Nissl
		Left	Coronal	Nissl
Case 18	*Nemestrina*	Right	Coronal	Nissl, Myelin (120), SMI-32 (60)
		Left	Coronal	Nissl, Myelin (60)
Case 13	*Fascicularis*	Right	Coronal	Nissl
		Left	Coronal	Nissl, SMI-32 (60)
Case 14	*Nemestrina*	Right	Coronal	Nissl
		Left	Coronal	Nissl
Case 20	*Nemestrina*	Right	Coronal	Nissl
		Left	Coronal	Nissl
Case 23	*Fascicularis*	Left	Coronal	Nissl, Myelin (60)
		Right	Coronal	Nissl
Case 29	*Fascicularis*	Left	Coronal	Nissl, Myelin (60)
Case 38	*Nemestrina*	Left	Coronal	Nissl, Myelin (60)

* Number in parentheses indicates the distance in μm from the Nissl stained section.

of the adjacent postarcuate convexity cortex. In fact, the architecture of this cortical sector, especially of the postarcuate bank, is often poorly discriminated in the standard coronal plane, because of the oblique or almost vertical direction of the sulcus. In addition, sections cut tangential or perpendicular to the IAS or parasagittal sections, offered optimal views of different rostro-caudal levels of the postarcuate bank and/or of the postarcuate convexity cortex for the identification of boundaries between rostro-caudal subdivisions.

In all hemispheres, every fifth section was stained with the Nissl method (thionin, 0.1% in 0.1M acetate buffer pH 3.7). In 9 animals (12 hemispheres, 7 of them cut coronally, 4 parasagitally and 1 perpendicular to the IAS), sections adjacent or very close to those stained with thionin were stained for myelin (Gallyas, 1979).

The immunoarchitectonic study of the rostral PMv was based on the analysis of the distribution of the immunoreactivity (ir) for the antibody SMI-32 and for the calcium-binding protein calbindin (CB). SMI-32-ir was analyzed in 11 animals (14 hemispheres, 4 of them cut coronally, 9 parasagitally and 1 perpendicular to the IAS) and CB-ir in 5 animals (7 hemispheres, 2 of them cut coronally, 4 parasagittally and 1 perpendicular to the IAS). In these hemispheres, every tenth section was immunoreacted. Immediately after cutting, sections were rinsed in phosphate-buffered saline (PBS) for 10–15 min. Endogenous peroxidase activity was eliminated by incubation in a solution of 0.6% H_2O_2 and 80% methanol for 15 min at room temperature. Sections were rinsed in PBS for another 10-15 min and incubated in a solution of one of the following primary antibodies: mouse monoclonal SMI-32 (Sternberger Monoclonals, Baltimore, MA, USA) dilution 1:5000 in 0.3% Triton (Sigma, St Louis, MO, USA), 2% normal horse serum (Vector, Burlingame, CA, USA), in PBS or monoclonal anti-calbindin D-28K (Swant, Bellinzona, Switzerland), dilution 1:5000 in 0.3% Triton, 5% normal horse serum in PBS. After incubation and rinsing in PBS (15 min), sections were processed with the avidin-biotin method by using a Vectastain ABC kit (Vector) and 3,3'-diaminobenzidine (DAB, Sigma) as chromogen. The reaction was intensified with cobalt chloride and nickel ammonium sulphate. Immunoreacted sections were then mounted on gelatine-coated slides from saline, air dried, dehydrated in graded alcohols, and cover slipped. In order to avoid

possible sources of variability among sections from the same case, all sections selected for one type of immunostaining were processed all together in the same solutions.

1.2. Qualitative analysis

The cytoarchitectonic analysis was carried out with a Wild M420 Universal macroscope equipped with Apozoom objective for low-power observations, and with a Nikon Optiphot-2 and a Zeiss Axioscop 2 microscope for medium and high power observations. In each section, the outer and inner cortical borders (pial and white matter borders) and the location of the boundaries between the various identified cytoarchitectonic areas were plotted with the aid of inductive displacement transducers mounted on X and Y axes of the microscope stage. The transducer signals were digitized and stored by using software developed in our laboratory that allows the visualization of section outlines, of gray-white matter borders and of architectonic borders. Data from individual sections were also imported into 3D reconstructions software (Bettio et al., 2001), which allowed us to obtain volumetric reconstructions of the monkey brain. The analysis of myelin-stained and SMI-32 and CB immunoreacted sections was carried out independently from the cytoarchitectonic analysis by using the same procedures. Myelo- and immuno-architectonic borders were then correlated with cytoarchitectonic borders.

1.3. Quantitative analysis

A quantitative analysis of the distribution of SMI-32 and CB immunoreactivity was carried out in the ventral agranular frontal areas, using procedures virtually identical to those adopted in a previous study focused on the caudal ventrolateral prefrontal cortex (Gerbella el., 2007).

The distribution of SMI-32ir was analyzed quantitatively in three hemispheres (PR17, M4l and MEF16l), from three different macaque species and cut in two different planes of section. Coronal sections were not used for this analysis, because of the very oblique cutting of the postarcuate bank. This analysis was aimed to evaluate the density of immunopositive cells in different cytoarchitectonic areas and cortical layers. By using the above mentioned computer based charting system, immunopositive neurons were plotted, at a magnification of 200X, in cortical transverses 250 μm wide from the pial surface through the entire cortical thickness. In each hemisphere, eight transverses were plotted for each of five different areas, as cytoarchitectonically

defined. Thus, this analysis was based on a total number of 40 transverses from each hemisphere and a total number of 24 transverses (8 transverses per case) for each area. The plotted transverses were selected from different sections and different parts of each area. By using a camera lucida attached to the microscope, borders between different cortical layers were transferred on the plots from adjacent Nissl-stained sections.

For each area, the density of the SMI-32 immunopositive cells, was analyzed separately for layers II/III and V, where virtually all these neurons were observed. Density was defined in terms of number of immunopositive cells, plotted in a given layer, divided by the thickness of that layer expressed in millimetres, for a transverse 250 μm wide. Although in the supragranular layers SMI-32 immunopositive cells were all located in layer III, layers II and III were considered together because of the difficulty in setting the border between them. The obtained data were tested with a two-way ANOVA for repeated measures (factors: Area, Layer, 5X2 ANOVA), followed by post-hoc Bonferroni correction for multiple comparisons.

The distribution of CBir was analyzed quantitatively in three hemispheres (PR17, M3l and MEF16l), from three different macaque species and cut in two different planes of section, in terms of density of immunopositive cells in different cytoarchitectonic areas and cortical layers. As reported in other studies (for review, see Hof et al., 1999), CB immunopositive neurons included two main populations of cells. One, by far the most represented, consisted of darkly and more lightly stained nonpyramidal cells, the other of pyramidal cells, most of them only lightly stained. However, in the areas object of the present study, the number of the observed CB immunopositive pyramids was very low or almost negligible. For this reason, this type of CB positive cells was not considered for this analysis. CB immunopositive nonpyramidal cells were plotted at a magnification of 400X, in cortical transverses 250 μm wide from the pial surface through the entire cortical thickness. The total number of transverses analyzed and the criteria for their selection were the same as in the analysis of SMI-32ir described above.

Two types of analyses were carried out in order to compare the distribution of CB immunopositive nonpyramidal cells across different areas. The first analysis aimed to evaluate their density in the studied areas. To this purpose, the total number of cells, plotted in transverses

250 μm wide, was divided by the cortical thickness expressed in millimetres. It should be noted however that in the agranular frontal cortex the border of layer VI with the white matter generally relatively gradual and difficult to draw with precision. Thus, we considered for this and the following analysis the cortical thickness from the pial surface to the border between layers V and VI. In this respect, it is worth noting that in all areas under study, layer VI CB immunopositive neurons were sparse and homogenously distributed. The obtained data were tested with a two-way ANOVA for repeated measures (factors: Cell type, Area, 2X5 ANOVA) followed by post-hoc t-test with Bonferroni correction for multiple comparisons. The second analysis aimed to obtain an estimate of the differences in the laminar distribution of CB immunopositive nonpyramidal neurons in each area. To this purpose, the number of these cells, plotted in a given layer of a cortical transverse 250 μm wide, was divided by the thickness of that layer expressed in millimetres. Given that the distribution of CB immunopositive nonpyramidal cells in supragranular layers was highly heterogeneous, with a much higher concentration in layer II and uppermost part layer III, these two layers, considered as a whole, were subdivided into four sublaminae of equal thickness. Thus, five different layers/sublayers were analyzed: the four layer II/III sublaminae and layer V. The obtained data were tested with a two-way ANOVA for repeated measures (factors: Area, Layer/Sublamina, 5X5 ANOVA), followed by post-hoc Bonferroni correction for multiple comparisons

1.4. Architectonic maps

In all cases used in the present study, architectonic maps were obtained by reporting the location of architectonic borders on drawings of dorsolateral views of the studied hemispheres. Furthermore, in order to obtain more realistic views of the location and extent of the identified architectonic areas, data from individual sections, spaced 600 μm, obtained with the above mentioned computer based charting system, were imported into a 3D reconstruction software (Bettio et al., 2001). By using this software, the individual sections were firstly manually translated or rotated for their alignment. The alignment was based on the location of the track left in the white matter by a needle inserted orthogonally to the plane of sectioning and of several cortical and subcortical anatomical landmarks. Furthermore, local non-linear transformations were applied to correct distortions due to the histological processing. Finally, a 3D rendering of the cortical surface

was created showing the extent of the identified architectonic areas. The obtained 3D reconstructions could be also re-sliced in any desired plane, for comparing data from hemispheres cut with different planes of sectioning, or dissected to expose cortical surfaces buried within sulci. The location of areas lying on the cortical convexity was visualized in standard dorsolateral views of the hemispheres. Areas located in the postarcuate bank were visualized in non-standard views of the hemispheres in which the bank was exposed with appropriate dissection of the 3D reconstruction.

1.5. Photographic presentation

Photomicrographs shown in the present study were obtained by capturing images directly from the sections with a digital camera attached to the macroscope or to the microscope. Individual images were then imported in Adobe Photoshop, in which they were assembled into digital montages and reduced to the final enlargement. Image brightness and contrast were adjusted, if necessary, to reproduce the original histological data.

2. Hodology

2.1. Surgical procedure and tracers injection

The connectivity of the different sectors of area F5 was investigated in ten macaque monkeys (7 *Macaca nemestrina,* 2 *Macaca fascicularis* and 1 *Macaca mulatta*). In all cases, except for cases C21 and C10, neural tracers were injected in different subdivisions of area F5. In C21 the tracer injection was made in F1, and in C10 the tracer injection was made in the cervical segments C4-C5 of the spinal cord.

Each animal was anaesthetized with either ketamine hydrochloride (15-20 mg/kg i.m.) or sodium thiopental (10-15 mg/Kg i.v.) and placed in a stereotaxic apparatus under aseptic conditions. In all animals except for C10, an incision was made in the scalp, the skull was trephined to remove the bone overlying the target region and the dura was opened.

In all monkeys but C10, the injection sites were chosen by using AP stereotaxic coordinates as a frame of reference and the IAS, the spur, the inferior precentral dimple and the central sulcus as anatomical landmarks. In C21, the hand field of the primary motor cortex (area F1) was

electrophysiologically defined before the injections, using the intracortical microstimulation. Trains of 50 ms duration were generated by a constant current stimulator (7-40 μA) and were delivered at 300 Hz through tungsten microelectrodes (Impedance 1.5MΩ).

Once the appropriate site was chosen, fluorescent tracers (Fast Blue [FB] 3% in distilled water, diamidino Yellow [DY] 2% in 0.2M phosphate buffer at pH 7.2, EMS-POLYLOY GmbH, Gross-Umstadt, Germany, cholera toxin B sub-unit conjugated with Alexa 594 [CTB-A] 1% in phosphate-buffered saline, Molecular Probes and Microruby [MR] 10% in 0.2M phosphate buffer PH 7.4, Invitrogen-Molecular probes), wheat germ agglutinin-horseradish peroxidase conjugated [WGA-HRP] 4% in distilled water, SIGMA, St.Louis, Missouri, biotinylated dextran amine [BDA] 10% phosphate buffer 0.1M, pH 7.4; Molecular Probes, Eugene, Oregon, and fluororuby [FR], 10% in distilled water, Molecular Probes, Eugene, Oregon, were slowly pressure injected through a glass micropipette (tip diameter 100±50μm) attached to a 1ml Hamilton microsyringe (Reno, NV, USA). Figure 4 and table 2 summarize the locations of injections, the injected tracers and their amounts.

The tracers injected into the cortical convexity were delivered 1,5 mm below the cortical surface, while those injected in the posterior bank of the arcuate sulcus were delivered at various depths from the cortical crown. After the injection, the pipette remained in place for 15 to 30 min to prevent spread of the tracer. The dural flap was then sutured, the bone replaced and the superficial tissues sutured in layers.

In the animal in which the tracer was injected in the spinal cord (C10), following a laminectomy, the dura was opened and the segments of the spinal cord selected for the injection exposed. The horseradish peroxidase [HRP], 30% in 2% lysolectin, SIGMA, (6 injections of total amount of 10 μl) was pressure injected with 5 μl Hamilton microsyringe in the lateral funiculus at C4-C5 spinal cord level.

During surgery, hydration was maintained with saline (about 10 cc/ h, i.v) and temperature was maintained with a heating pad. Heart rate, blood pressure, respiratory depth and body temperature were continuously monitored. Upon recovery from anaesthesia, the animal was returned to its home cage and closely monitored.

TABLE 2. Monkey species, localization of the cortical injections, and tracers employed In the experiments

Monkey	Species	Hemisphere	Area	Tracer %	Amount (µl)
Case 14	*M.nemestrina*	Left	F5p	FB (3)	0,2 µl x 1
Case 21	*M.nemestrina*	Right	F1(convexity)	FB (3)	0,2 µl x 1
		Right	F1(bank)	MR (10)	1 µl x 1
Case 25	*M.nemestrina*	Right	F5c	WGA-HRP (4)	0,2 µl x 1
Case 30	*M.nemestrina*	Right	F5a	DY (2)	0,2 µl x 1
		Left	F5a	WGA-HRP (4)	0,2 µl x 1
Case 31	*M.nemestrina*	Right	F5p	WGA-HRP (4)	0,2 µl x 1
		Left	F5p	FR (10)	1µl x 2
Case 33	*M.nemestrina*	Left	F5c	FB (3)	0,2 µl x 1
Case 34	*M.fascicularis*	Left	F5a	BDA (10)	1µl x 2
Case 35	*M.mulatta*	Left	F5c	FB (3)	0,2 µl x 1
		Left	F5a	DY (2)	0,2 µl x 1
		Right	F5p	BDA (10)	1µl x 2
Case 36	*M.fascicularis*	Left	F5c	CTB-A 594 (1)	1µl x2

-In C10 (*M. nemestrina*), horseradish peroxidase (HRP, 10%) was injected in the cervical segments of the spinal cord (C4-C5). *For the abbreviations see the list.*

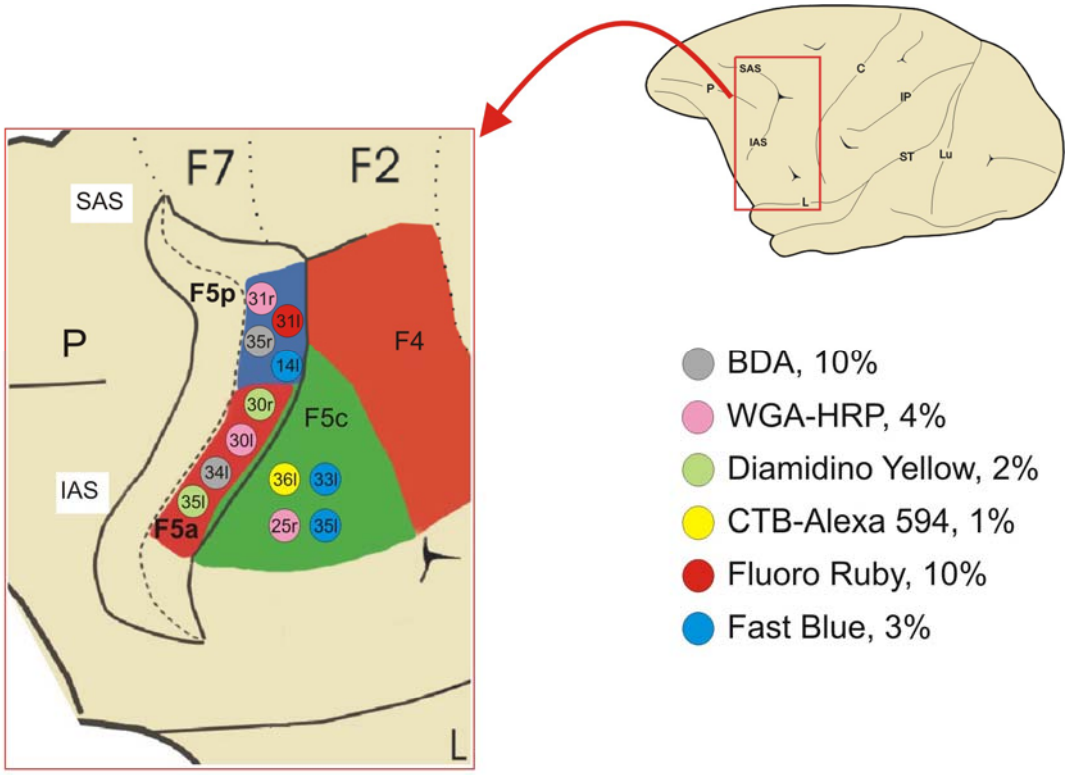

Fig. 4. Schematic diagram showing the injection sites localization in F5p, F5a and F5c. on *the left,* the inferior arcuate sulcus (IAS) was opened in order to show the posterior bank. The sharp lines correspond to the lips of anterior and posterior banks. Dashed line correponds to the fundus of the AS. Each neural tracer is represented with a full colored circle. *For Abbreviations see the list*.

2.2. Histological procedure

After appropriate survival periods following cortical (28 days for BDA and FR**,** 12-14 days for FB, DY and CTB-A, and 2 days for WGA-HRP) or spinal cord (3 days for the HRP) injections, each animal was anesthetized with ketamine hydrochloride (15 mg/kg i.m.) followed by an i.v. injection of sodium thiopental (60 mg/Kg) and perfused through the left cardiac ventricle with saline, 3.5-4% paraformaldehyde and 5% glycerol in this order. All solutions were prepared in phosphate buffer 0.1M, pH 7.4. Each brain was then blocked coronally on a stereotaxic apparatus, removed from the skull, photographed and placed in 10% buffered glycerol for 3 days and 20% buffered glycerol for 4 days. Finally, it was cut frozen in coronal sections 60 µm thick. In cases C10 and C31 the spinal cord was removed and after cryoprotection, cut transversally or horizontally respectively at 60 µm.

In all the cases injected with fluorescent tracers, one section of each five was mounted immediately, air-dried and quickly coverslipped for fluorescence microscopy. In cases C25r, C30l and C31r, one section of each five was processed for WGA-HRP histochemistry with tetramethylbenzidine as chromogen (Mesulam, 1982). In cases, C31l and C34l, one series of each fifth section was processed for the visualization of FR or BDA respectively, using a Vectastain ABC kit (Vector Laboratories, Burlingame, CA, USA) and 3,3'-diaminobenzidine (DAB) as chromogen. The reaction product was intensified with cobalt chloride and nickel ammonium sulphate.

In all cases, one series of each fifth section was stained with the Nissl method (thionin, 0.1% in 0.1M acetate buffer pH 3.7). In cases C10 and C31 one section of each five of the spinal cord was processed for the HRP histochemistry (C10) or for FR immunocytochemistry (C31l). One section of each five was stained with Nissl method.

2.3. Data analysis

2.3.1. Injection sites

The injection sites were defined according to the criteria previously described in detail by Luppino and collaborators (2001, 2003). Two concentric zones were defined for each tracer injection: a central zone, defined as the core and a surrounding zone, defined as the halo. The core of WGA-HRP, FR, BDA injection sites was considered to be the densely stained regions

adjacent to the needle track. The halo was considered to be the region with a less intense background staining and in which almost all neurons were labeled.

The core of the fluorescent tracers injection sites was considered to include an inner zone (zone I), sharply delineated around the needle track, which appeared necrotic and intensely fluorescent and a second zone (zone II), less sharply delineated and less brilliantly fluorescent, in which almost all of the neurons and many glial cells showed bright fluorescence. The halo was defined as the region which contained some background tissue fluorescence and in which almost all neurons and some glial cells were labelled. Zones I and II should correspond to the effective area of uptake and transport of fluorescent tracers (Kuypers and Huisman, 1984; Condé, 1987; Luppino et al., 2001, 2003).

In order to verify the locations of the cortical injection sites, Nissl stained material was used to identify the various areas. The borders between different areas and the extent of injection sites were then plotted on individual section drawings and mapped onto a dorsolateral view of the hemisphere. The injection sites of all the cases presented in this study were restricted within the limits of a single cytoarchitectonic area.

2.3.2. Distribution of the labeling

Retrogradely labeled neurons were plotted Under U.V. illumination and with the aid of a longpass barrier filter allowing one to visualize wave lengths greater than 395 nm, the fluorescent neurons were identified as follows: FB-labeled neurons by a sky-blue fluorescence in the cytoplasm; DY-labeled neurons by a yellow-green fluorescent nucleus; CTB-A 594 labeling was analyzed by using standard rhodamine filter. CTB-A 594-labeled neurons were identified for a red granular fluorescence in the cytoplasm.

The retrograde and anterograde (WGA-HRP, BDA and FR injections) labeling was plotted in each section every 600 µm, together with the outer and inner cortical borders with the aid of inductive displacement transducers mounted on the X and Y axes of the microscope stage. The transducer signals were digitized and stored by using software developed in our laboratory (*Inside* software) that allows the visualization of section outlines, of gray and white matter borders, and of labeled cells or terminals.

Data from individual sections were then imported into a three-dimensional (3D) reconstruction software (Bettio et al., 2001), creating volumetric reconstructions of the hemispheres from individual histological sections containing connectional data. The results of this processing allowed us to obtain realistic visualizations of the labeling distribution for a more precise comparison of data from different hemispheres. Distribution of labeling on exposed cortical surfaces was visualized in standard mesial, dorsolateral, or orbital views of the hemispheres.

The distribution of the labeling in the lateral fissure (LF) was visualized in two-dimensional (2D) reconstructions obtained by using *Inside* software, according to the following procedure: in each plotted section, the cortex included in the region of interest was subdivided into columnar bins by lines perpendicular to the cortical surface and connecting the outer and inner cortical contours. In order to minimize the distortion caused by cortical curvature, the cortex was then unfolded at the level of a virtual line connecting the midpoints of all the perpendicular lines, approximately positioned at the border between layers III and IV. The unfolded sections were then aligned and the labeling distributed along the space between two consecutive plotted sections (600 μm).

2.3.3. Areal attribution of the labeling

The parcellation of Matelli and co-workers (see also Geyer et al., 2000a) was adopted to attribute the labeling in the motor cortex (Matelli et al., 1985). While areas in the prefrontal cortex were identified following Preuss and Goldamn-Rakic, (1991) and Carmichael and Price, (1994) subdivisions. The labeled areas of the IPL were identified according to architectonic criteria from Gregoriou et al. (2006), the intraparietal areas according to the criteria defined by Borra et al. (2007). Finally, for the parietal operculum, we matched our data with the functional maps of the SII region of Krubitzer et al. (1995) and Fitzgerald et al. (2004).

C-Results

C. Results

1. Architectonics of the ventral premotor cortex

We identified three architectonically distinct areas in the rostral PMv that, all together, occupy the cortical sector corresponding to area F5, as histochemically defined (Matelli et al., 1985). Two of them are located within the inferior postarcuate bank, one more posteriorly (and dorsally), the other more anteriorly (and ventrally). They will be referred to as “posterior” (F5p) and “anterior” (F5a) F5, respectively. The third area occupies most of the shoulder of the inferior postarcuate bank and the adjacent postarcuate convexity cortex. It will be referred to as “convexity” (F5c) F5. F5p and F5c border caudally with a caudal PMv architectonic area corresponding to histochemical area F4.

The identification of these areas has been primarily based on the analysis of Nissl-stained material. In this respect, it should be noted the following (Gregoriou et al., 2006; Gerbella et al., 2007). First, given that very often architectonic features change gradually from one region to another, usually in the range of about 0.5 mm, borders between areas have been set at the intermediate points of these transitions. Second, given that some general and primary architectonic features (e.g., cell density and size) often show some interindividual variability, the definition of the cytoarchitectonic areas has been mostly based on *relative* changes, within individual cases, in single layer characteristics and in individual histological elements, reliably and consistently observed across different cases. By employing this approach and by using different planes of sectioning, we were able to set reliable cytoarchitectonic criteria, despite the interindividual variability of cytoarchitectonic features.

To seek a possible validation of the cytoarchitectonic subdivision of the rostral PMv, we combined this approach with the myeloarchitectonic and two chemoarchitectonic ones. This multiarchitectonic analysis proved to be very helpful in providing independent and complementary criteria for the characterization of the various identified rostral PMv areas.

The analysis of myelin-stained material, in spite of some variability in the quality of fiber staining from one section to another, showed that, in several cases, the identified cytoarchitectonic areas differed also in their myeloarchitectonic features. Myeloarchitectonic changes, however,

were rather more gradual with respect to the cytoarchitectonic ones and less effective for a precise delineation of architectonic borders.

SMI-32ir and CBir are two chemoarchitectonic approaches which provide complementary information on the organization of some aspects of the efferent and intrinsic components of the cortical circuitry (Campbell and Morrison, 1989; Hendry et al., 1989). In the primate neocortex, SMI-32ir reveals, almost everywhere, subpopulations of layers III and V pyramidal cell bodies and proximal portions of their apical and basal dendrites (Campbell and Morrison, 1989). SMI-32 immunopositive cells and neuropil display, however, specific regional and laminar distribution patterns, used in other studies for the delineation of occipito-parietal (Hof et al., 1999), temporal (Cusick et al.,1995), parietal (Gregoriou et al., 2006) dorsal premotor (Geyer et al., 2000b), cingulate (Nimchinsky et al., 1996) and prefrontal (Carmichael and Price, 1994) areas. In contrast, CBir is present in a subpopulation of cortical nonpyramidal and pyramidal neurons (e.g., DeFelipe et al., 1989; Hendry et al., 1989), in which, though with some variability across different cortical regions, nonpyramidal neurons are by far the most represented. In general, in the primate neocortex, CB immunopositive cells are highly concentrated in layers II and uppermost III and sparser in deeper layers. Other studies have shown that regional differences in the distribution of CB immunopositive nonpyramidal or pyramidal cells can be used for the characterization of different sensory (Kondo et al., 1999), temporal (Kondo et al., 1994) and prefrontal (Carmichael and Price, 1994; Condé et al., 1994; Dombrowski et al., 2001; Gerbella et al., 2007) areas. Both these chemoarchitectonic approaches proved to be very helpful for a further and independent validation of the results of the cytoarchitectonic analysis. In this respect, it should be noted that, likely because of slight differences in fixation and immunostaining procedures, some variability was observed, from one case to another, in the absolute staining intensity of the immunopositive cells and neuropil. Nevertheless, qualitative analysis of SMI-32ir, based on relative changes, within individual cases, in the number of immunopositive cells and laminar position and intensity of cell and neuropil immunostaining, showed that the various PMv cytoarchitectonic areas very well corresponded to different chemoarchitectonic fields. These observations were supported by quantitative analysis of the density of immunopositive pyramids in layers II/III and V. Furthermore,

qualitative and quantitative analysis of CB immunoreacted material showed that, in spite of a similar general pattern of CBir, differences in the number and laminar distribution of immunopositive cells were very helpful for the characterization of different PMv areas. Changes in CBir from one area to another were, however, relatively more gradual than in SMI-32ir.

In the next sections, the architectonics of the rostral PMv areas F5p, F5a and F5c and of the neighboring cortical areas will be firstly described in terms of cyto- myelo- and chemo-architectonic features. The results of the quantitative analyses of the distribution of SMI-32 and CB immunoreactivity will be described comparatively in a separate section.

1.1 Area F5p

Area F5p was identified in the more posterior part of the inferior postarcuate bank. In the standard coronal plane this cortical sector is cut almost tangentially to the cortical surface and its architecture was very poorly delineated (Figs. 5B and 6C). Parasagittal, perpendicular to the IAS and tangential to the arcuate sulcus sections (Figs. 7A, 9A and 10A), provided optimal and complementary views of the location and architectonic features of this area. The combined analysis of these sections showed that F5p is characterized by the presence of relatively large layer V pyramids. These cells, though varying in absolute size across different cases, represented one major distinguishing architectonic feature of this rostral PMv area. Higher magnification views (Figs. 8A, 9C, 10A and 11A) showed that F5p is also characterized by a barely discernible layer II and a layer III relatively homogeneous in cell density. Layer III pyramids, as a whole, were relatively small, but showed a size gradient with a slight, but evident increase in size from the upper to the lower part of it. Layer V was clearly sublaminated: layer Va is cell dense and populated by small pyramids, layer Vb is relatively densely populated by medium sized pyramids and hosts the relatively large pyramids typical of this area. Layer VI is homogeneous and displays a radial cellular organization.

Myeloarchitectonic analysis showed that area F5p was relatively heavily myelinated (Figs. 12A, 13A, and 14A). Vertical bundles of fibers were dense and relatively thick, ending within a very dense and coarsely delimited plexus of mixed vertical and horizontal fibers. In those sections in

which this sector was cut almost orthogonally to the cortical surface, this plexus presented an evident increase in staining intensity in correspondence of the outer band of Baillarger.

F5p could be very clearly delineated with SMI-32ir. One outstanding chemoarchitectonic feature of this area was the presence in layer V of relatively large, darkly stained pyramids distributed along its entire extent (Figs. 15A, 16B, 16C and 17A). These immunopositive pyramids appeared to correspond to virtually the entire population of the relatively large layer Vb pyramids identified in adjacent Nissl-stained sections. In layer III, numerous, darkly stained, small immunopositive pyramids and relatively dense immunopositive apical dendrites were observed in its lower half (Fig. 17A).

In CB immunostained sections, darkly stained nonpyramidal cells were highly concentrated in layer II and in the uppermost part of layer III, where immunopositive neuropil was densely stained (Figs. 18A, 19A and 19C). In the remaining part of layer III, these cells were much sparser and the neuropil staining much weaker. In correspondence of layer Va, there was a relatively higher number of large, multipolar, darkly stained cells. These cells, which represent a subset of CB immunopositive cells typically encountered in layer V and VI (Hof et al, 1999) displayed darkly stained dendritic arbors forming an horizontal plexus within layer Va that, at low power views, appeared as a faint band of neuropil.

1.2. Area F5a

F5a was identified in the inferior postarcuate bank, anteriorly (and ventrally) to F5p. In Nissl-stained sections, the most distinctive feature of this area, evident even at very low power view (Figs. 5C, 7A and 7B), was a relatively prominent layer V, which characterized F5a among the three rostral PMv areas identified in the present study. Higher magnification views (Figs. 6D, 8C, 9D,10B and 11B) showed that this layer displayed a not very distinct sublamination, being populated mostly by relatively densely packed medium-sized pyramids, only slightly larger and sparser in the lower part. Layer II was barely discernible and layer III was, in general, densely and homogeneously populated by small pyramids. However, the lowest part of this layer typically displayed an almost continuous single row of relatively sparse, deeply stained and relatively large pyramids which, though with some interindividual variability, tended to be even larger than those

observed in layer V. These relatively large layer III pyramids were very often clearly evident even at low power views and represented a further distinguishing cytoarchitectonic feature of F5a. In correspondence with the layers III/V border, in all cases, some small granular cells were observed, intermingled with pyramidal cells. Though these granular cells varied in number and density from one case to another (Figs. 11D and 11E), independently of the macaque species, in any case we were able to identify in this area the presence of a layer IV, even in a rudimentary form.

F5a was considerably less myelinated than F5p (Figs. 12C, 12D, 13B, 13C and 14B). Vertical bundles of fibers were relatively thin and both bands of Baillarger were clearly evident, which represented a distinguishing architectonic feature of this area.

SMI-32ir was relatively low in F5a, especially in comparison with the two other rostral PMv areas (Figs. 15A, 15B, 16A, 16B, 16D and 17B). In layer III, immunopositive apical dendrites were relatively poor and only an almost continuous single row of darkly stained, relatively large pyramids was observed in the lowest part of this layer. These cells appeared to correspond to the large layer III pyramids observed in Nissl-stained sections and represented a distinguishing chemoarchitectonic feature of this area. Layer V was very poorly stained and populated by sparse and lightly stained small pyramids.

CBir pattern was very helpful for the characterization of F5a, where the overall immunostaining was relatively high in comparison with the two other rostral PMv areas (Figs. 18A, 18B, 19B and 19D). In particular, darkly stained CB immunopositive cells, though highly concentrated in the most superficial layers, were very numerous through the almost entire extent of layer III, where immunopositive neuropil was quite densely stained. Furthermore, F5a displayed a relatively higher concentration of multipolar, darkly stained cells in layer V, with respect to F5p. Accordingly, the horizontal plexus formed by the dendritic arbores of these cells was much denser and more clearly visible at low power views than in F5p.

1.3. Area F5c

F5c was identified on the postarcuate convexity cortex, close to the IAS. At low power views (Figs. 5B, 5C, 7B and 9B), this area was distinguished from its neighbours for a very poorly laminated appearance, due to its overall cell population rather homogeneous in size and density.

Higher magnification views (Figs. 6B, 8B, 9E and 11C) showed that layer III was homogeneously populated by small pyramids without any evident size gradient. Layer V was sublaminated, relatively cell dense and populated by quite small pyramids. In layer Vb these cells were only slightly larger and sparser in layer Va. A radial cellular organization was evident in lower layer III and in layers V and VI, with thin vertical columns of cells very close to each other. The poor lamination, the columnar organization, the lack of a size gradient in layer III and the overall smallness of layer V pyramids, all represented reliable criteria for the definition of the border of F5c with F5p and F5a.

F5c was heavily myelinated (Figs. 12D, 13B, 13C and 14C) and characterized by the presence of thin and very close vertical bundles, most of them ascending up to the superficial layers, where a relatively high myelin content represented a distinguishing myeloarchitectonic feature of this area. The outer band of Baillarger was densely stained and more neatly delineated than in F5p. An inner band of Baillarger was not evident.

SMI-32ir was relatively higher than in F5a, especially in layer III, where numerous small immunostained pyramids were observed in the lower part of it (Figs. 15B, 16A, 16B, 16D and 17C). Apical dendrites were numerous as well, but less than in area F5p. Layer V was poorly labeled and only very sparse and lightly stained cell were observed. The very poor immnunostaining in this layer clearly distinguished F5c from F5p.

CBir pattern in F5c was basically similar to that observed in F5p, except for a denser staining of the neuropil band observed in layer V (Figs. 18B, 19B and 19E).

1.4. Cortical areas neighbor to F5p, F5a and F5c

Posteriorly to F5c and to the dorsal part of F5p, we identified a caudal PMv architectonic area very well corresponding to histochemical area F4. Accordingly, it has been designated as F4. The cytoarchitecture of this area was optimally analyzed in coronal sections (Fig 5A), in perpendicular to the IAS sections (Fig. 9A) and in parasagittal sections, taken, however, at more medial levels than those shown in Figure 7, in which the postarcuate convexity cortex is cut more perpendicularly to its surface (Fig. 20A). In F4, layer III was relatively cell sparse and displayed an evident increase in cell size from the upper to the lower part of layer III, where numerous medium-

sized pyramids were observed (Figs. 6A, 20A and 20C). The relative cell sparseness and the evident size gradient in layer III represented major, reliable cytoarchitectonic criteria for distinguishing the border of F4 with F5p and F5c. Layer V was clearly subdivided into a cell dense layer Va, populated by small pyramids and less dense than in F5p, and a relatively cell sparse layer Vb, where large pyramids were observed. Although with some degree of interindividual variability in their number and size, in most of the cases these large layer V pyramids tended to be larger and more numerous than in F5p. Furthermore, a dorsoventral gradient was observed within F4, in which these cells tended to be slightly smaller and denser more ventrally (Fig. 5A). The appearance of a much less evident size gradient in layer III, of a much sparser layer Va and, even more, of numerous giant layer Vb pyramids, arranged in multiple rows, clearly distinguished the caudal border of F4 with the precentral area F1. In myelin stained sections, F4 was slightly less myelinated than F5p and characterized by very close and conspicuous vertical bundles and an evident (when optimally visualized) outer band of Baillarger (Figs. 12B, 13A, 13D and 14D). SMI-32ir was higher than in F5p in both layer III, where positive cell bodies and apical dendrites were more numerous and in layer V, which was more densely populated by positive pyramids (Figs. 15A, 15B, 16C, 16D and 17D). These immunopositive pyramids tended to be smaller more ventrally in F4. Based on this gradient in immunopositive layer V cells, it has been previously suggested (Geyer et al., 2000b) that F4 possibly consists of a dorsal and a ventral subdivision. This gradient was indeed observed, in the present study, in SMI-32ir as well as in Nissl-stained section. These changes were, however, rather gradual and we did not found further architectonic support for this subdivision. Finally, CBir was, in general, lower than in F5p and F5c in terms of positive cell bodies and neuropil, though with a quite similar laminar distribution of positive cells (Figs. 18A, 18B, 19A and 19F). The neuropil band observed in layer V in F5p, F5a and F5c, was much less pronounced in F4.

Ventrally, F5c bordered with an area displaying markedly distinct architectonic characteristics (Figs. 5C, 6B and 20D). Major cytoarchitectonic features of this area (Fig. 20D) were the presence of a layer III rather dense and homogeneous in cell size and density, a faint, rudimentary layer IV, where granular cells were intermingled with layers III and V pyramids, and an homogeneous layer

V, densely populated by small pyramids. This area could be distinguished from F5c also for a decrease in myelin content with a less distinct outer band of Baillarger (Figs. 13C and 14E), a considerably sharp decrease in number and size of SMI-32 immunopositive layer III pyramids (Figs. 16A and 17F) and by an increase in CB immunopositive cells and neuropil. This area occupied a ventral convexity sector and bordered ventrally, close to the frontal operculum, with area PrCO as defined by Roberts and Akert (1963). On the basis of its multiarchitectonic features, we found this area much more similar to the frontal opercular cortex than to the PMv. Accordingly, we have provisionally designated it as Dorsal Opercular (DO) area.

In the very rostralmost part of the postarcuate convexity cortex and of the postarcuate bank, striking architectural changes marked the rostral border of F5c and F5a (Figs. 5D, 6E, 7B and 10B). The distinguishing cytoarchitectonic features of this cortical sector were an evident layer IV and a prominent layer V, populated by densely packed, small and deeply stained pyramids. This sector was also characterized by a very low myelin content (Figs. 12C, 12D and 14F), a very poor SMI-32ir (Figs. 15B and 17E) and a very high CBir (FigS. 18A, 18B and 19H). All together these architectonic features strongly suggest that this sector should be considered as part of the granular frontal cortex. We have, therefore, generically designated it as Granular Frontal (GrF). It should be noted, however, that in a previous multiarchitectonic study, focused on the caudal ventrolateral prefrontal cortex (Gerbella et al., 2007), we have suggested that this very rostral part of the postarcuate cortex is in continuity with area 12l as defined by Carmichael and Price, (1994).

Finally, while F5p appeared to occupy virtually the entire extent of the postarcuate bank, bordering with area 8/FEF (Gerbella et al., 2007), F5a tended to occupy only the lateral two/thirds-three/fourths of the bank. If it is considered that the ventral border of the prearcuate area 45B is located deeply in the prearcuate bank (Gerbella et al, 2007), then F5a and 45B appear to be separated by a small cortical sector mostly located along the fundus of the IAS (Figs. 20B and 20E). Because of its location, the architectonic features of this field could not be optimally visualized in any of the used planes of sectioning. Nevertheless, it appeared to be characterized by the presence of a size gradient in layer III, in which, however, layer IIIc medium-sized pyramids were denser and smaller than in area 45B. A faint layer IV and a poorly developed, homogenous

layer V also characterized this field. Thus, it is possible that this fundal sector of the IAS represents a distinct field, with architectonic features intermediate between those of F5a and area 45B. Given that this field appear to be neither part of the PMv, nor of area 45B, we have provisionally designated as “Fundal Inferior Arcuate” (FIA) area. We will discuss later the possibility that this field corresponds, at least in part, with area 44, as defined by of Petrides et al. (2005).

1.5. Quantitative analysis

To seek for possible additional and more objective criteria supporting the above described subdivision of the rostral PMv, our qualitative analysis has been complemented by a quantitative analysis of the distribution of SMI-32 or CB immunopositive cells in F5p, F5a and F5c. Furthermore, to have a more complete view of the chemoarchitecture of all the various areas of the ventral agranular frontal cortex, F4 and the precentral area F1 were also included in this analysis.

In SMI-32 immunostained material, differences were observed across the studied areas in the density of immunopositive pyramids in layer II/III and in layer V (Fig. 21A). The two-way ANOVA performed on the values of laminar density of SMI-32 immunopositive cells showed a significant main effect of Area [$F(4;92)=28.827$, $p<0.001$] and a significant interaction effect (Area x Layer) [$F(4;92)=27.439$, $p<0.001$]. Post-hoc analysis showed that, in layer III (Fig. 21A), the immunopositive cell density in F4, F5p and F5c was significantly higher than in F1 ($p<0.05$) and F5a ($p<0.005$). In layer V (Fig. 17B), the density of immunopositive pyramids in the two caudal areas F1 and F4 was significantly higher than in the three rostral areas F5p ($p<0.005$ for F1 and $p<0.05$ for F4), F5c ($p<0.001$) and F5a ($p<0.001$). Moreover, in F5p it was significantly higher than in F5c ($p<0.001$) and F5a ($p<0.001$) and in F5c it was significantly higher than in F5a ($p<0.05$). Finally, post-hoc analysis also showed that the ratio between layer III and layer V immunopositive pyramids was <1 in F1 ($p<0.001$) and F4 ($p<0.05$) and >1 in F5c ($p<0.001$) and F5a ($p<0.005$).

All together, these data indicated that F1 and F4 display a higher density of immunopositive pyramids in layer V, with respect to layer III and differed from more rostral areas for a higher density of immunopositive cells in layer V. F4, however, differed from F1 for a lower density of layer V immunopositive cells. In F5p the density of immunopositive pyramids in layer III and in layer V is similar. This area differed from F4 for a lower density of immunopositive pyramids in

layer V and from F5c and F5a for a higher density of immunopositive pyramids in layer V and in layers III and V, respectively. In both F5c and F5a, layer III immunopositive pyramids are denser than in layer V. Finally, F5a differed from F5p and F5c for a lower density of immunopositive pyramids in both layers III and V. Accordingly, SMI-32ir proved to be a very helpful approach for the architectonic definition of all the various ventral agranular frontal areas, on the basis of both qualitative and quantitative criteria.

In the analysis of CB immunostained material we firstly observed that the number of CB positive pyramids in all the studied areas was almost negligible, except for F5a, where, however, these cells represented no more than 5% of the whole population of CB positive cells. For this reason, CB positive pyramids were not considered for quantitative analysis. This paucity of CB positive pyramids represents a major chemoarchitectonic difference between the agranular frontal and the caudal ventrolateral prefrontal cortex, where these cells are, for example in prefrontal areas 45A and 46, about 10% of the whole population of CB positive cells (Gerbella et al., 2007).

The quantitative analysis of the density and/or laminar distribution of CB immunopositive nonpyramidal neurons showed several chemoarchitectonic differences among the five studied ventral agranular frontal areas. The one-way ANOVA for repeated measures of the density values of CB immunopositive nonpyramidal neurons showed a significant main effect of Area [$F(4;92)=189.901$, $p<0.001$]. Post-hoc analysis showed that the studied areas significantly differed each other ($p<0.001$) in terms of density of CB positive nonpyramidal cells, except for F5p and F5c. In particular, in F4 the density was about 20% higher than in F1, in F5p and F5c was about 25% higher than in F4 and in F5a was about 30% higher than in F5p and F5c (Figs. 21C and 21D).

The two-way ANOVA of the values of laminar density of CB immunopositive nonpyramidal cells showed a significant main effect of Area [$F(4;92)=115.581$, $p<0.001$] and Layer/Sublamina [$F(4;92)=688.548$, $p<0.001$] and a significant interaction effect (Area x Layer/sublamina) [$F(16;368)=21.094$, $p<0.001$]. In spite of a general similarity across the five studied areas, some significant differences were observed in layer II/III sublamina and in layer V. In particular, post-hoc analysis showed that the differences observed across the studied areas in terms of overall density were reflected into similar significant differences ($p<0.005$) at the level of the first and second layer

II/III sublamina. Furthermore, in F5a, as evident also at a qualitative level of analysis, the density of CB immunopositive nonpyramidal cells in the lower layer II/III sublaminae and in layer V, was significantly higher than in all the other studied areas ($p<0.001$ for all comparisons except for F5a vs. F5p in layer V, which was $p<0.05$).

All together, these data indicated that the architectonic areas of the ventral agranular frontal cortex can be distinguished each other also on the basis of differences in overall and/or laminar density of CB positive nonpyramidal cells, except for F5p and F5c, which showed a very similar distribution pattern of CBir. In particular, F1, F4 and the two more rostral areas F5p and F5c, mostly differed in terms of density of CB positive nonpyramidal cells in the most superficial layers. The rostralmost area F5a markedly differed from the other areas for a much higher overall density of CB positive nonpyramidal cells and for a higher density of these cells in the lower half of layer II/III and in layer V.

1.6. Location and extent of areas F5p, F5a and F5c

To obtain an estimate of the distribution of the identified rostral PMv areas, a 3D reconstruction was generated from the individual sections for each case studied. The location and the extent of areas F5p, F5a, F5 and of the neighbouring areas F4 and DO, are shown in two reconstructed hemispheres (Cases 18r) in Figure 22. For each hemisphere, the frontal lobe is shown from a dorsolateral view and from a rostrolateral view in which the posterior bank of the IAS was exposed with dissection of the 3D reconstruction along the fundus of the arcuate sulcus. Both location and extent of these areas are quite consistent and the areal distribution was very similar in the rest of the cases studied.

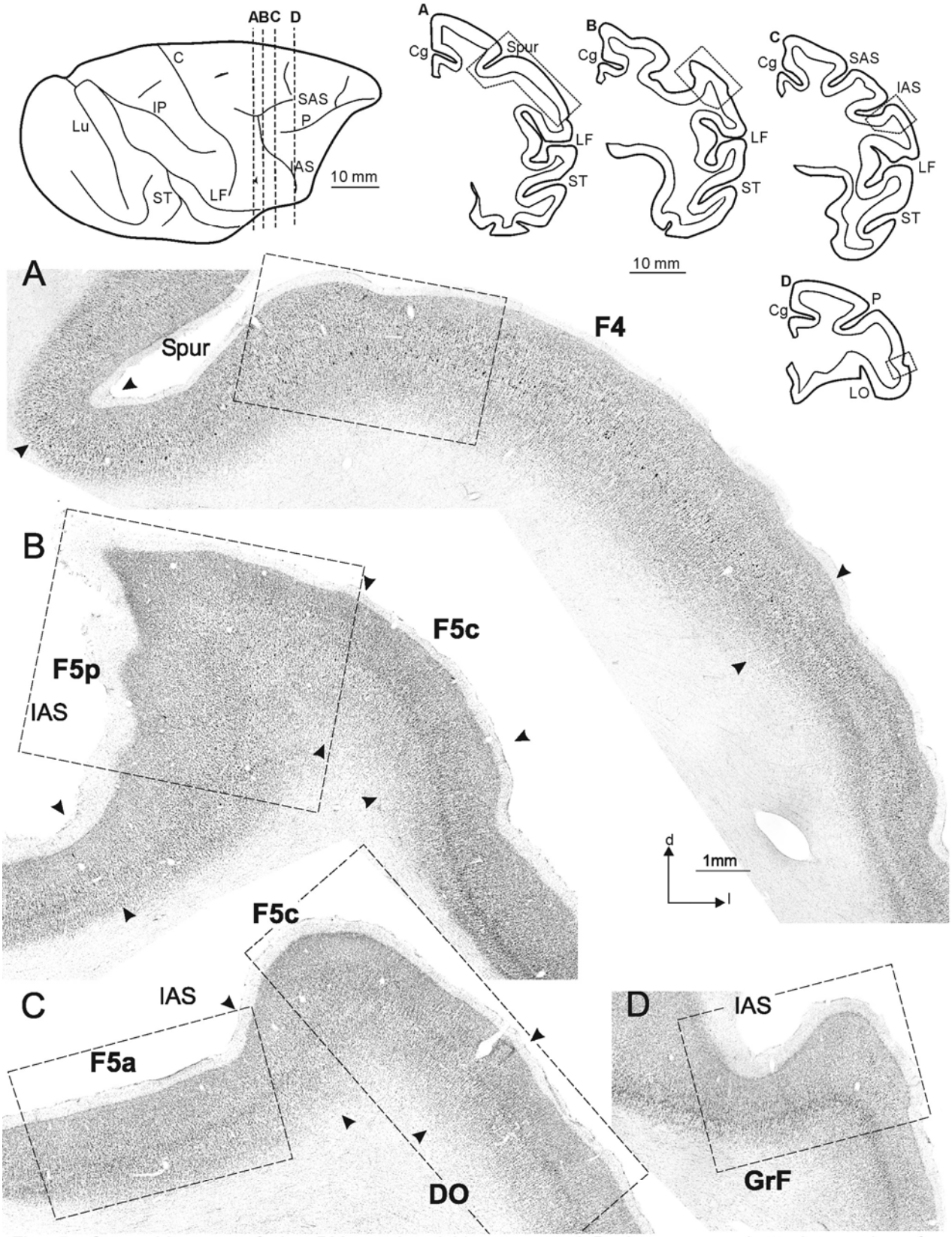

Fig. 5. Cytoarchitecture of the PMv and neighbor areas. A-D, Low-power photomicrographs of a series of Nissl-stained coronal sections, in a caudal to rostral order, taken from Case 18r. In all photomicrographs, arrows indicate the borders between cytoarchitectonic areas. Section orientation in A applies to all photomicrographs and section drawings. The scale bar in A applies to A-D. The levels at which the sections were taken are indicated by dashed lines on the drawings of the dorsolateral view of the hemisphere. Dashed boxes on the section drawings indicate the locations of the photomicrographs and the scale bar in B applies to A-D drawings. Dashed boxes in A-D photomicrographs indicate the location of the higher magnification views shown in Fig. 6. For *Abbreviations see the list.*

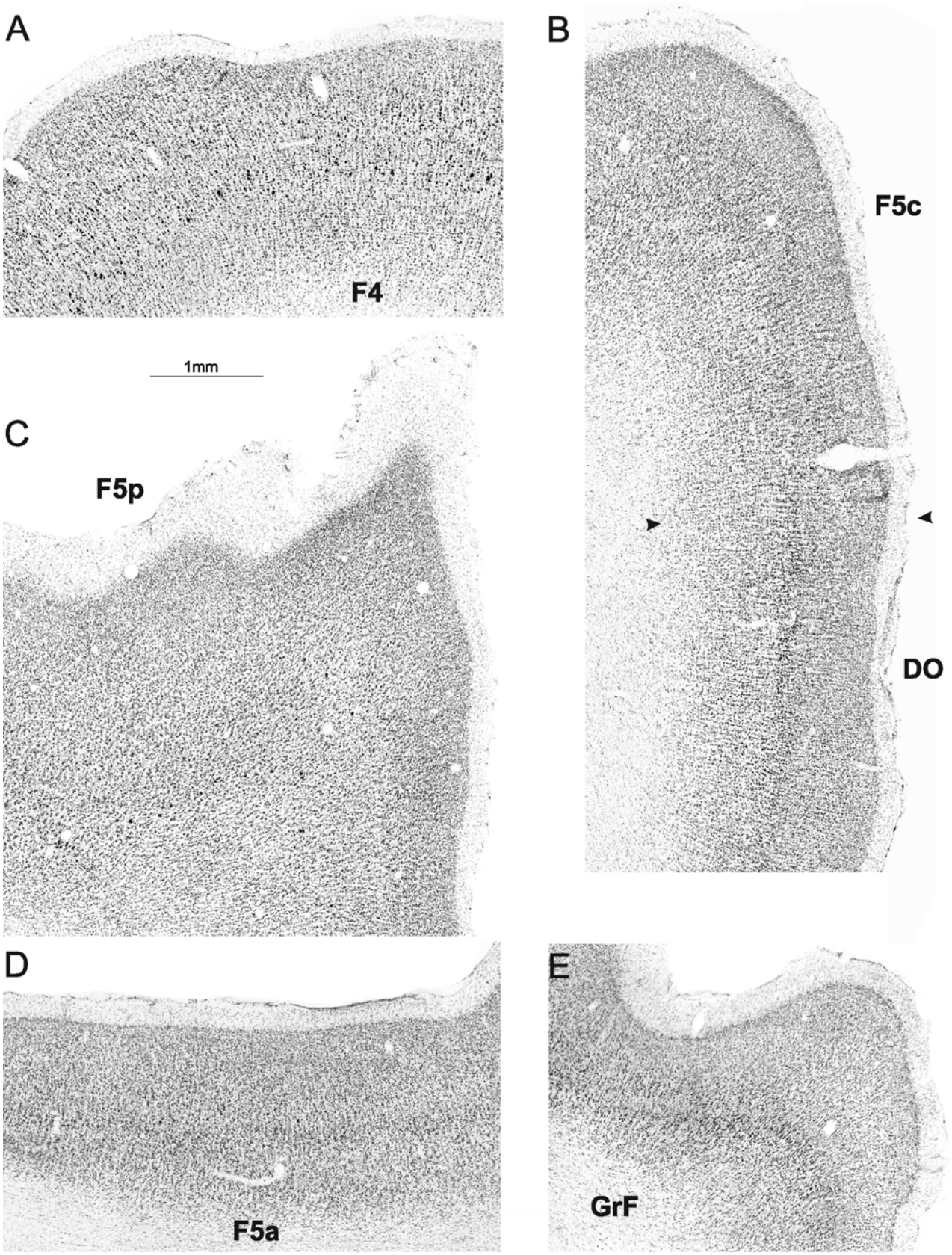

Fig. 6. Cytoarchitecture of the PMv and neighbor areas. A-E, Higher magnification views of areas F4 (A), F5c and DO (B), F5p (C), F5a (D) and GrF (E). The location of the photomicrographs is indicated by dashed boxes in the sections shown in Fig. 5. Scale bar in C applies also to A-E. Arrows mark the intermediate points of cytoarchitectonic transitions. For *Abbreviations see the list*.

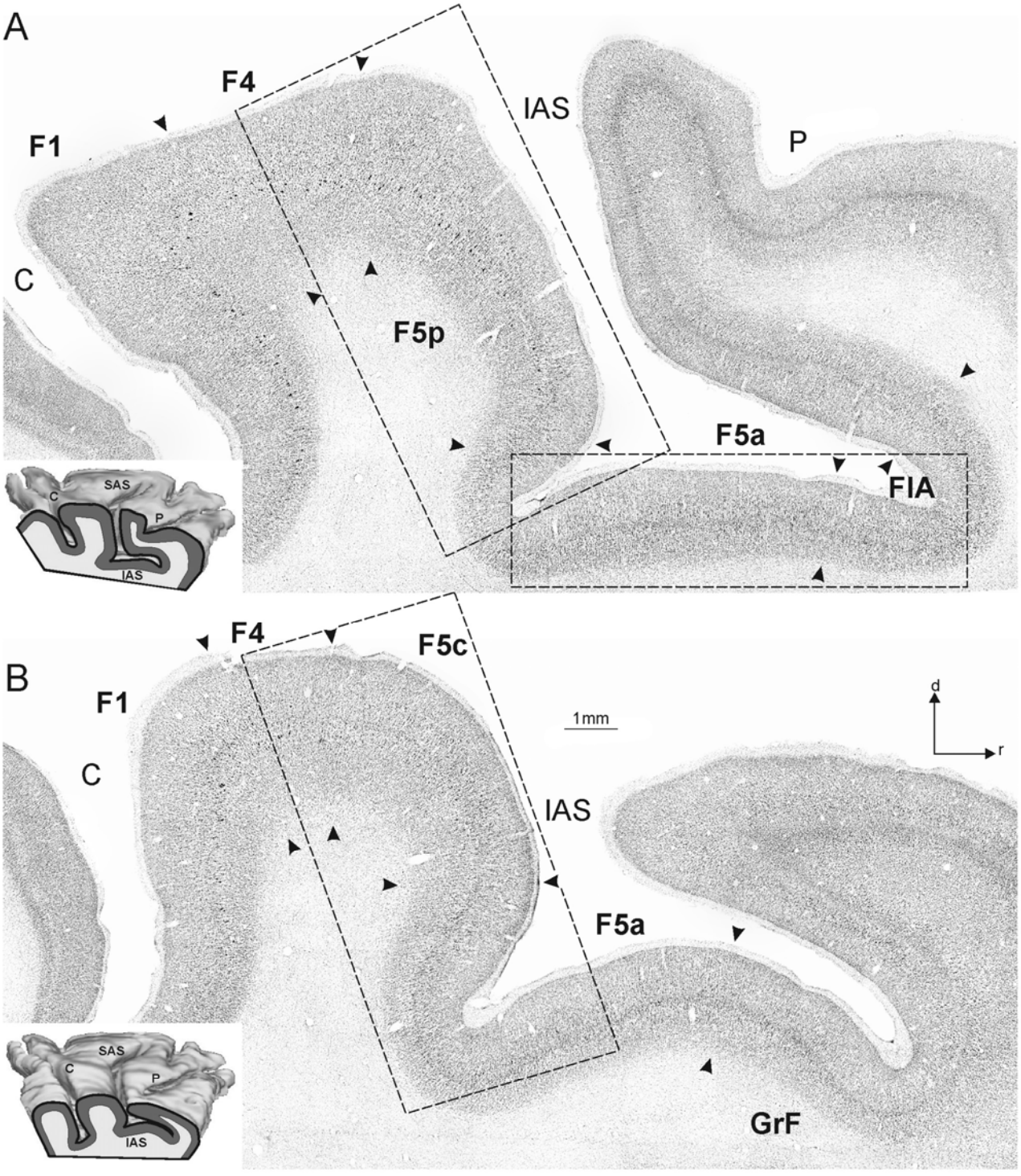

Fig. 7. Cytoarchitecture of the PMv and neighbor areas. A and B, Low-power photomicrographs of medial and lateral Nissl-stained parasagittal sections, taken from Case M3r. Section orientation and scale bar in B apply also to A. In both A and B, 3D reconstruction of the hemispere shows the level at which the section was taken. Dashed boxes in A and B indicate the location of the higher magnification views of the Fig. 8. Other conventions as in Fig. 5. For *Abbreviations see the list*.

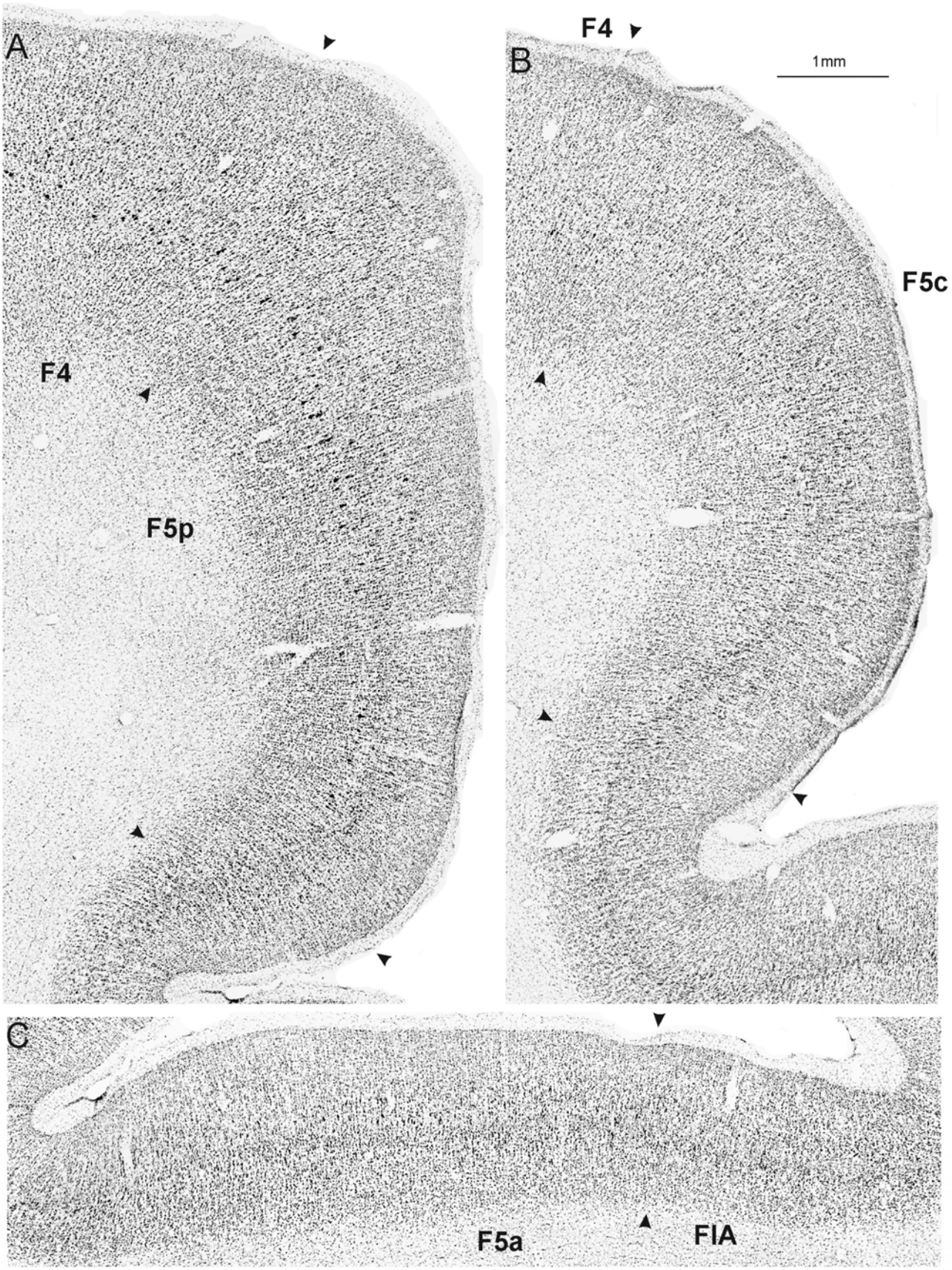

Fig. 8. Cytoarchitecture of the PMv and neighbor areas. A-C, Higher magnification views of areas F5p (A), F5c (B), F5a and FIA (C). The location of the photomicrographs is indicated by dashed boxes in the sections shown in Fig. 7. Other conventions as in Fig. 5. Scale bar in B applies to A-C. For *Abbreviations see the list*.

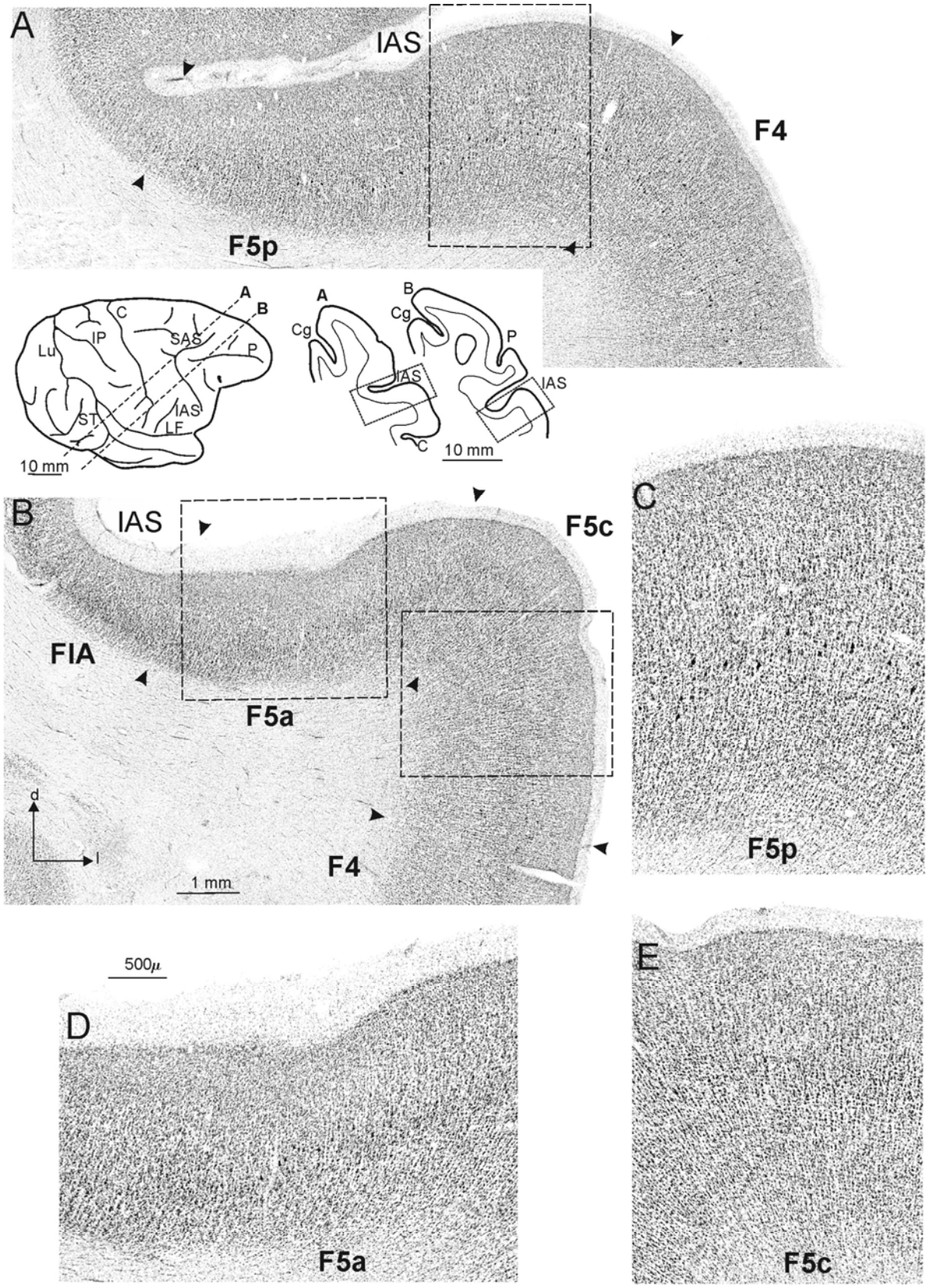

Fig. 9. Cytoarchitecture of the PMv and neighbor areas. A and B, Low power photomicrographs of two Nissl-stained perpendicular to the arcuate sulcus sections, in a dorsal to a ventral order taken from Case Pr17. Section orientation and scale bar in B apply to A. Dashed boxes on the photomicrographs indicate the location of the higher magnification views. C-E Higher magnification views of areas F5p (C), F5a (D) and F5c (E). Scale bar in D applies to D-E. Other conventions as in Fig. 5. For *Abbreviations see the list*.

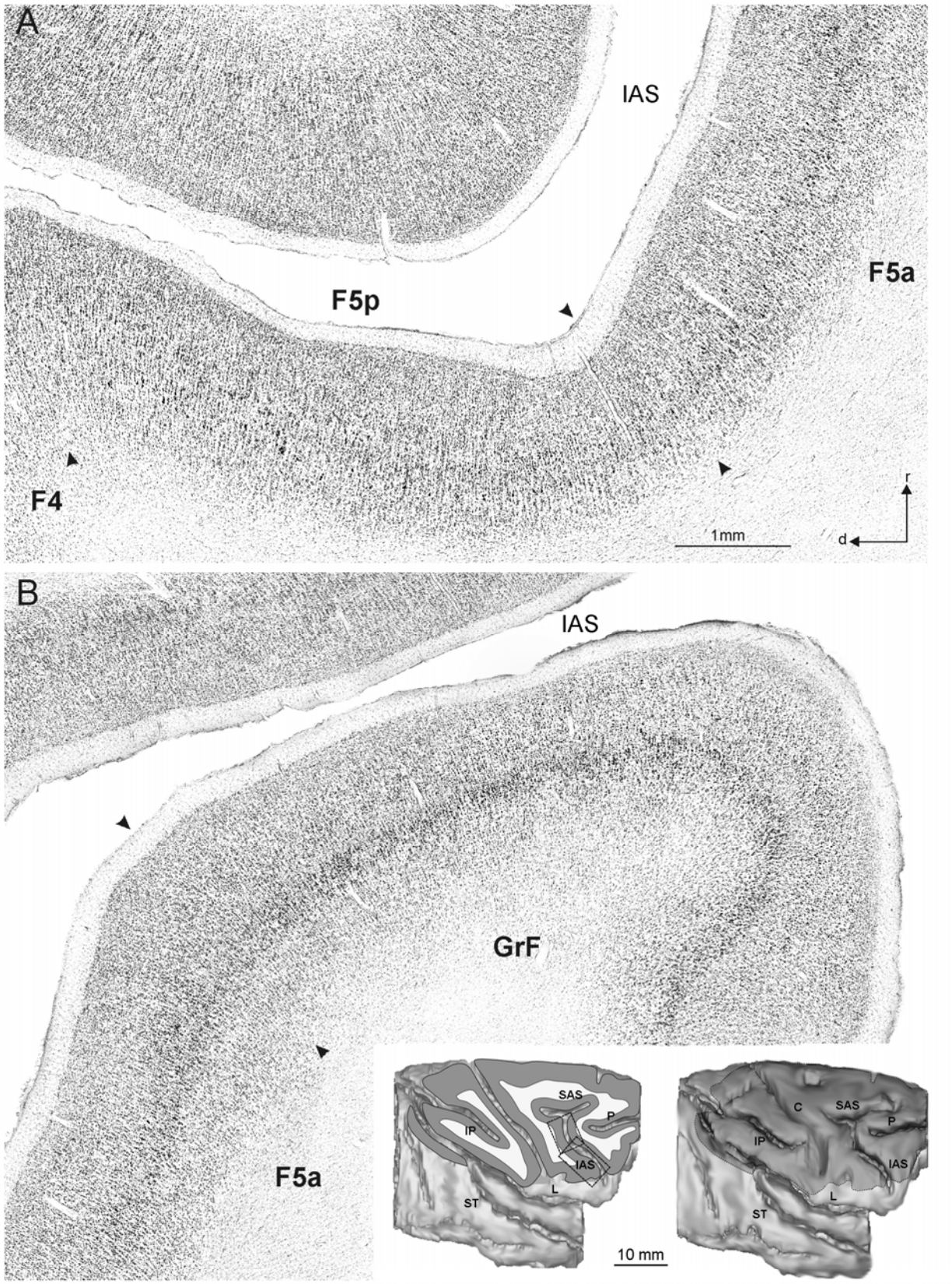

Fig. 10. Cytoarchitecture of the PMv and neighbor areas. A and B, Higher magnification views of a Nissl-stained tangential to the arcuate sulcus section, taken from Case PR18. A- Higher magnification view of the cytoarchitectonic transitions between areas F4 and F5p, F5p and F5a. B- Higher magnification view of the cytoarchitectonic transition between F5a and GrF. Scale bar in B applies to A. The right 3D reconstruction of the right hemisphere shows in darker grey the brain sector dissected in order to expose the approximate level of the section, shown in the left 3D reconstruction. The dashed box on the reconstruction indicates the locations of the photomicrographs. Section orientation in A applies to B. Other conventions as like in Fig. 5. For *Abbreviations see the list*.

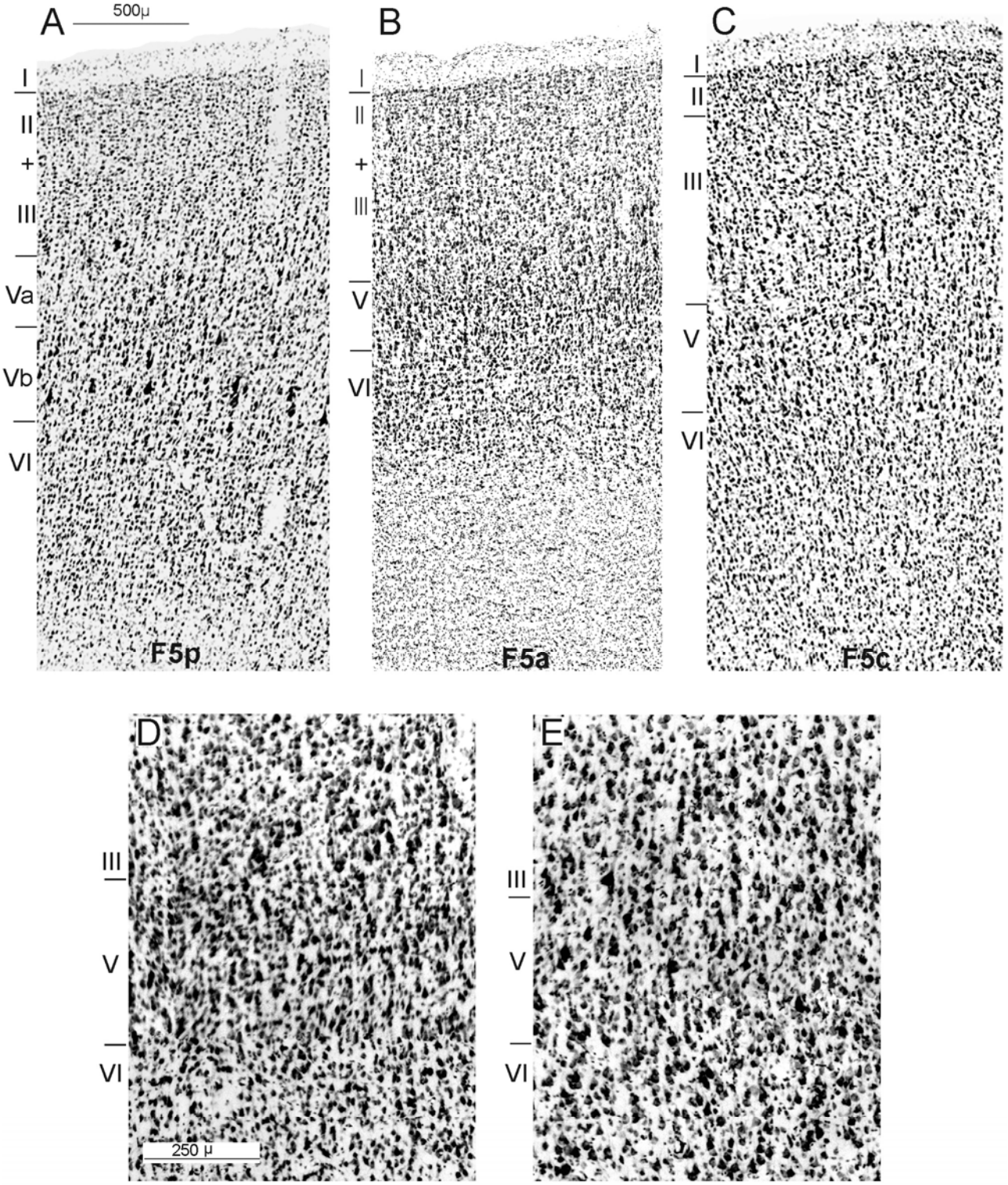

Fig. 11. Cytoarchitecture of the PMv and neighbor areas. A-C, Higher power photomicrographs of representative fields of cytoarchitectonic areas F5p (A), F5a (B) and F5c (C), taken from Case M3r. Scale bar in A applies to B and C. D and E, Higher power photmicrographs of area F5p taken from Cases M4l and M3r respectively. These views are centered on Layers III-V to allow direct comparison of granular cells density in two representative different cases. Scale bar in D applies to E. For *Abbreviations see the list.*

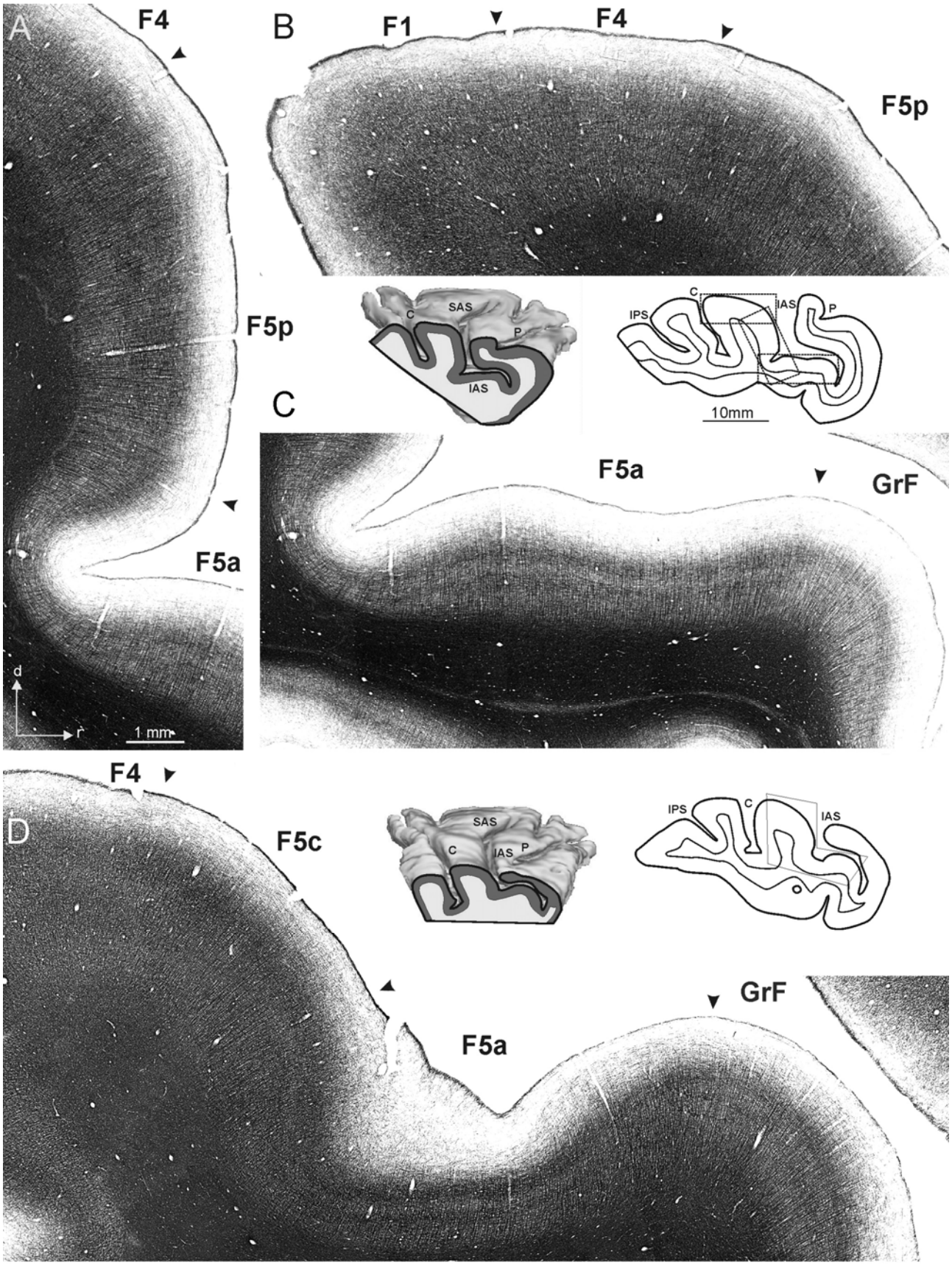

Fig. 12. Myeloarchitecture of the PMv and neighbor areas. A-D, Low-power photomicrographs of myelin-stained parasagittal sections, taken from Case M4l. 3D reconstructions of the hemisphere shows the medio-lateral levels at which the sections from which the photomicrographs were taken. Section orientation and scale bar in A apply also to B-D. Arrows on the photomicrographs indicate the location of cytoarchitectonic borders reported from adjacent Nissl-stained sections. Other conventions as in Fig. 5. For *Abbreviations see the list*.

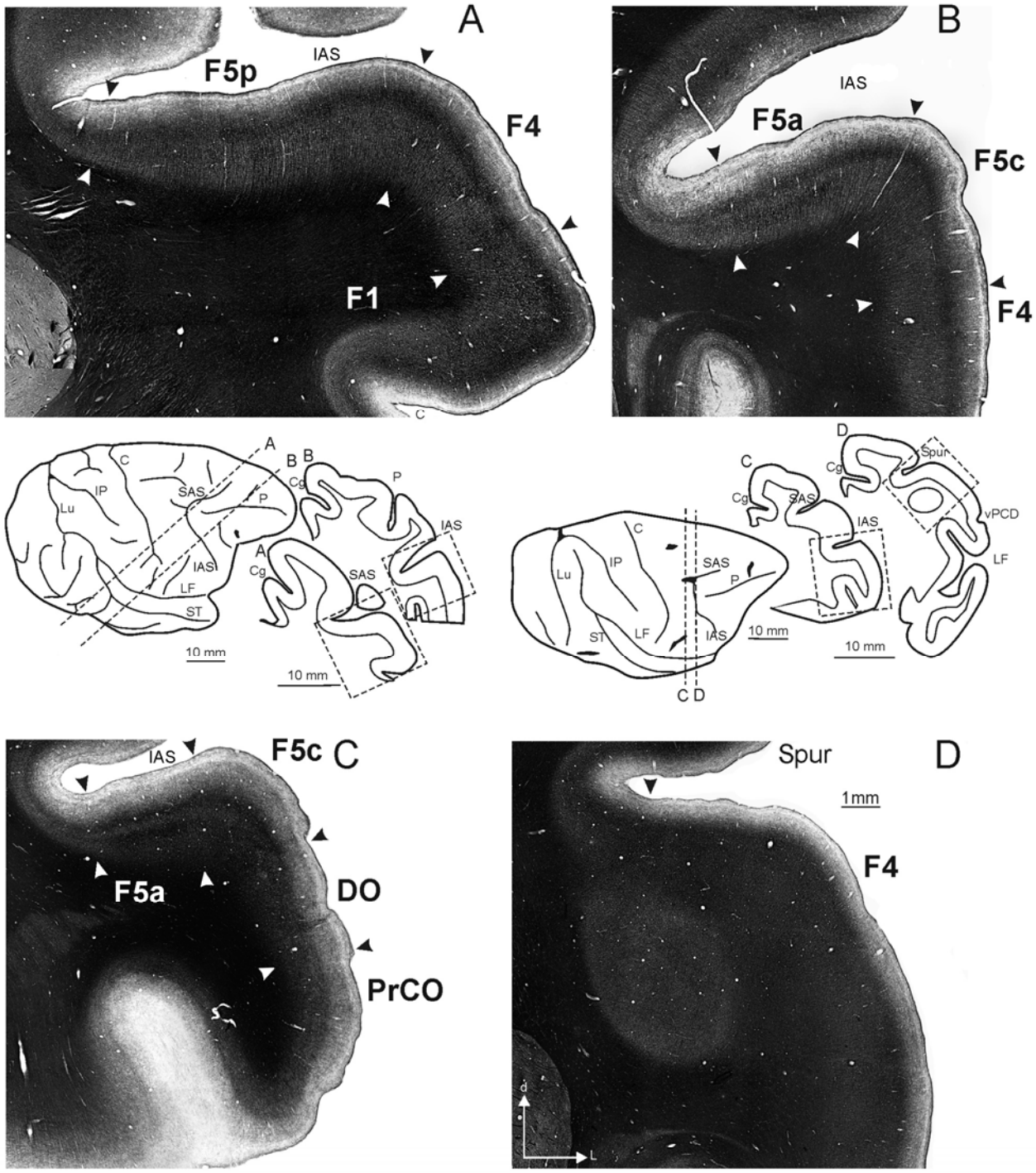

Fig. 13. Myeloarchitecture of the PMv and neighbor areas. A and B, Low-power photomicrographs of two myelin-stained perpendicular to the IAS sections, in a dorsal to ventral order, taken from Case Pr17. C and D, Low-power photomicrographs of two myelin-stained coronal sections, in rostral to caudal order, taken from Case 29l. Section orientation in D applies to all photomicrographs and section drawings. Scale bar in D applies to A-D. Arrows on the photomicrographs indicate the location of cytoarchitectonic borders reported from adjacent Nissl-stained sections. Other conventions as in Fig. 5. For *Abbreviations see the*

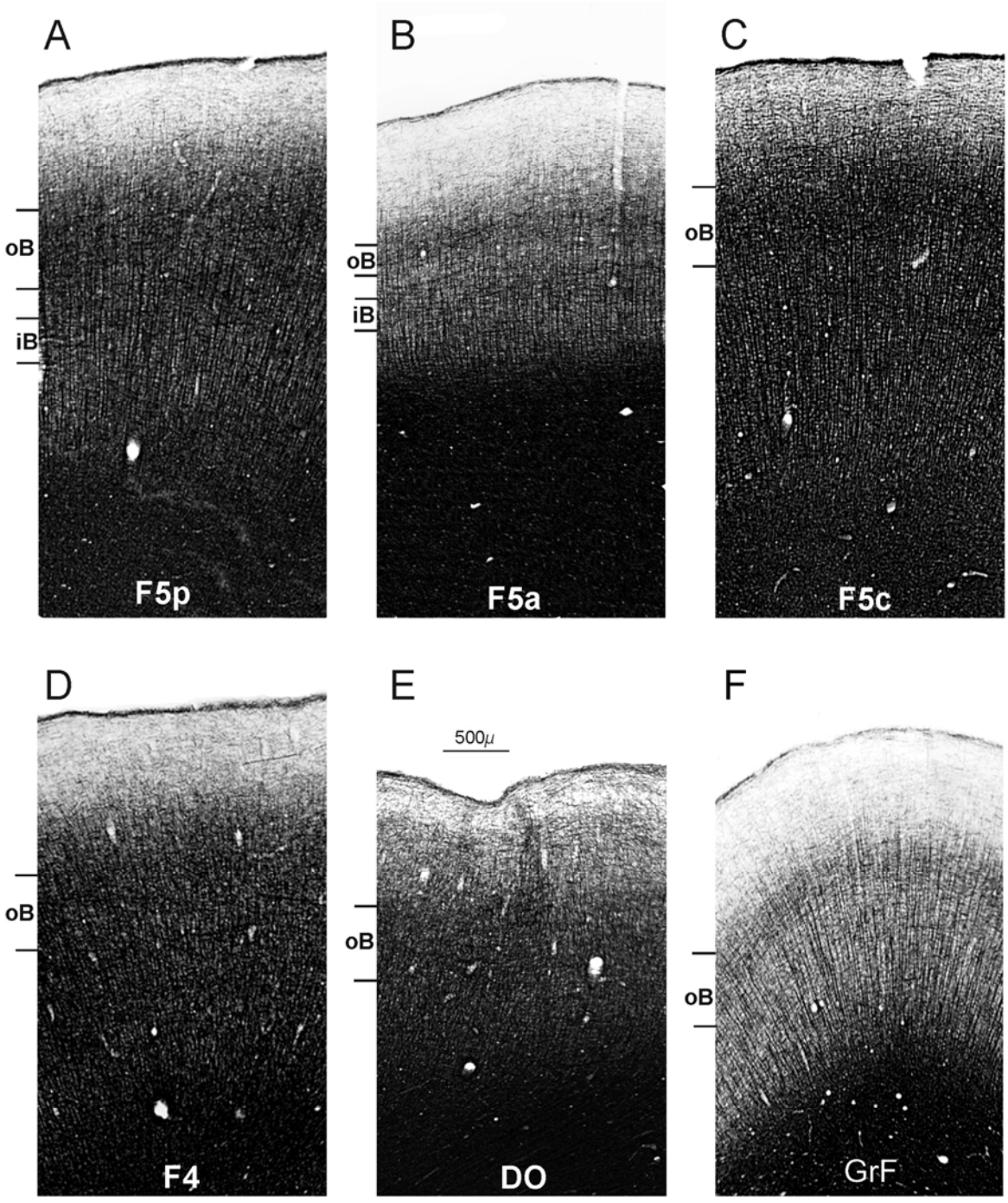

Fig. 14. Myeloarchitecture of the PMv and neighbor areas. A-F, Higher magnification views of representative myeloarchitectonic fields of areas F5p (A), F5a (B), F5c (C), F4 (D), DO (E) and GrF (F). A-C and F are taken from Case M4l. D and E are taken from Case 29l. Scale bar in E applies to A-F. For *Abbreviations see the list*.

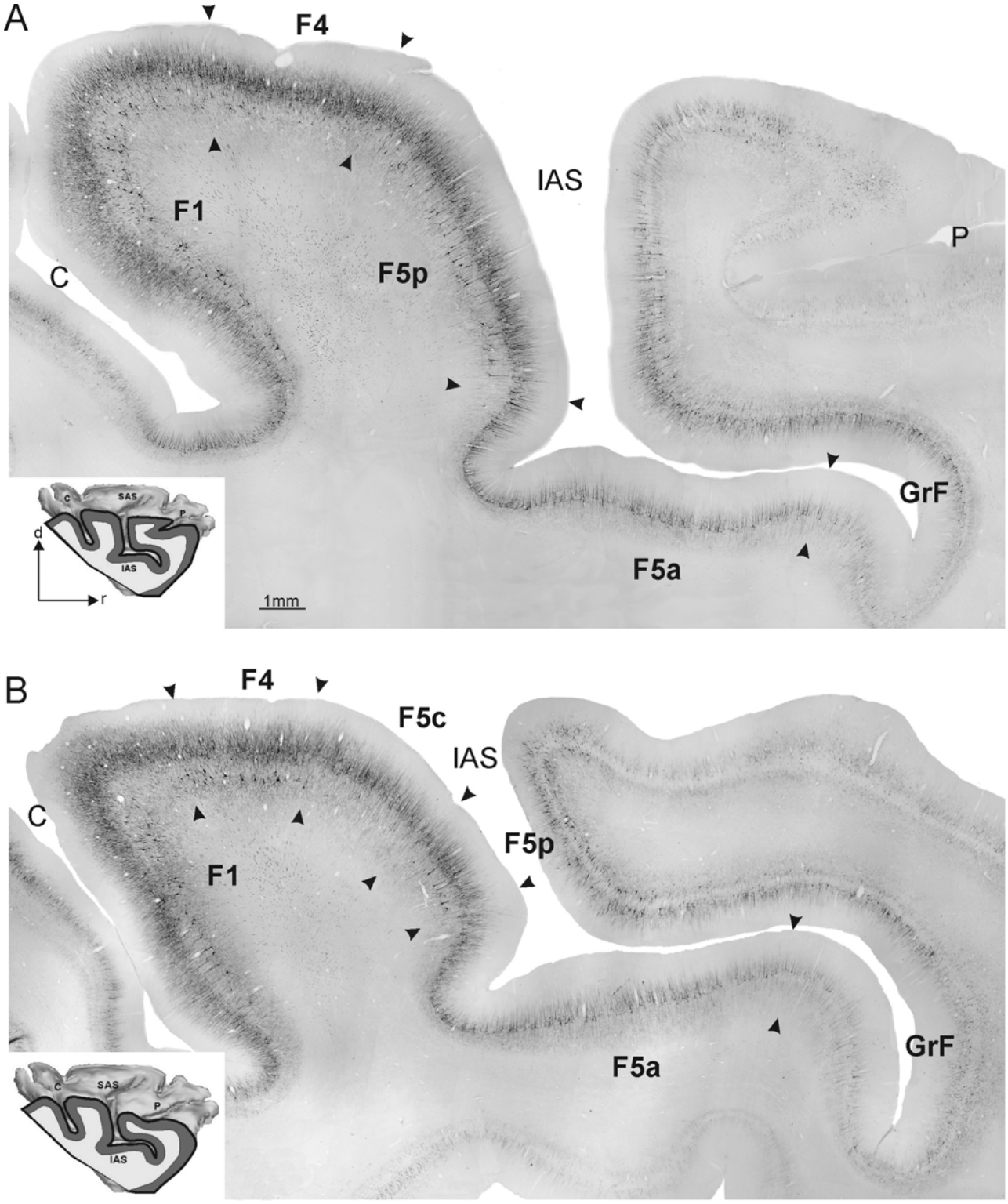

Fig. 15. Distribution of SMI-32ir in the PMv and neighbor areas. A and B, Low-power photomicrographs of SMI-32 immunostained parasagittal sections taken from Case M4l. Section orientation and scale bar in A apply also to B. Arrows on the photomicrographs indicate the location of cytoarchitectonic borders reported from adjacent Nissl-stained sections. Other conventions as in Fig. 7. For *Abbreviations see the list.*

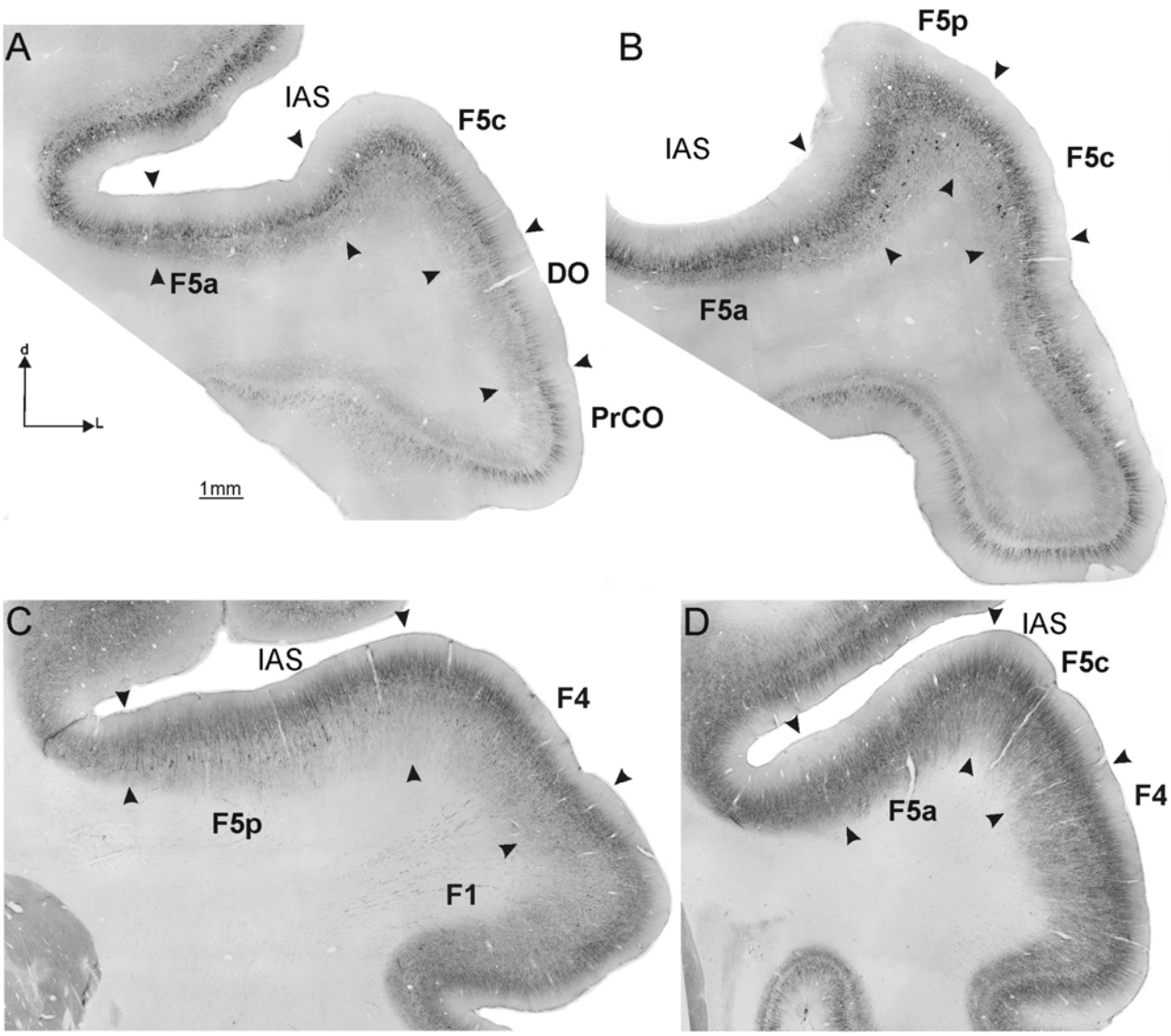

Fig. 16. Distribution of SMI-32ir in the PMv and neighbor areas. A and B, Low-power photomicrographs of SMI-32 immunostained coronal sections, in rostral to caudal order, taken from Case 18r. C and D, Low-power photomicrographs of two SMI-32 immunostained perpendicular to the IAS sections, in a dorsal to a ventral order, taken from Case Pr17. Section orientation and scale bar in A apply to all photomicrographs. Arrows on the photomicrographs indicate the location of cytoarchitectonic borders reported from adjacent Nissl-stained sections. For *Abbreviations see the list.*

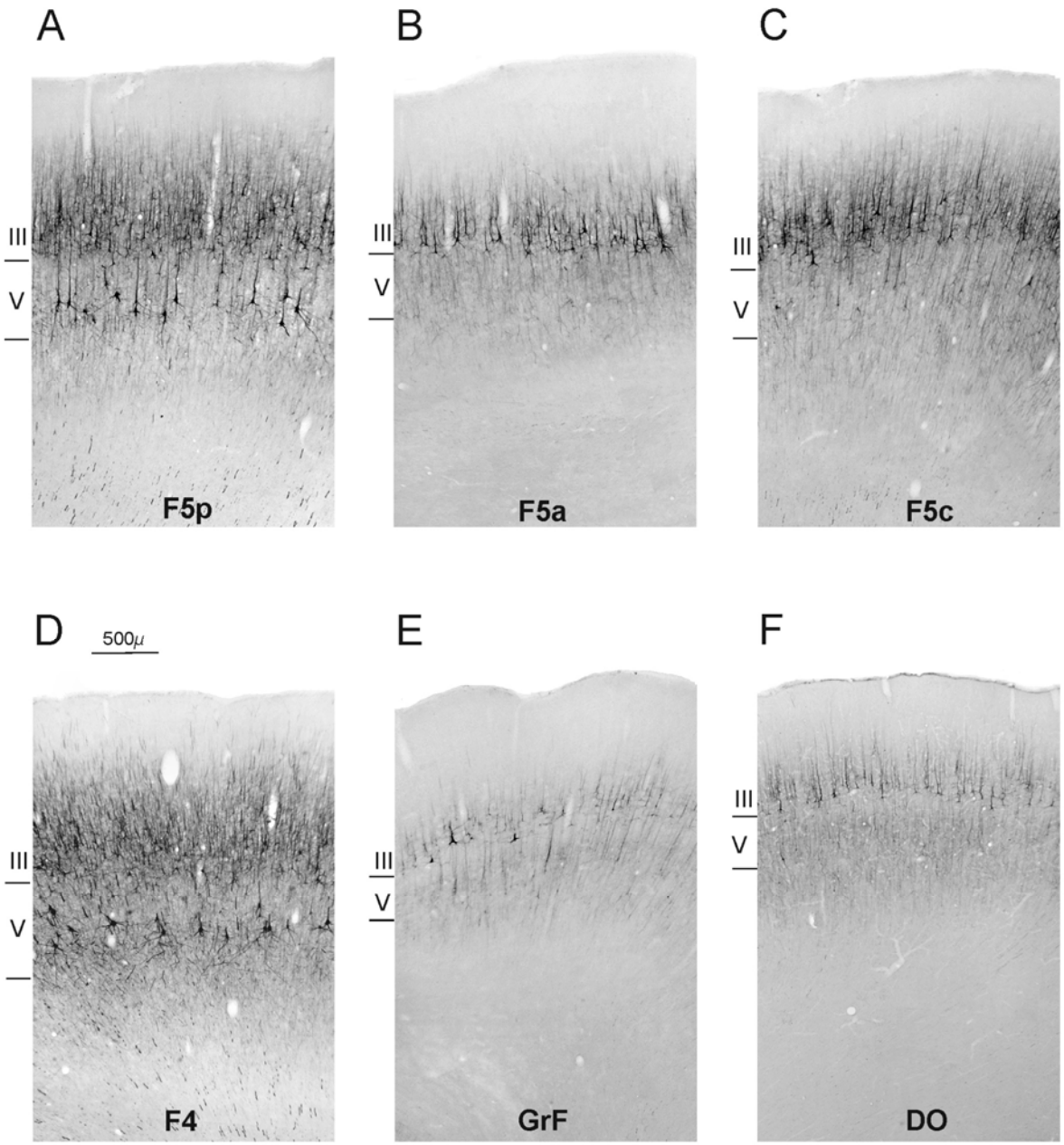

Fig. 17. Distribution of SMI-32 in the PMv and neighbor areas. A-F, higher magnification views of representative SMI-32 immunostained fields of areas F5p (a), F5a (B), F5c (C), F4 (D), GrF (E) and DO (F). All views are taken from Case M4l, but F which is taken from Case 18r. Scale bar in D applies to A-F. For *Abbreviations see the list*.

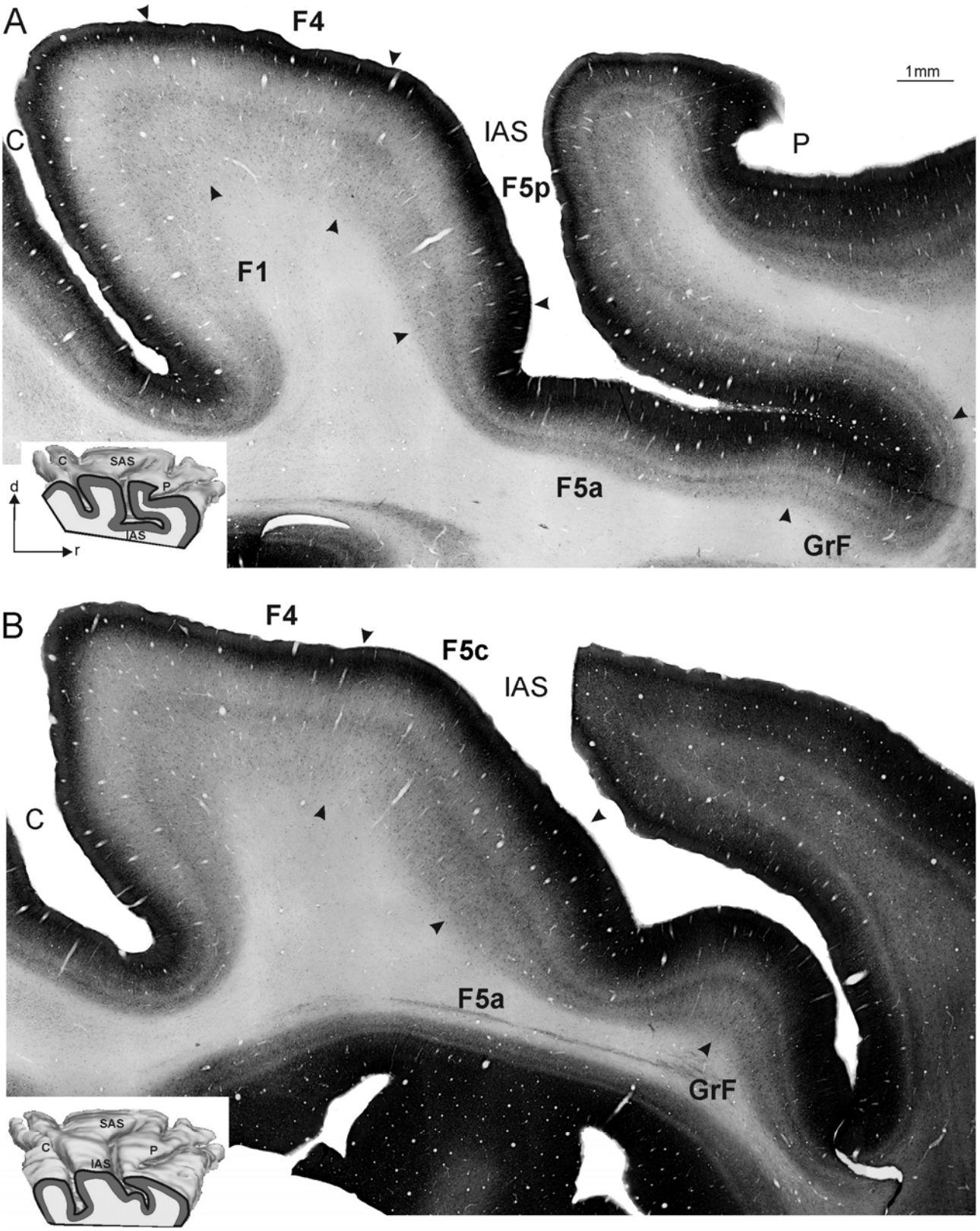

Fig. 18. Distribution of CBir in the PMv and neighbor areas. A and B, Low-power photomicrographs of CB immunostained parasagittal sections taken from Case MEF16l. Section orientation and scale bar in A apply also to B. Arrows on the photomicrographs indicate the location of cytoarchitectonic borders reported adjacent Nissl-stained sections. Other conventions as in Fig. 7. For *Abbreviations see the list*.

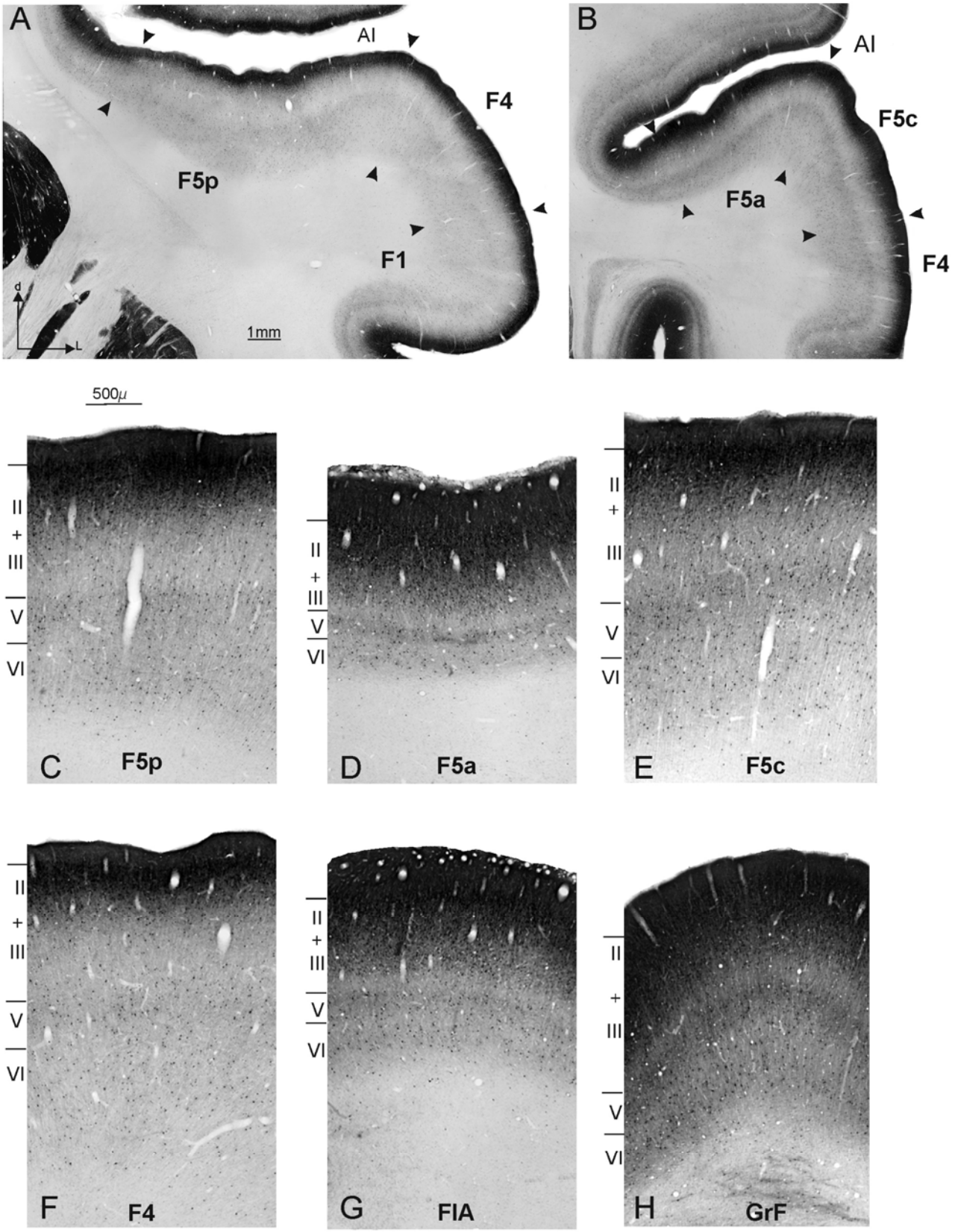

Fig. 19. Distribution of CBir in the PMv and neighbor areas. A and B, Low-power photomicrographs of CB immunostained perpendicular to the IAS, in a dorsal to a ventral order, taken from Case Pr17. Arrows on the photomicrographs indicate the location of cytoarchitectonic borders reported from adjacent Nissl-stained sections. Section orientation and scale bar in A apply also to B. C-H, Higher magnification views of representative CB immunostained fields of areas F5p (C), F5a (D), F5c (E), F4 (F), FIA (G) and GrF (H) taken from Case MEF16l. Scale bar in C applies to C-H. For *Abbreviations see the list*.

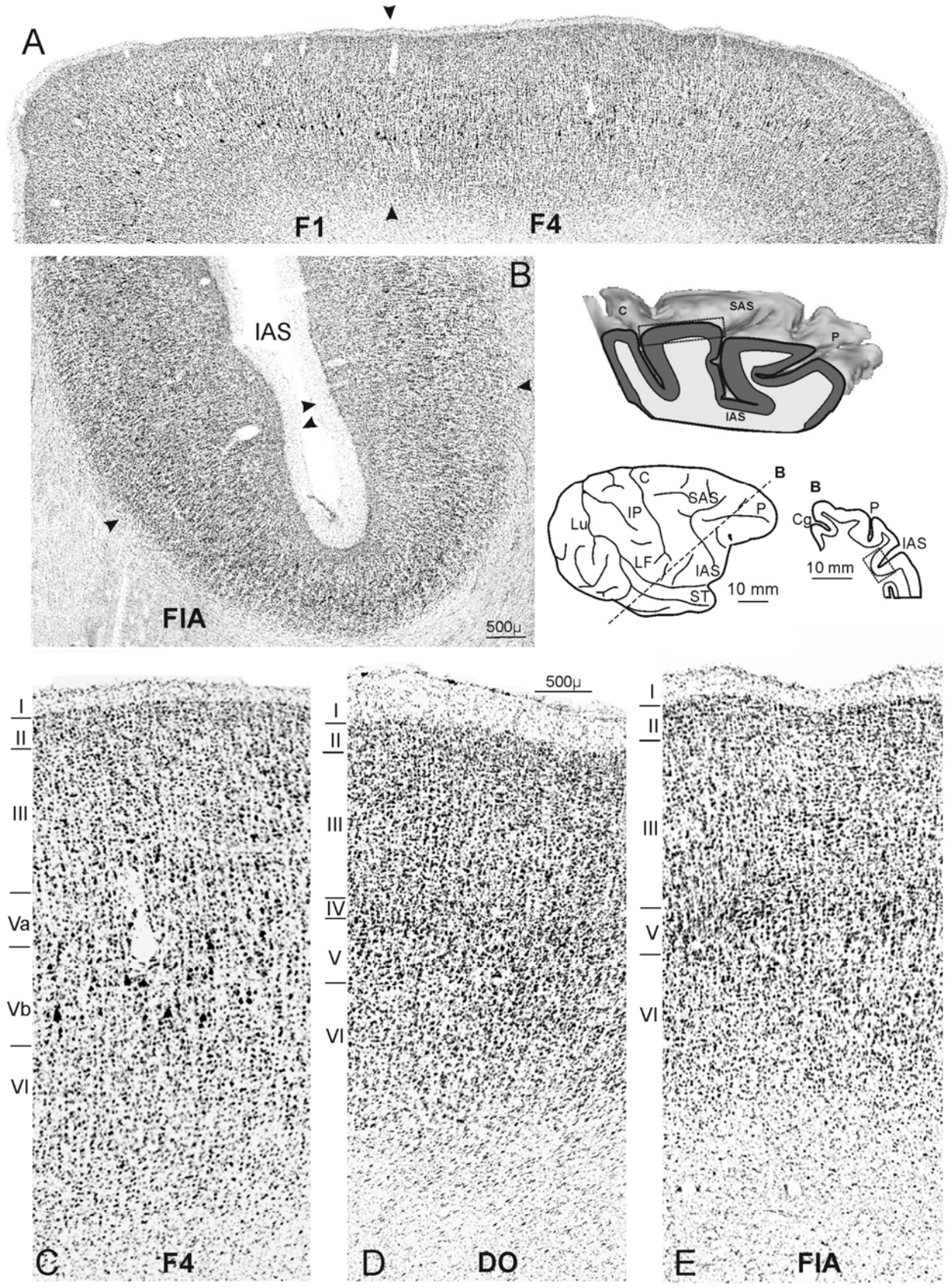

Fig. 20. Cytoarchitecture of the PMv neighbor areas. A and B, Low-power photomicrographs of Nissl-stained parasagittal and perpendicular to the IAS sections taken from Cases M3l and Pr17 respectively. Scale bar in B applies to A. C-D, Higher-power photomicrographs of representative fields of cytoarchitectonic areas F4 (C), DO (D) and FIA (E) taken from Case M3r. Scale bar in D applies to C and E. Other conventions as in Figs. 5 and 7. For *Abbreviations see the list*.

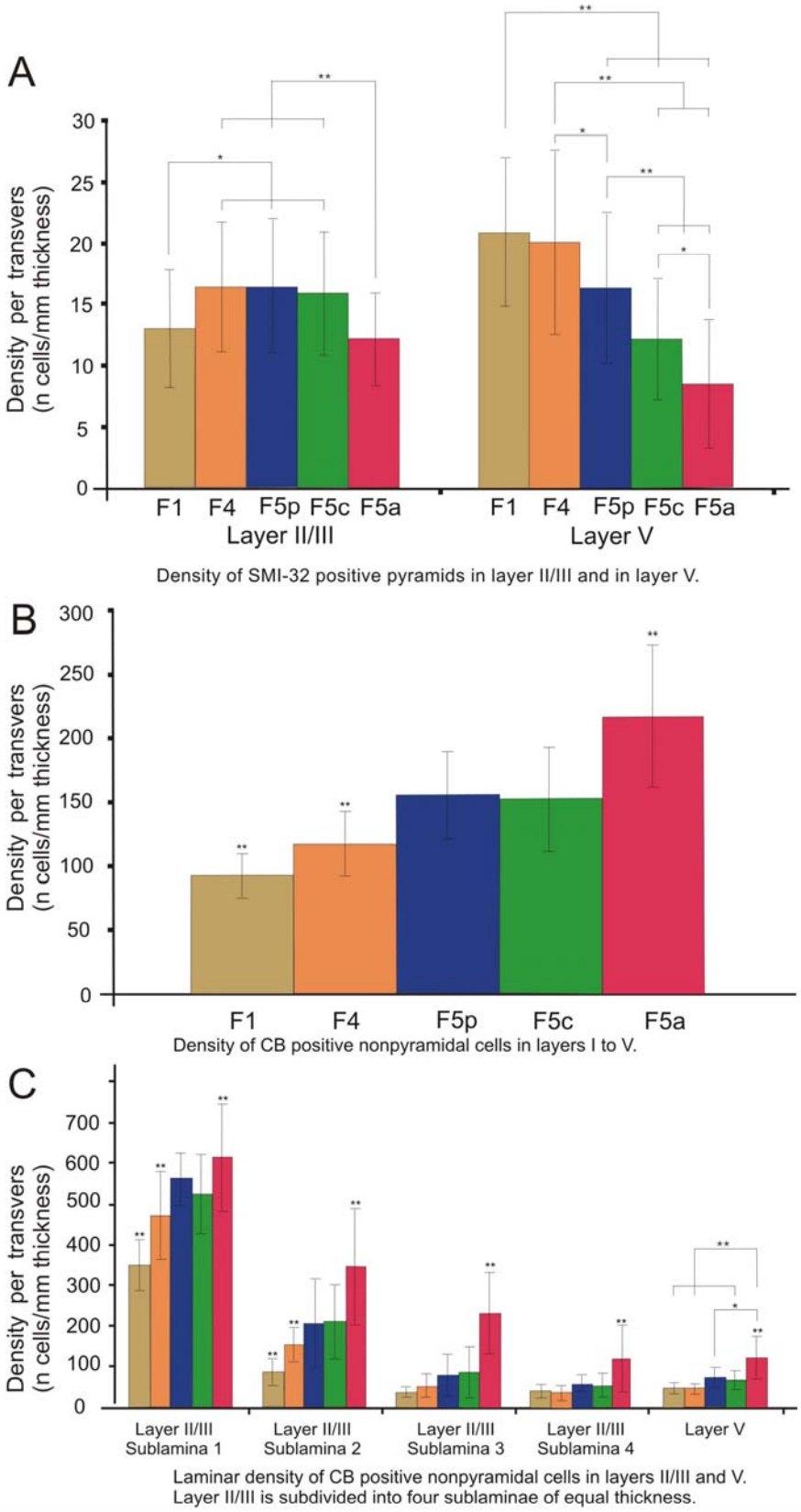

Fig. 21. Distribution of SMI-32 and CB immunoreactivity in F1, F4 , F5p, F5c and F5a. Mean (±SD) values of the density of SMI-32 immunopositive pyramids in layer II/III and layer V (A), the density of CB immunopositive nonpyramidal cells in layers I-V(B) and neurons and laminar density of CB immunopositive nonpyramidal cells (C), expressed in terms of number of cells/mm thickness. Data are from 3 animals (MEF16l, M3l, and Pr17r). The values are referred to a total number of 40 transverses from each hemisphere and a total number of 24 transverses (8 transverses per case) for each area. Statistics: ANOVA for repeated measures followed by post hoc Bonferroni corrections for multiple comparisons.** significance level of $p < 0.01$,* significance level of $p < 0.05$.

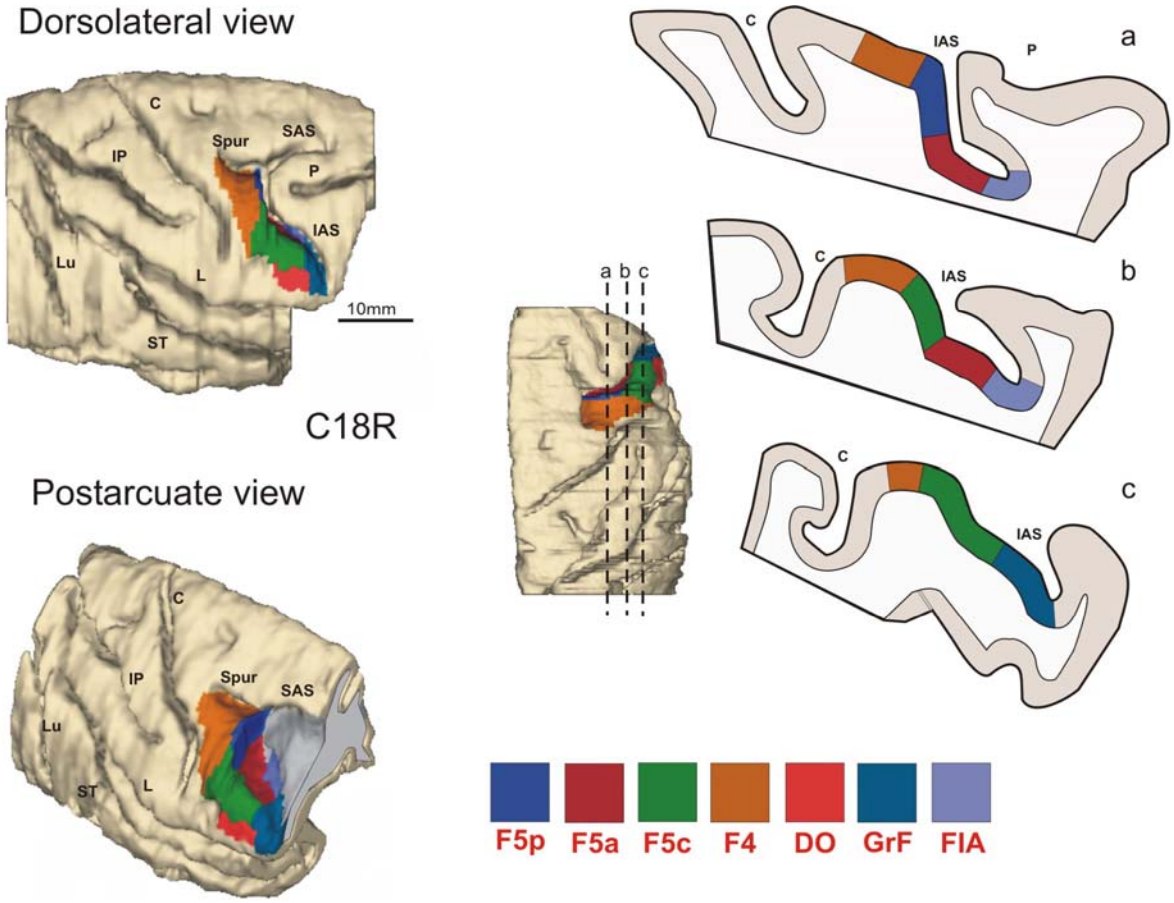

Fig. 22. Location and extent of the ventral premotor areas identified in this study. On *the left of the figure* are represented the 3D reconstruction of the right hemisphere from C18r, shown in dorsolateral and postarcuate views. In the postarcuate view, the posterior bank of the IAS was exposed with dissection of the 3D reconstruction along its fundus. On *the right of the figure,* a-c, parasagittal re-slicings taken from C18r, from the medial to the lateral level show in different colors the PMv and neighbor areas. The levels at which the re-slicings were made, are represented in the middle of the figure in a dorsal view of the hemisphere. In *the bottom of the figure,* the legend represents the name and the corresponding color of each area. For *Abbreviations see the list.*

2. Cortico-cortical connections of F5p, F5a and F5c

As shown in the previous section, the rostral PMv area F5 is not an homogeneous area, but can be subdivided, architectonically, into three areas: F5a, F5c and F5p. Both F5a and F5p are located in the posterior bank of the IAS, F5c lies caudally on the adjacent convexity. Each of these three premotor areas was a target of multiple neural tracers injection. The histological analysis allowed us to attribute the injection site to the targeted area and only the cases in which the injection sites were restricted within the limits of a single architectonic area will be presented.

Our results showed that the three premotor areas are reciprocally connected, but each one displayed differential connections with frontal and parietal areas, giving an additional anatomical support to our architectonical parcellation of the PMv area F5.

2.1. Connections of area F5p

Area F5p was injected in three cases (C14l, C31r, C31l, C35r) with retrograde (FB), anterograde (BDA) and retro-anterograde (WGA-HRP, FR) tracers.

The distribution of the labeling was very similar across cases. The intensity of the labeling varied, however, from one case to another. Likely because of differences in tracers sensitivity.

The cortical connections of area F5p are shown in figures 23, 24 and 25, in which the distribution of the labeling is represented in mesial and lateral views of the injected hemisphere, in representative coronal sections (Fig. 23) and in 2D reconstruction of the parietal operculum (Fig. 25).

The results showed that F5p displays strong connections with area F1. These connections involved the hand-related field (Fig. 23, 3D reconstruction lateral view, section e). This finding was confirmed by our tracer injections made in F1 (C21r), in which the hand-related field was identified with intracortical microstimualtion before the injection (Fig. 24). In both FB and MR injections made in C21r, we observed that the connections of F1 with the PMv involved the posterior bank of the IAS, mainly its posterior sector which corresponds to F5p. Very few labeling was observed also with its anterior sector (Fig. 24, 3D reconstruction views, a and b parasagittal sections).

F5p was strongly connected, with the arm-related premotor field of the adjacent area F4 (Gentilucci et al., 1988; Graziano et al., 1994; Fogassi et al., 1996), (Fig. 23, 3D reconstruction lateral view,

section d). F5p was also connected with the PMd area F2, mainly with its ventral rosral sector (Fig. 23, 3D reconstruction lateral view, sections c and d) where the distal arm movements are represented (Raos et al., 2003). Connections with the mesial areas F6 (Pre-SMA) and F3 (SMA proper) and cingulate areas 24d and 24c (Luppino at al., 1991, 1993) were also observed (Fig. 23, 3D reconstruction mesial view). Weak connections with the prefrontal cortex involving the caudal sector of area 46v as defined by Preuss and Goldman-Rakic (1991) were seen as well (Fig. 23, 3D reconstruction lateral view, section a).

F5p received parietal afferents mainly from the IPL areas PF and PFG (Gregoriou et al., 2006; Rozzi et al., 2006). These connections were relatively more dense with PF than with PFG. Few labeling with area PG was observed as well (Fig. 23, 3D reconstruction lateral view, sections f-h). F5p was also connected with the intraparietal areas AIP (Fig. 23, sections f and g) and PEip (Fig. 23, section h), (Borra et al., 2007). F5p was a target of projections from the SII region. Comparison with data from Krubitzer et al. (1995) and Fitzgerald et al. (2004), suggests that these projections involved mostly the hand field of SII (Fig. 23, sections f and g; Fig. 25).

Finally, our HRP injection in the lateral funiculus, at C4-C5 spinal cord level, showed that while the PMd contains a dense population of corticospinal neurons (Fig. 26 A, 3D reconstruction views), the PMv was devoid of labeling except for a sector of the posterior bank of the IAS which showed a patch of labeled neurons (Fig. 26, Postracuate view, sections a and b). This sector corresponds very well to area F5p. This last finding was confirmed by our FR injection in F5p (C31L) which showed that fibres and terminals targeting the ventral most part of lamina VII were seen in all cervical segments. Terminals were very dense in the upper cervical segments (C2-C4) weakly dense in the lower cervical segments (C7-C8) which are involved in the forelimb distal muscles (Fig. 26B), (See Kuypers, 1981).

2.2. Connections of area F5a

Area F5a was injected in three cases (C30r, C30l, c34l and C35l) with retrograde (DY), anterograde (BDA) and retro-anterograde (WGA-HRP) tracers.

Representative cortical connections of area F5c taken from cases C34I-BDA and C35I-DY are shown in figures 25, 27, 28 and 29. The distribution of labeled neurons is represented in mesial, lateral and orbital views of the injected hemisphere and in representative coronal sections (Figs. 27, 28). Labeled neurons in the parietal operculum are shown in 2D reconstruction (Figs. 25, 29).

Our data showed that F5a connections with the motor area F1 were almost absent (Fig. 27, 3D reconstruction lateral view). F5a, however, displayed relatively strong connections with the PMv area F4 (Gentilucci et al., 1988; Graziano et al., 1994; Fogassi et al., 1996), (Fig. 27, 3D reconstruction-lateral view, section g). F5a was also connected with area F6 (Pre-SMA) and cingulate areas, 24c, 24d and 24a (Luppino et al., 1991, 1993), (Fig. 27, 3D reconstruction mesial view, sections d, e and f; Fig. 28, 3D reconstruction mesial view, sections e and f). Strong connections were observed with the GrF area, rostral frontal opercular areas and PrCO (Robert and Akert, 1963), (Fig. 27, 3D reconstruction lateral view, sections e and f; Fig. 28, 3D reconstruction lateral view, section f). Relatively robust prefrontal connections were observed with rostral area 46v as defined by Preuss and Goldman-Rakic (1991), (Fig. 27, 3D reconstruction lateral view, sections b-d; Fig. 28, 3D reconstruction, sections c and d) and areas 12r and 12l as defined by Carmichael and Price (1995), (Fig. 27, 3D reconstruction lateral view, sections a-e; Fig. 28, 3D reconstruction lateral view, sections a, b and e).

Area F5a displayed strong parietal connections with mostly the IPL area PF. Connections with area PFG were less dense than those with PF. Weak connections involved area PG as well (Gregoriou et al 2006; Rozzi et al., 2006), (Fig. 27, 3D reconstruction lateral view, sections i and j; Fig. 28, sections i-m). Relatively strong labeling involved also the intraparietal area AIP (Borra et al., 2007), (Fig. 27, sections i and j).

F5a was strongly connected with the SII/PV complex as defined by Krubitzer el al. (1995) and Disbrow et al. (2003). These connections involved mostly the hand representations (Fig. 27 section h, Fig. 28, sections I and j, Figs. 25 and 29).

2.3. Connections of area F5c

Area F5c was injected in four cases (C25r, C33l, C35l and C36l) with retrograde (FB, CTB-A 594) and retro-anterograde (WGA-HRP) tracers.

Representative cortical connections of area F5c taken from cases (C33l-FB and C35l-FB) are shown in figures 25, 28, 29 and 30. The distribution of labeled neurons is represented in mesial, lateral and orbital views of the injected hemisphere and in representative coronal sections (Figs. 28, 29) and the distribution of the labeled neurons in the parietal operculum in 2D reconstruction (Figs. 25, 30).

Some variability was observed across cases as for connections of F5c with F1. In fact, these connections were almost absent in C33l-FB (Fig. 30, 3D reconstruction lateral view), while they involved the face/mouth related field of F1 in C35l-FB (Fig. 28, 3D reconstruction lateral view, section i). F5c was strongly connected with area F4, mostly with face/mouth related field (Gentilucci et al., 1988; Graziano et al., 1994; Fogassi et al., 1996), (Fig. 28, 3D reconstruction lateral view and section h; Fig. 30, 3D reconstruction and section g). Relatively strong connections were also observed with area F3 mostly involving its face/mouth field (Luppino et al., 1991, 1993), (Fig. 28, 3D reconstruction mesial view and section g; Fig. 30, 3D reconstruction mesial view and section f). The cingulate connections of area F5c involved areas 24c and 24a.

F5c was connected with the caudal frontal opercular areas (Fig. 30, 3D reconstruction lateral view and section g). These connections were relatively stronger in C33l.

Prefrontal connections were relatively robust and involved a more rostral sector of area 46v (Preuss and Goldman-Rakic, 1991), (Fig. 28, 3D reconstruction lateral view and section c; Fig. 30, 3D reconstruction, sections b-d) and area 12r (Carmichael and Price., 1995), (Fig. 28, 3D reconstructions, sections a and b; Fig. 30, 3D reconstruction lateral view, sections a-c).

F5c received strong afferents from the IPL area PF (Fig. 28, section j). Furthermore, Connections were observed also with area PFG (Fig. 28, section k) and the intraparietal area AIP (Gregoriou et al 2006; Rozzi et al., 2006; Borra et al., 2007), (Fig. 28, sections j and m),

Connections with SII and PV involved mostly face/mouth representations (Krubitzer et al., 1995; Disbrow et al., 2003; Fitzgerald et al., 2004), (Figs. 25; 28-sections I and j, 29, 30-sections h and i).

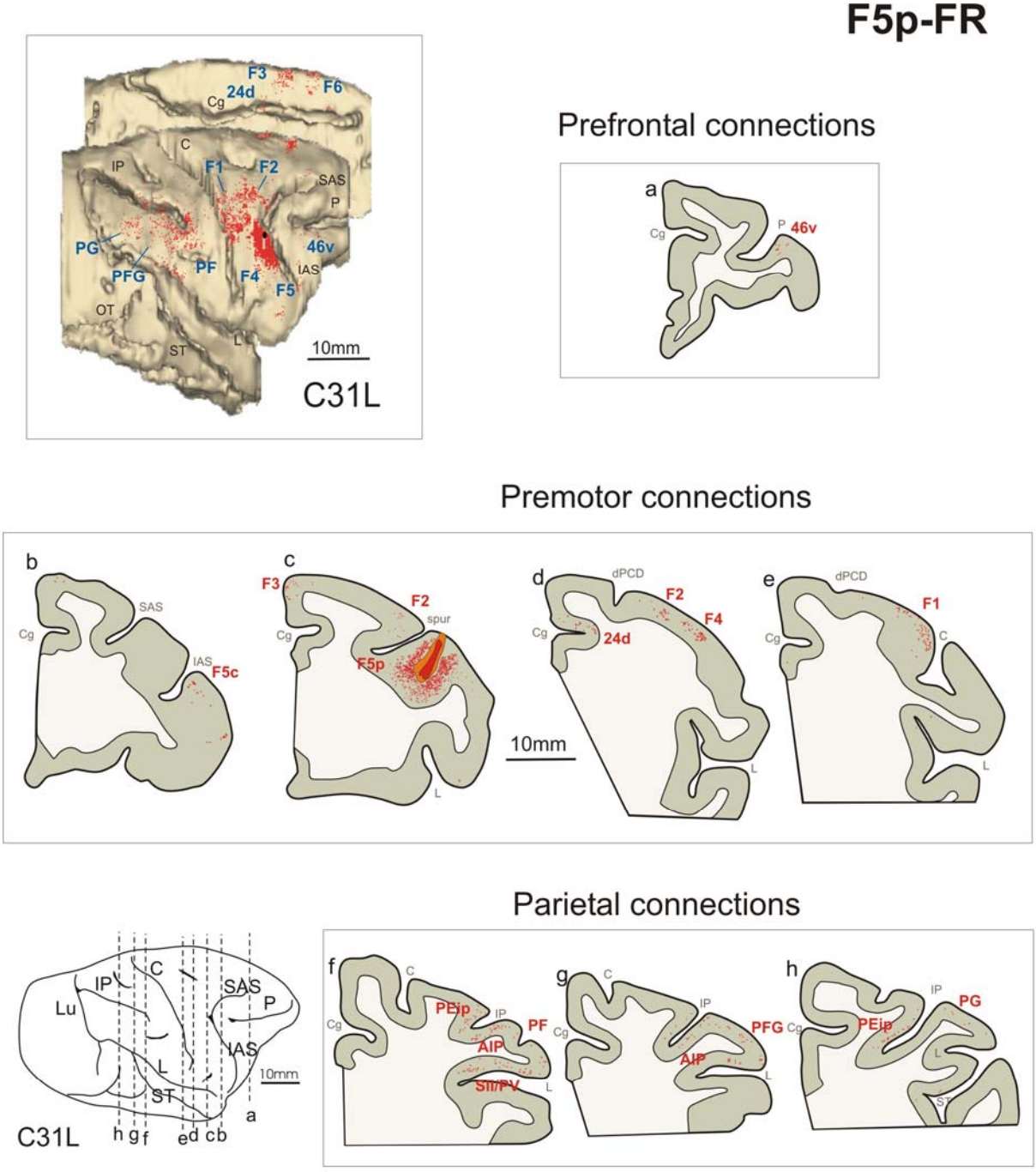

Fig. 23. Distribution of retrograde labeling following the FR injection in F5p. *Upper left part of the figure,* 3D reconstruction of the injected hemisphere showing the labeled neurons on mesial and lateral brain views. The black dot marks the injection site. a-h, drawings of selected coronal sections showing the labeled neurons in the different cortical areas.The core of the injection and the surrounding halo are colored in red in section c. The levels at wich the sections were taken are indicated in the *lower left part of the figure*. For *Abbreviations see the list*.

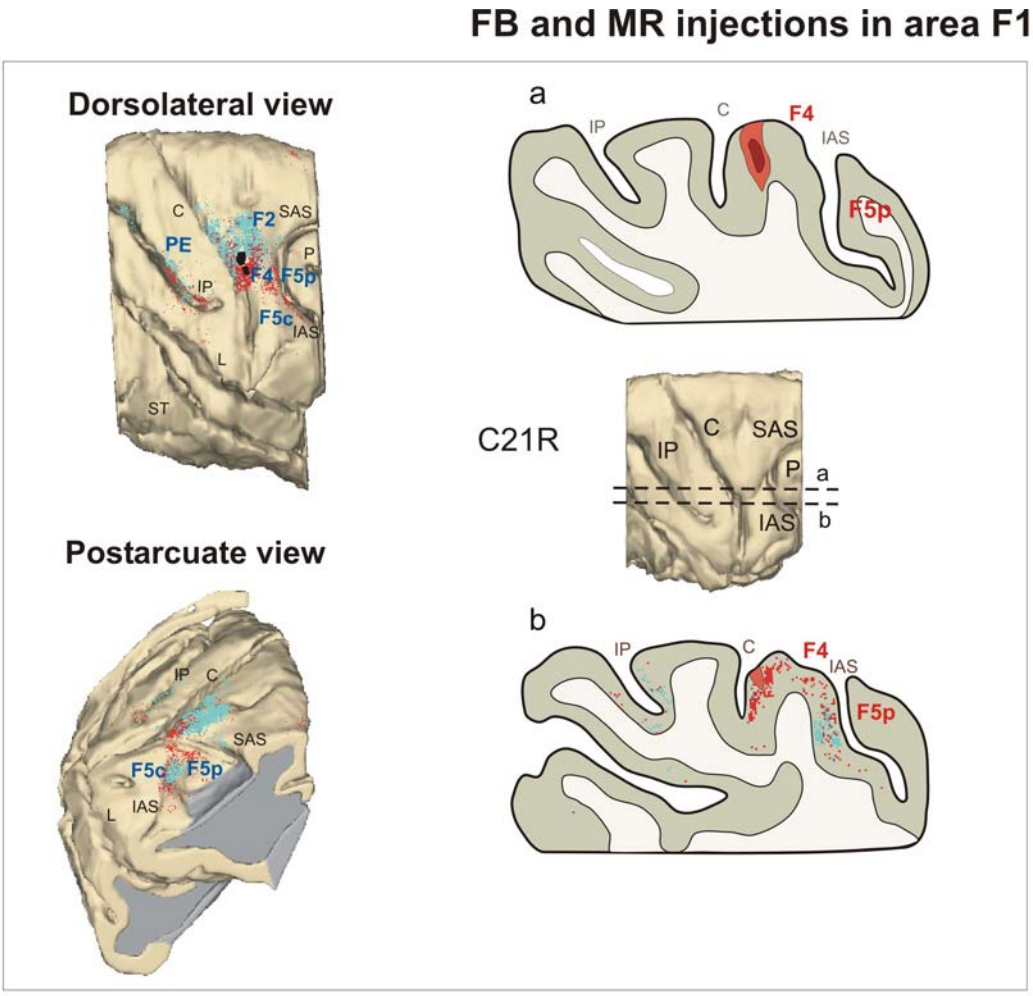

Fig. 24. Distribution of retrograde labeling following the FB (In blue) and MR (In red) injections in the hand field of F1. On *the left part of the figure*, the 3D reconstructions of the injected hemisphere showing the distribution of the labeled neurons in dorsolateral and postarcuate views. On *the right part of the figure*, are represented parasagittal brain re-slicings showing retrogradely labeled neurons, and the levels at which the re-slicings were made. *For Abbreviations see the list.*

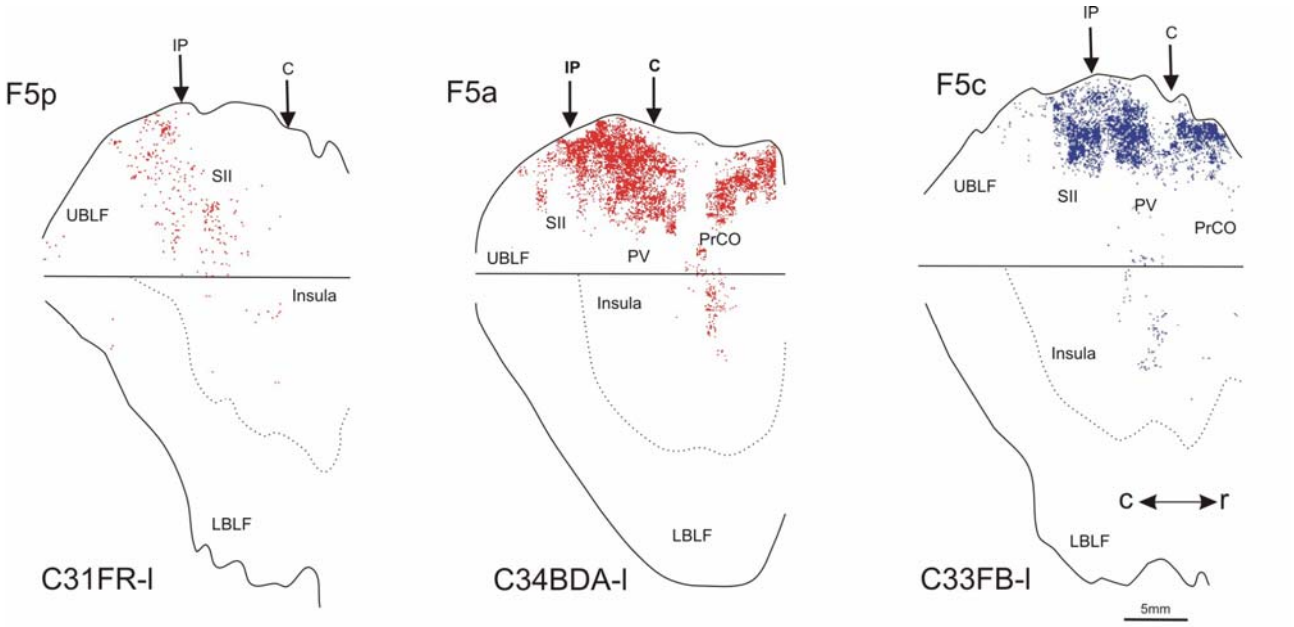

Fig. 25. Cortical connections of areas F5p, F5a and F5c with the parietal operculum. The distribution of the labeling is shown in 2D reconstruction of the LF and of the insula, aligned in correspondence with the fundus of the upper bank of the sulcus indicated by a straight line. The continous curved lines mark the lip of the upper and lower banks of the LF. The curved dotted line marks the border between the insula and the inferior bank of the LF. Rostral is on the right. Arrows mark the central (C) and intraperietal sulci (IP) . Scale and orientation bars shown for C 33 apply to C34BDA and C31FR. *For Abbreviations see the list*.

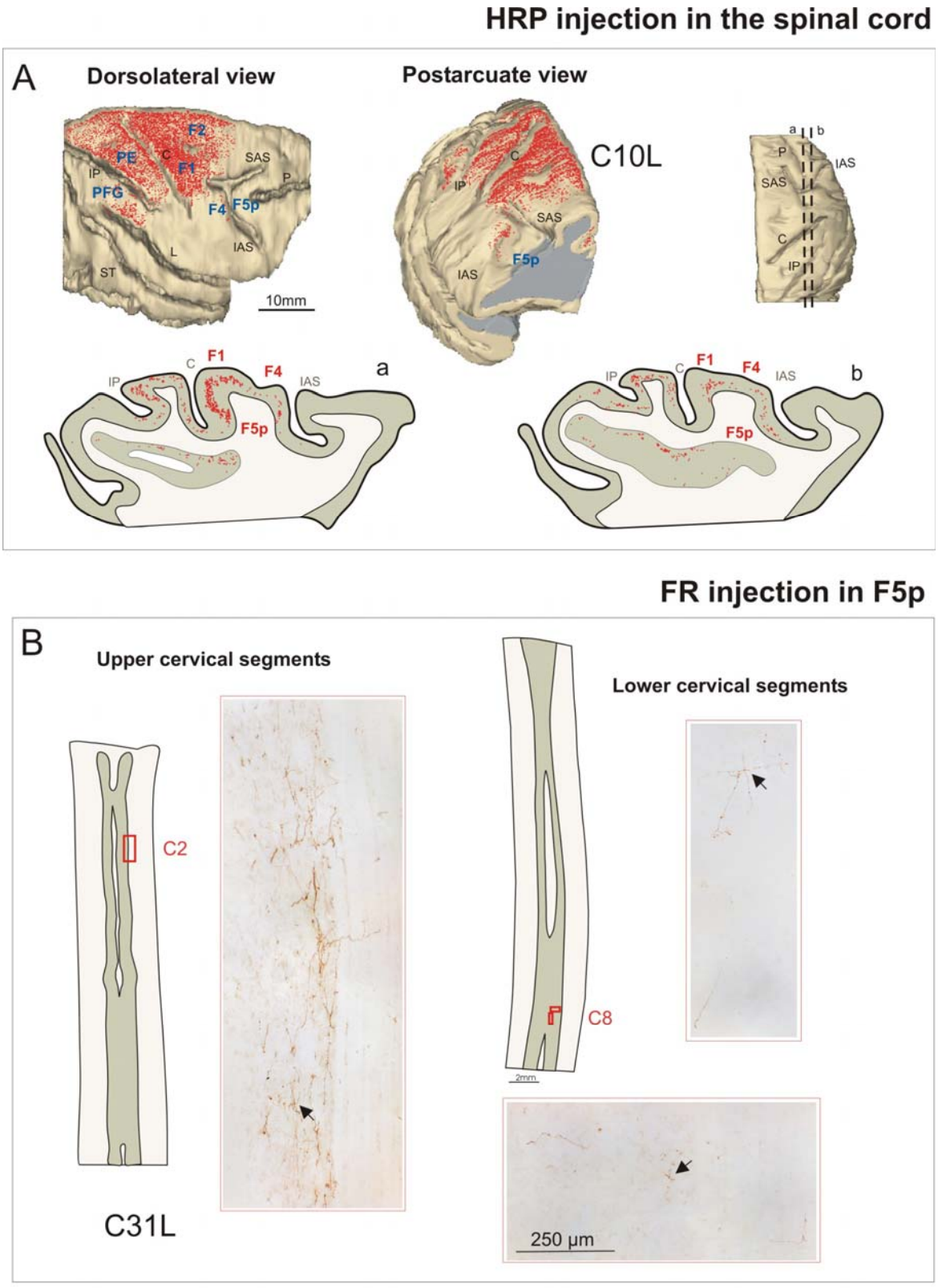

Fig. 26. Corticospinal efferents of area F5p. A-Distribution of retrogradely labeled corticospinal neurons observed following HRP injections in the lateral funiculus of the spinal cord at the upper cervical levels shown in dorsolateral and postarcuate views of the hemisphere controlateral to the injections. a and b, parasagittal brain re-slicings showing retrogradely labeled neurons taken from medial to lateral order. In *the upper right part of the figure* are indicated the levels at which the re-slicings were made. B- The photomicrographs show corticospinal fibers (indicated with black arrows) in the lower (on *the right*) and the upper (on *the left)* cervical segments, originating from area F5p after FR injection. Drawings show the segmental levels at which the photomicrographs were taken. *For Abbreviations see the list*.

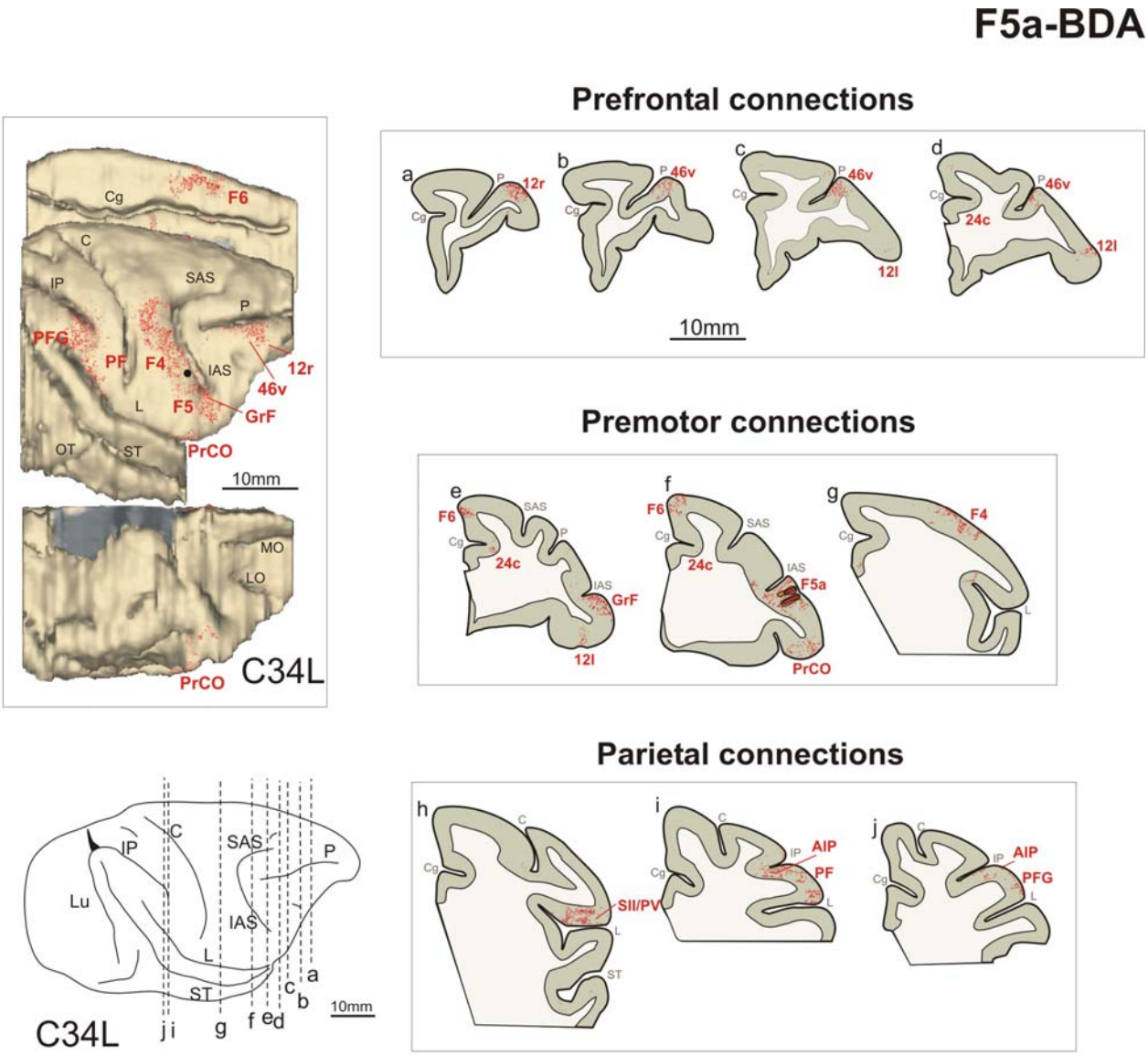

Fig. 27. Distribution of anterograde labeling following the BDA injection in F5a. *Upper left part of the figure,* 3D reconstruction of the distribution of the anterograde labeling shown on mesial, lateral and orbital brain views. The black dot marks the injection site. a-j, drawings of selected coronal sections showing the labeled fibers in the different cortical areas. The core of the injection and the surrounding halo are colored in red in section f. The levels at wich the sections were taken are indicated in the *lower left part of the figure*. *For Abbreviations see the list*.

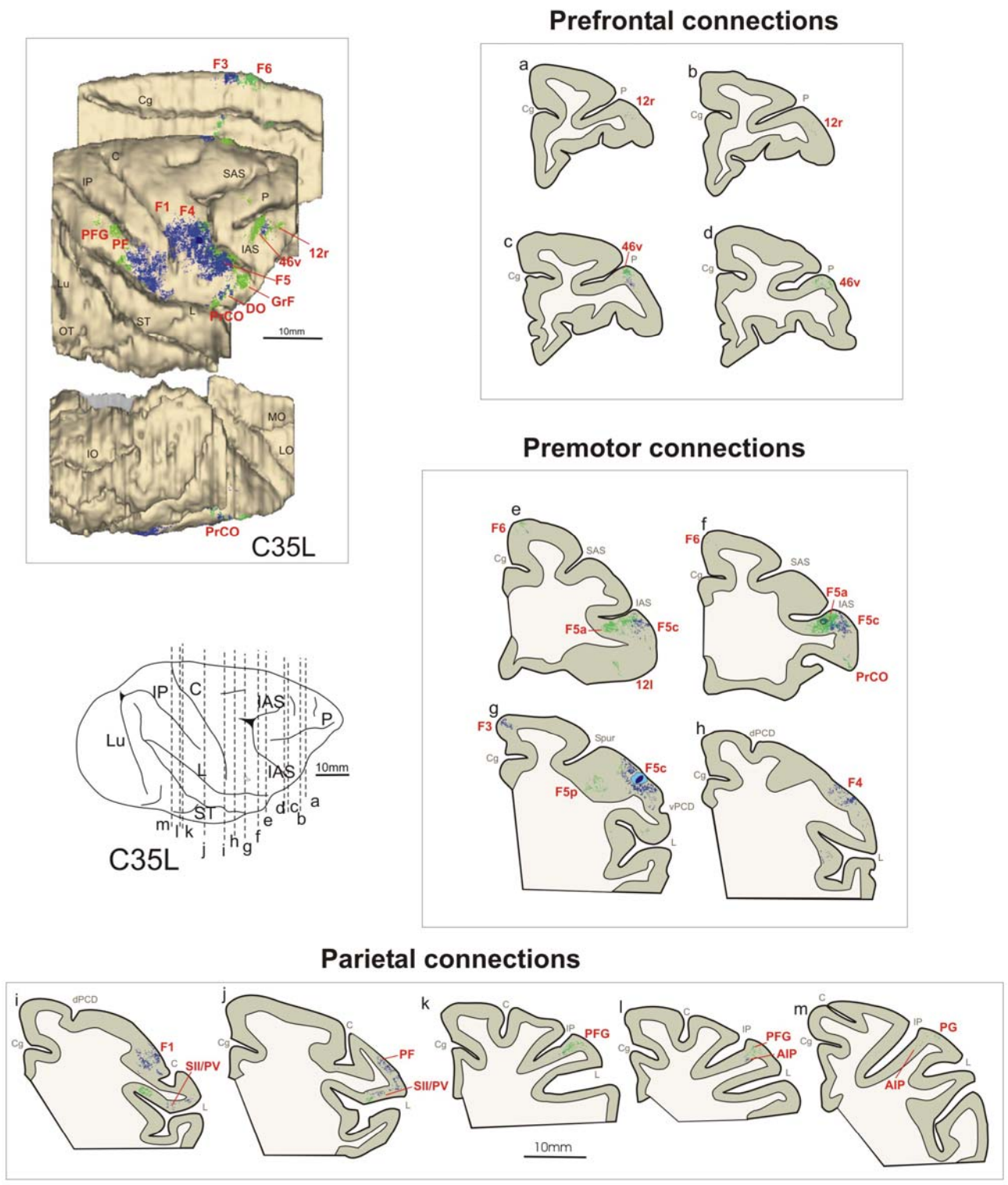

Fig. 28. Distribution of retrograde labeling following the FB and DY injections in F5c and F5a respectively. *Upper left part of the figure,* 3D reconstruction of the distribution of the retrograde labeled neurons (FB in blue and DY in green) shown on mesial, lateral and orbital brain views. a-m, drawings of selected coronal sections showing the labeled neurons in the different cortical areas.The core of the injection and the surrounding halo are colored in blue for the FB (section g) and in green for the DY section f). The levels at which the sections were taken are indicated in *the lower left part of the figure*. *For Abbreviations see the list*.

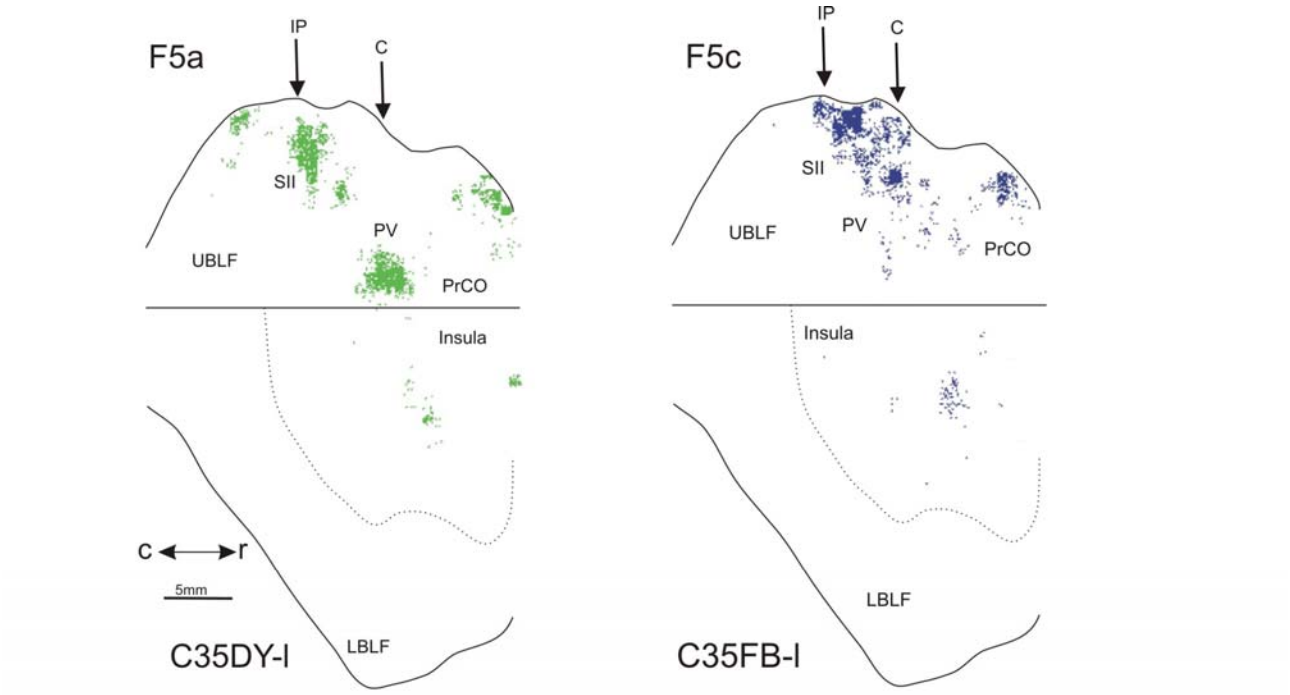

Fig. 29. Cortical connections of areas F5a and F5c with the parietal operculum. The distribution of the labeling is shown in 2D reconstruction of the LF and of the insula. Scale and orientation bars in C35 apply to C35. Conventions are like in Fig. 25. For *Abbreviations see the list*.

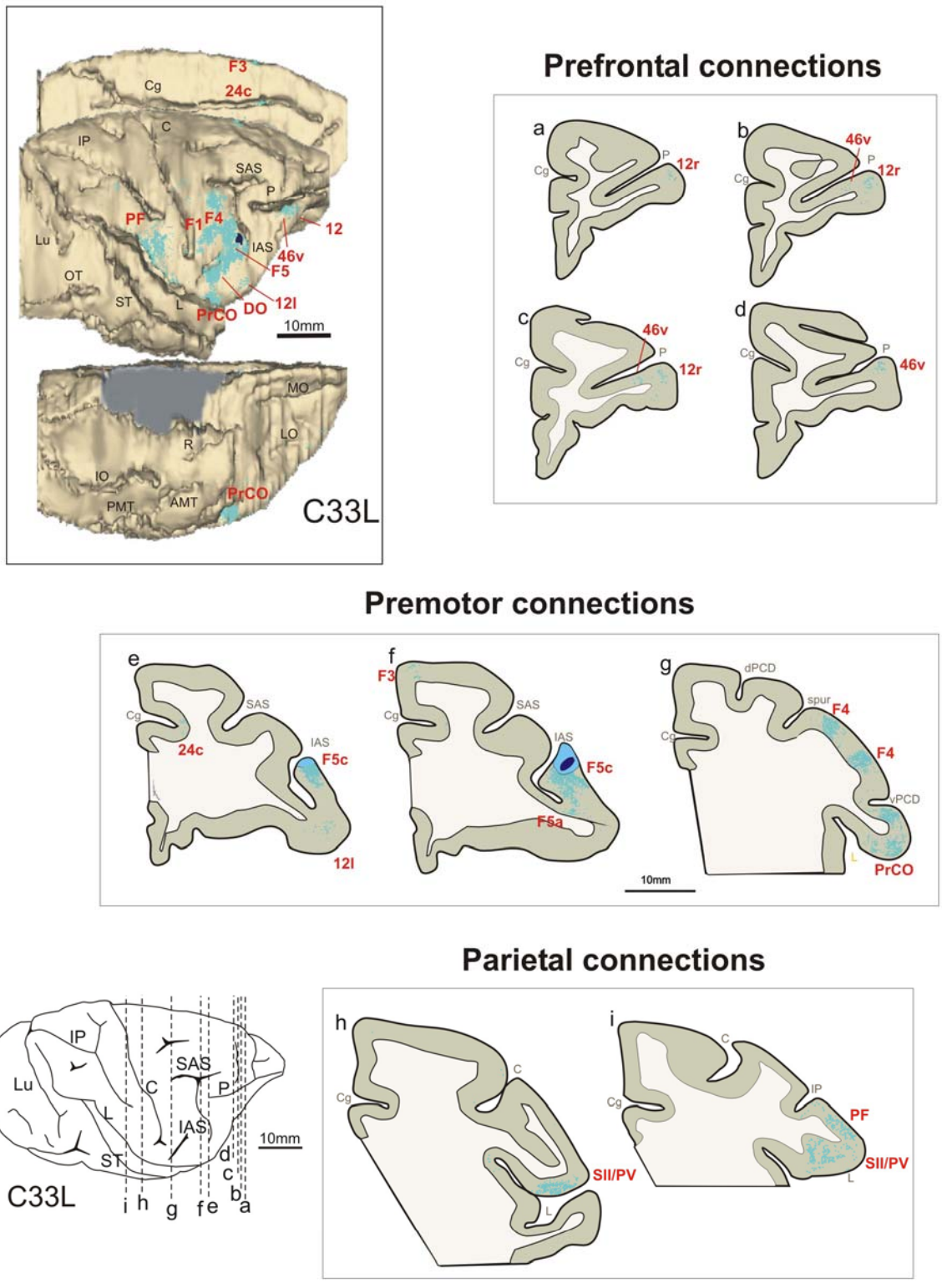

Fig. 30. Distribution of retrograde labeling following the FB injection in F5c. *Upper left part of the figure,* 3D reconstruction of the distribution of the retrograde labeled neurons shown on mesial, lateral and orbital brain views. The black dot marks the injection site. a-i drawings of selected coronal sections showing the labeled neurons in the different cortical areas.The core of the injection and the surrounding halo are colored in blue. The levels at which the sections were taken are indicated in *the lower left part of the figure*. *For Abbreviations see the list*.

D-Discussion

D-Discussion

In the present study we have provided a detailed description of the anatomical organization of the macaque rostral PMv area F5, using a combination of both, architectonics and hodological approaches. The major finding of our study is that area F5, as defined with cytochrome oxidase histochemistry (Matelli et al., 1985), consists of three anatomically distinct areas. One of these areas -F5c- extends on most of the postarcuate convexity cortex immediately adjacent to the IAS. The other two areas -F5p and F5a- lie within the postarcuate bank at different antero-posterior levels. F5c and F5p border caudally with an architectonic area distinct from the precentral area F1 and well corresponding to histochemical area F4 (Matelli et al., 1985).

In the next sections, the results of the architectonical study will be firstly compared with those already reported in the literature, and which were focused on the macaque PMv. Subsequently, the connectional features of the new architectonically defined premotor areas F5p, F5a and F5c, will be discussed on the basis of the differential connectivity observed in the present study. Finally, on the basis of the available functional data, we will discuss the possibility that the three rostral PMv areas F5p, F5a and F5c, correspond to distinct cortical entities, involved in different aspects of executive and/or cognitive motor functions.

1. Architectonics of the macaque ventral premotor cortex

The present data extend other architectonic subdivisions of the macaque PMv and provide a new multiarchitectonic frame of reference for this agranular frontal region. One major argument against the validity of the classic cyto- and myeloarchitectonic architectonic approaches is represented by the variability of the maps proposed by different investigators. Indeed, architectonics has been often accused of giving uncertain results, due to its subjective nature and to the variability of the criteria used for defining borders between areas. In the current study, in an attempt to provide robust results and establish reliable criteria we used different planes of sectioning relying mainly on the ones that were perpendicular to the cortex of interest, eliminating thereby, as far as possible, ambiguities generated by the distortion of architectonic features. Furthermore, the architectonic characterization of the PMv areas identified in the present study

was obtained primarily on the basis of the analysis of Nissl stained material (by far the most informative approach for this type of studies) in a large number of different cases. Nevertheless, the cytoarchitectonic approach has been combined with myeloarchitectonic and qualitative and quantitative chemoarchitectonic analysis which provided independent and complementary criteria fully supporting the cytoarchitectonic subdivision.

The macaque PMv has been the object of several other studies that have resulted in markedly different parcellation schemes, in which both the number and the extent of the identified areas vary. Nevertheless, these studies have led up, basically, to two different views of the architectonic organization of this region.

One of these views holds that the PMv consists of different areas, located at different dorsoventral levels. The Vogts (Vogt and Vogt, 1919) firstly subdivided this cortical region into four architectonic fields: a dorsal most one, reckoned as part of an area 4 sub-sector (area 4c) and three other ones, designated, from the dorsal to the ventral, as 6aα, 6bα and 6bβ. In particular, areas 6aα and 6bα occupy different dorsoventral sectors of the postarcuate convexity cortex, while area 6bβ is mostly located around the ventral tip of the IAS. A similar subdivision, based on cyto- and myeloarchitectonic criteria, has been proposed by Barbas and Pandya, (1987). According to them, the PMv hosts a dorsalmost area, designated as 4C, but distinct from area 4 and two more ventral areas -6Va and 6Vb- that appear to roughly correspond to areas 6aα and 6bβ of the Vogts (Vogt and Vogt, 1919), respectively. Area 6bβ of the Vogts was considered by Barbas and Pandya, (1987) as part of the prefrontal area 12. Finally, a dorsoventral subdivision of the PMv has been also proposed by Preuss and Goldmann Rakic, (1991), mostly on the basis of myeloarchitectonic criteria. Two PMv areas were, however, identified in this study, a more dorsal and much larger area 6Va and a more ventral and smaller one 6Vb. In particular, area 6Va appears to include areas 4C, 6Va and, possibly, part of area 6Vb of Barbas and Pandya, (1987), while area 6Vb appears to include the ventral part of area 6Vb of Barbas and Pandya, (1987), extending ventrally into area 12.

The other view of the architectonic organization of the macaque PMv holds that this region consists of different areas located at different rostrocaudal levels. This view has been firstly

proposed by Von Bonin and Bailey, (1947), on the basis of cytoarchitectonic criteria. In this study, rostral to area FA (corresponding to area 4), two areas were identified in the ventral part of the agranular frontal cortex: a more caudal one, designated as FBA and a more rostral one, designated as FCBm. Using a completely different architectonic approach, i.e., cytochrome oxidase histochemistry, a very similar subdivision has been proposed by Matelli et al., (1985). In this study, on the basis of regional differences in the laminar pattern of enzymatic activity, Matelli et al., (1985) identified two histochemically distinct PMv areas: a caudal one -F4- and a rostral one -F5- which well correspond to areas FBA and FCBm of Von Bonin and Bailey, (1947), respectively.

The present study, at least as far as the inferior postarcuate convexity cortex is concerned, strongly supports this last view. In fact, our data provide robust multiarchitectonic evidence for a rostrocaudal subdivision of this region into two areas: a more caudal one -F4- and a more rostral one -F5c- which appear to very closely correspond to the cytoarchitectonic areas FBA and FCBm of Von Bonin and Bailey, (1947), respectively. As a consequence, these two areas only partially overlap with the PMv subdivisions identified by Barbas and Pandya, (1987) or Preuss and Goldmann-Rakic, (1991). In particular, F4 appears to include at least area 4C and the caudalmost part of area 6Va of Barbas and Pandya, (1987), or the caudal part of area 6Va of Preuss and Goldmann-Rakic, (1991). F5c appears to coincide with the rostral part of area 6Va and, possibly of area 6Vb of Barbas and Pandya, (1987) and with a rostroventral sector of area 6Va of Preuss and Goldmann-Rakic, (1991). The limited photographic material provided by Barbas and Pandya, (1987) and Preuss and Goldmann-Rakic, (1991) makes any comparison between their data and the data presented in the current study difficult. Nevertheless, according to Barbas and Pandya, (1987) area 4C is characterized by the presence of large layer V pyramids and both outer and inner Baillarger bands, while area 6Va displays prominent layer III and V neurons and a well developed outer Baillarger band. This myeloarchitectonic difference, however, was not noticed by Preuss and Goldmann-Rakic, (1991), who described their area 6Va as densely myelinated, with a prominent outer Baillarger band. In agreement with Von Bonin and Bailey, (1947), we found that F4 displays an evident size gradient and relatively large layer V pyramids along its entire dorsoventral extent. These features clearly distinguish this area from area F5c, which is poorly laminated and

displays considerably smaller layer III and V pyramids. In this respect, it is noteworthy that the gradual reduction in size observed in F4 in dorsoventral direction was not considered as a sufficient criterion for a dorsoventral subdivision of this area. Indeed, our data also showed that F4 has an homogeneous myeloarchitetonic pattern and chemoarchitectonic features which clearly distinguish this area from both area F5c and F1. Accordingly, our data suggest that area 4C and the caudal part of area 6Va of Barbas and Pandya, (1987) actually correspond to a single architectonic area -F4- and that a rostral area with the cytoarchitectonic features of F5c has not been recognized by these authors. Moreover, given that F4 and F5c display relatively subtle myeloarchitectonic differences, which can be better visualized in planes of sectioning orthogonal to their border (e.g. parasagittal sections), it is not surprising that Preuss and Goldmann-Rakic, (1991) did not note a rostrocaudal myeloarchitectonic difference in coronal sections within their area 6Va.

In our study, we found that the postarcuate convexity cortex immediately adjacent to the IAS was largely occupied by a single architectonic area -F5c- without any dosrsoventral subdivision, possibly equivalent to areas 6Va and 6Vb of Barbas and Pandya, (1987) and Preuss and Goldmann-Raki,c (1991). It is very likely, however, that this discrepancy is only apparent. In fact, the major criterion identified in these studies for setting the border between areas 6Va and 6Vb was a marked decrease in myelin content in 6Vb, with respect to 6Va, that is exactly what we have observed at the transition between F5c and area DO. Moreover, the location of area 6Vb in the coronal sections presented by Barbas and Pandya, (1987) and Preuss and Goldmann-Rakic, (1991) is remarkably similar to that of area DO. In our 3D reconstructions, area DO is located very ventrally in the dorsolateral convexity cortex, rostral to the inferior precentral dimple. Its location appears quite compatible with that of area 6Vb in the 2D reconstruction presented by Preuss and Goldmann-Rakic, (1991), but ventral to that of area 6Vb in the 2D reconstruction presented by Barbas and Pandya, (1987). However, considering the relatively dorsal location also of the extent of areas 3a and 3b in the frontal cortex, it is possible that in the 2D reconstruction of Barbas and Pandya, (1987) area 6Vb has been somewhat misplaced in dorsal direction. Thus, in this case, the major difference between the present data and those of Barbas and Pandya, (1987) and Preuss

and Goldmann-Rakic, (1991) is not in the number of identified areas, but in the attribution of this ventral frontal area to a given architectonic cortical domain. As described in the result sections, multiarchitectonic evidence strongly suggests that this area is much more similar to the frontal opercular cortex than to the PMv.

One major finding of the present study is the identification of two architectonically distinct areas -F5p and F5a- buried within the postarcuate bank. Architectonic differences between the postarcuate bank and the postarcuate convexity cortex have not been reported in any of the above mentioned architectonic studies of the PMv. It is noteworthy, however, that all these studies have been mostly based on the analysis of coronal sections, in which the architecture of the postarcuate bank is very difficult to discriminate. Indeed, in our study, for the identification of areas F5p and F5a was crucial the analysis of sections cut in several different planes. However, in a series of architectonic studies focused on the caudal ventrolateral prefrontal cortex, Petrides and Pandya, (1994; 2002) have described in the anterior part of the postarcuate bank a cytoarchitectonic area, designated as area 44, considered, for its cytoarchitectonic features as the homologue of the human area 44 (caudal part of the Broca's region). In their schematic unfolded views of the IAS, this area, characterized by a size gradient in layer III and a barely discernible layer IV, was placed by Petrides and Pandya in the anterior part of the postarcuate bank. Thus, its location very closely coincides with that of area F5a. Indeed, though we failed in identifying in F5a an even rudimentary layer IV, several architectonic features, suggest that this area displays somewhat transitional features between those of the PMv and of the granular frontal cortex. Among them are the rather homogeneous layer V, the significant decrease in myelin content and in SMI-32ir and the significant increase in CBir, with a density of CB immunopositive non pyramidal neurons comparable to that observed in caudal ventrolateral prefrontal areas (Gerbella et al., 2007). In a more recent study, however, using sections cut perpendicularly to the IAS, Petrides et al., (2005) have redefined the location of area 44. Accordingly, this dysgranular area lies anteriorly along the fundus of the IAS and only slightly extends in the postarcuate bank that is mostly reckoned as part of the agranular premotor cortex. Thus, though the very limited photographic material provided by Petrides et al., (2005) makes any comparison rather difficult, it is possible that area 44, as defined

by these authors, does not correspond to area F5a, but is the equivalent of our area FIA, where a faint layer IV was observed.

2. Comparative connectivity of the premotor areas F5p, F5a and F5c

It is largely accepted in neuroscience that the cerebral cortex contains many functionally distinct domains, usually referred to as “areas”. There is no consensus, however, on what precisely constitutes a cortical area and what the best criteria for their definition are (see, e.g., Van Essen, 1985). In general, three main experimental approaches, the architectural, the connectional and the functional one, are considered most useful for their definition and converging evidence from these three approaches is generally considered a strong argument for their reliable identification and delineation (see, e.g., Felleman and Van Essen, 1991; Lewis and Van Essen, 2000 ; Van Essen, 1985).

In an attempt to give a reliable and strong anatomical support to the architectonic parcellation of the PMv area F5 established in the present study, we made a series of neural tracer injections in each newly defined premotor area (F5p, F5a and F5c), to see whether the architectonic subdivision of F5 could be validated by a differential connectivity of each area and to provide an anatomical background to the functional segregation showed within area F5.

Beside the present study, many other hodological investigations have been already focused on the premotor cortex (Pandya and vignolo, 1971; Godshalk et al., 1984; Matelli et al., 1986; Barbas and Pandya, 1987; Tokuno and inase, 1994; Gosh and Gattera., 1995; Tanné-Gariépy et al., 2002). However, most of these studies used different architectonical maps of the premotor cortex for the attribution of the injection sites. Consequently, most of the tracer injections made in these studies were not perfectly confined to our area F5, usually extending beyond its architectonic limits. Moreover, when the tracer injection was restricted to area F5, the injection sites were relatively large, likely including more than one rostral PMv subdivision as architectonically defined in this study.

Nevertheless, most of these studies agree that the rostral PMv sector -corresponding to our area F5- displays afferent and efferent connections with the adjacent caudal PMv (F4) area, with the PMd, mainly its caudal sector (F2), with areas in the mesial aspects of the hemisphere (F3 and F6)

and with area 4 (F1). Connections with the posterior parietal cortex which involved the IPL areas, mainly the rostral sector -area 7b- have been described by several studies (e.g. Petrides and Pandya,1984; Tanné-Gariépy et al., 2002; Rozzi et al., 2006). It has been shown that other parietal afferents to F5 originated also, from the intraparietal areas AIP and PEip (Borra et al., 2007; Marconi et al., 2001) and from the opercular area SII (Disbrow et al., 2003).

Connections with the prefrontal cortex have been reported by several hodological investigations (Barbas and Pandya, 1987; Matelli et al., 1986; Preuss and Goldman-Rakic, 1989; Deacon, 1992; Lu et al., 1994; Carmichael and Price, 1995). These connections arise from both area 46v and area 12.

In agreement with these studies, our results indicate that F5p, F5a, and F5c as a whole displayed connections with frontal and parietal areas, but each one of these premotor areas was characterized by a different pattern of connections.

Area F5p was connected with the adjacent premotor area F4, mainly with the arm-related field (Gentilucci et al., 1988; Graziano et al., 1994; Fogassi et al., 1996) and was connected also with the rostral sector of the PMd area F2 (F2vr) where arm movements are mostly represented (Raos et al., 2003). F5p displayed relatively strong connections with the hand field of areas F3 and F6 in the mesial wall of the hemisphere as defined by Luppino et al., (1991). All the tracer injections made by these authors in the arm/hand fields of areas F3 and F6 involved the posterior sector of F5 (F5p), which fits perfectly with our observations after F5p tracer injections.

The strong involvement of F5p in motor execution is also demonstrated by the presence of a consistent connectivity with the hand field of F1.

F5p is also a target of parietal afferences which arise from the IPL. In fact, we demonstrate in the present study, along with in our previous investigations in which we targeted the IPL areas with different tracer injections (Rozzi et al., 2006), that the IPL projections to F5p originated mainly from PF, PFG and PG. According to Hyvärinen (1981), this IPL sector contains a hand/arm field and neurons responsive to visual and somatosensory stimuli. F5p received consistent projections also from the intraparietal area AIP, which is congruent with our recently published data focused on the connectivity of this parietal area (Borra et al., 2007), in which we provided evidence of direct

anatomical connections of AIP with the infero-temporal cortex. Thus AIP could have a role in linking the paieto-frontal network of areas involved in sensory-motor transformations for grasping - among which area F5p- with areas involved in object recognition (Borra et al., 2007).

The analysis of the labeling distribution within the upper bank of the lateral fissure, following the F5p injection and the matching of the labeling distribution with the maps provided by Krubitzer et al. (1995) and Fitzgerald et al. (2004) indicate that F5p is mostly connected with the hand field of SII/PV complex. This data suggests that F5p could integrate the somatosensory information necessary for manual object exploration and recognition (Disbrow et al., 2003).

A strong anatomical link between area AIP and SII has been shown by Borra et al., (2007). Accordingly, it has been suggested that SII may contribute to the control of grasping movements, not only as theorized by Fagg and Arbib, (1998), through the connections with F5 (Disbrow et al., 2003; Tanne-Gariepy et al., 2002), but also through connections with AIP. These connections appear to involve sectors in the SII region, in which neurons have mostly proprioceptive responses and are active during object manipulation (Krubitzer et al., 1995; Fitzgerald et al., 2004).

Thus, area F5p could play a major role in translating the objects features into potential hand action appropriate to interact with an object.

One major distinguishing connectional feature of area F5p is that this area is the only PMv area sending direct projections to cervical segments of the spinal cord. Mainly the upper cervical segments (C2-C4). These data are in agreement with those from Dum and Strick, (1991) and He et al., (1993) in which they injected neural tracers in different cervical segments. In addition, our data show that some fibres originating from F5p targeted also the lower cervical (C7-C8).

In another study made by Jenny and Inukai, (1983), in which they investigated how the motoneurons controlling the arm and hand muscles are distributed in the cervical spinal cord, these authors showed that the motoneurons which control hand movements are located primarily in in the lower cervical segments (C8-T1).

A clear discrepancy emerges if we take in consideration what is area F5p at the upstream (a potential hand field) and what should process in the downstream (predominant projections to the upper cervical segments). The functional significance of this arrangement is not fully elucidated.

One of the possible interpretations of this disparity was suggested by He et al (1993). These authors speculated that this disparity could reflect a projection of corticospinal efferents from the F5p (rostral PMv in their terminology) to propriospinal neurons in C2-C4 that in turn innervate the motoneurons in lower cervical segments that control hand muscles (Martino and Strick, 1987; Dum and Strick, 1989; see also Gentilucci et al., 1988). Though, there is evidence of such propriospinal neurons in cat (Alstermark and Sasaki, 1985; Alstermark et al., 1990), they still remain to be demonstrated in primates.

Both, the hodological data found in the present study and the functional data available, indicate that F5p is a potential hand field which should integrate the hand/arm related informations from the parietal and the premotor areas to deliver it to the hand field of the primary motor cortex in order to control the hand motor outputs of F1. In addition, through its corticospinal projections, area F5p has a more direct access to motor outputs at the spinal cord levels.

F5a lacked connections with area F1, while F5c projections to F1 targeted the face/mouth field. Both F5a and F5c displayed connections with area F4. F5a with mostly the arm related field, while F5c tended to be connected mainly with the face/mouth related field of area F4.

The mesial areas F3 and F6 were a target of different neural tracer injections made by Luppino and co-workers (1993). These authors found that area F6 is connected with both the bank and the convexity parts of F5, while in the present study only area F5a displayed connections with area F6. As for F5c, our data are congruent with those from Luppino et al., (1993), in which we found that F5c displayed connections with F3, mainly with its face/mouth field.

These connectional patterns indicate that F5c could correspond to F5 sector implicated in the motor control of face/mouth effector, while F5a could correspond to F5 sector related to the hand motor control.

F5a displayed connections with the IPL areas PF, PFG and PG. F5c, however, received projections mainly and strongly from the rostral IPL area PF. Weak connections to F5c originating from PFG were observed as well. According to Hyvärinen (1981), area 7b contains a rostral, mostly somatosensory, mouth and face field, and as already mentioned, a caudal hand/arm field in which neurons are responsive to visual or visual and somatosensory stimuli. Recent data

suggested a role of this IPL sector in higher order aspects of visuomotor transformations and organization of goal-directed arm/hand and face movements. The caudal part of 7b have been shown to contain visually responsive neurons during the observation of arm, hand and mouth goal-directed movements made by the experimenter (Ferrari et al., 2003b, Gallese et al., 2002) suggesting a role of this area in action recognition.

Other parietal connections of areas F5a and F5c are with SII/PV complex. F5a was connected with, mostly, hand field of SII/PV complex. F5c, however, tended to be mostly connected with the mouth/face field of SII/PV complex as defined by Krubitzer et al (1995). It has been proposed that these connections indicate the involvement of these PMv areas in complex hand and mouth/face tactile behaviours (Disbrow et al., 2003).

Both area F5a and area F5c are connected with the frontal opercular areas, but these connections showed different topographical distribution. F5a was connected with the rostral opercular areas while F5c was connected with the caudal ones. These connections were almost absent after F5p tracer injections. These data fit partially with those from Cipolloni and Pandya, (1999) in which different neural tracer injections were made in different rostro-caudal sectors of the fronto-parietal opercular cortex. Similarly, these authors did not find any connections between the posterior sector of the bank of the IAS (F5p in our study) and the frontal opercular cortex, but no difference between the anterior sector of the bank of the IAS (F5a) and the postarcuate convexity (F5c) as to their connections with the frontal opercular cortex was reported by these authors. This discrepancy could be due to the large injection sites of their study which included several areas, in both the upper bank of the LF and the adjacent convexity.

Both F5a and F5c were connected with the prefrontal cortex. These connections form a direct link between the rostral PMv and the ventrolateral prefrontal region and constitutes an exclusive characteristic of the rostral PMv, given the lack of connections between the prefrontal cortex and caudal PMv.

Prefrontal connections of areas F5a and F5c involved both 46v and 12. The connections with area 46v shown in this study are in full agreement with the study of Preuss and Goldman-Rakic, (1989). These authors by injecting neural tracers in 46v, showed that area 6v -corresponding to our F5a

and F5c areas- displayed connections with different sectors of area 46v. The connections with area 12 are in agreement with those from Carmichael and Price, (1995).

The prefrontal connections of F5a and F5c differ, however, in two aspects: 1) area F5a tends to be connected with the more caudal sector of area 46v as defined by Preuss and Golman-Rakic, (1991), while F5c was connected with the more rostral sector of area 46v, 2) F5a displayed connections with both areas 12r and 12l as defined by Carmichael and Price, (1995), while F5c was connected only with area 12r. The possible functional significance of this difference has to be elucidated. It is well-known, however, that area 46v is a target of IPL projections. In fact, area 46v receives IPL projections arising from areas PF, PFG and PG (Rozzi et al., 2006). Area 12 is a target of projections from the infero-temporal cortex which provide it with visual information (Webster et al., 1994; Carmichael and Price, 1995). Area 12 is considered as a functional domain where the sensory non-spatial information is processed, in particular information related to the object identity and faces (Wilson, 1993). Thereby, the prefrontal connections of F5a and F5c, support the proposed role of these areas in higher order aspects of motor control and action recognition.

3. Functional considerations

In the last two decades, the ventral premotor cortex became a subject of extensive functional investigations, from the single-neuron recording to the functional magnetic resonance imaging. Early electrophysiological studies have shown that the rostral part of the PMv, corresponding to the histochemical area F5, is involved in the control of hand and mouth movements (Rizzolatti et al., 1981; Kurata and Tanji, 1986; Rizzolatti et al., 1988; Hepp-Reymond et al., 1994). In the F5 sector located posteriorly in the bank of the IAS, neurons showed changes in activity related to active movements of the hand (Rizzolatti et al., 1981; Gentilucci et al., 1988). Intracortical stimulation in this F5 sector, evoked movements of the fingers and wrist (Gentilucci et al., 1988, 1989) which suggests the implication of F5p in the motor control of the hand movements.

In the ventral part of F5, lying on the postarcuate convexity cortex, neurons coding mouth movements predominate, though mixed with hand- or both hand- and mouth-related neurons (Gentilucci et al., 1988).

More recent evidence, indicated clearly that these two different F5 sectors do not differ simply for their motor representation, but represent two functionally distinct rostral PMv subdivisions. One major difference between these two F5 sectors is represented by different visual properties of their visuomotor neurons, which have been subdivided into two main classes: 'canonical' and 'mirror' neurons (Rizzolatti et al., 2000). Canonical visuomotor neurons are mostly located in the posterior part of the inferior postarcuate bank. These neurons typically are active even when the monkey merely observes three-dimensional visual stimuli whose size and shape is congruent with the type of hand grasping action coded by the neuron (Rizzolatti et al., 1988; Murata et al., 1997; Raos et al., 2006). It has been proposed that these functional properties reflect the results of a visuomotor transformation processing, leading to the selection of motor programs of distal movements appropriate for hand-object interactions (Jeannerod et al., 1995).

Other studies have also shown that neurons in the posterior part of the postarcuate bank display object/grasp related tuning earlier than M1 neurons in the visual presentation and pre-movement periods and a greater preference for particular objects/grasps than did M1 neurons (Umiltà et al., 2007). Furthermore, this is the only F5 sector providing a robust, short-latency facilitation of motor outputs from primary motor cortex (M1) to contralateral intrinsic hand muscles (Shimazu et al., 2004; Cerri et al., 2003).

Mirror neurons are typically located, more ventrally, in the postarcuate convexity cortex close to the IAS, where extensive single unit recording studies showed that half of the cells code mouth actions, the other half coding hand or both hand and mouth actions (Ferrari et al., 2003a). Mirror neurons were initially identified as neurons active both when the monkey performs a motor action and when it observes a similar action made by another individual (Di Pellegrino et al., 1992; Gallese et al., 1996; Rizzolatti et al.,1996). Mirror neurons, however, can be activated also by the observation of ingestive or communicative mouth action (Ferrari et al., 2003a). It has been proposed that these functional properties reflect coding in visual terms of actions made by others

that are mapped onto the repertoire of motor representations coded in F5. The result of this mapping would be at the basis of recognition and understanding of actions made by others, a cognitive function of crucial importance in animals with a complex social behaviour, such as primates (Rizzolatti et al., 2001). The discovery that a PMv sector is possibly involved in communicative behaviour has been used to support to the notion, based on architectonic and phylogenetical considerations, that the rostral part of PMv is the homologue of at least part of the human Broca's language region (see Rizzolatti and Arbib, 1998).

These functional data are in favour of our architectonic and hodological findings, because they indicate clearly that F5 consists of at least two distinct subdivisions, a more dorsal one, playing a crucial role in the control of object-oriented hand actions and a more ventral one, involved in cognitive motor functions. These two subdivisions have been previously referred to as F5ab and F5c, respectively (Rizzolatti et al., 1998; Rizzolatti and Luppino, 2001). In the present study, we have identified two premotor areas, F5p and F5c, which appear to very likely represent the anatomical counterpart of these two F5 subdivisions. Thus, areas F5p and F5c should correspond to two distinct cortical entities.

The F5 sector corresponding to F5a, likely because of its anterior location in the postarcuate bank, has been so far only marginally involved in electrophysiological studies, except for the study of Petrides et al. (2005) in which, however, intracortical microstimulation in anaesthetized monkeys was not effective in evoking body movements. A recent functional magnetic resonance study in awake monkeys, however, showed up to be very useful for shedding light on the possible functional properties of F5a (Nelissen et al., 2005). The aim of this study was to map the frontal areas of the monkey involved in coding actions made by others. A constrained analysis using ROIs defined on the basis of preliminary architectonic data of the present study showed that both F5c and F5a, but not F5p, were activated by the observation of video clips of goal-directed object-oriented movements. F5c and F5a, however, showed a differential pattern of activation: while F5c was active only for the observation of a person grasping objects in full view, F5a was active also for the observation of an isolated hand grasping objects, a hand mimicking grasping and a robot arm grasping objects. These data, therefore, suggest that in F5c, where mirror neurons have been

recorded, actions done by others are represented in a more context-dependent way, while F5a appears to be involved in coding actions at a more abstract level, possibly related to the general meaning of the action. All together, these data showing that architectonic areas F5p, F5c and F5a, are functionally distinct, provide strong support for the presently proposed subdivision of the rostral PMv into three areas.

Conclusions and perspectives

In the present study, we established a new PMv parcellation based on a multimodal histological approach combining cyto- and myeloarchitectonics with SMI-32 and calcium binding protein (CB) immunohistochemistry, on the basis of which we provided a detailed description of the architectonic organization of the PMv and the neighbor areas. The major finding of this study is that the rostral PMv area F5, as histochemically defined by Matelli et al., (1985), is not an homogeneous area, but consists of three architectonically distinct areas: F5p, F5a and F5c. F5c extends on most of the postarcuate convexity cortex immediately adjacent to the IAS. The other two areas -F5p and F5a- lie within the postarcuate bank at different antero-posterior levels.

In order to get solid evidence in favour of our architectonically based parcellation of area F5, a series of tracer injections was made in each one of the three -architectonically- defined areas (F5a, F5p and F5c). The results showed clearly that each one of these areas displays a differential connectional pattern, suggesting that area F5 as was histochemically defined, is not a unique area but consists of three anatomical entities each of which could be involved in different aspect of the visuomotor integration.

On the basis of the results from the present study and the functional data available, we suggest that F5p should correspond to F5 sector where ‘canonical neurons’ are located, while area F5c could correspond to F5 sector where ‘mirror neurons’ are located. F5a, however, has been shown to be activated by action observation, but in less context-dependent way with respect to F5c. The role of this area in action observation has to be elucidated.

Thereby, the current study provides a new anatomical frame of reference of the macaque PMv that appears to be very promising for gaining new insight into the possible role of this premotor sector in different aspects of motor control and cognitive motor functions.

Acknowledgments

I am extremely indebted to Pr. Giuseppe Luppino for supervising my thesis. I specially appreciated your permanent availability. I really enjoyed working with you not only from an academic but also from a personal point of view.

I would like to express my profound gratitude to Pr. Giacomo Rizzolatti to give me a precious opportunity to do research in such excellent institute as I always dreamt. Thank you for making my dream reality.

I would like to express my gratitude to Pr. Stefano Rozzi, for initiating me to the monkey brain's techniques. Thank you for your availability every time I needed your help.

I am grateful to Pr. Driss Bossaoud at the INCM (Marseille-France) for encouraging me to go ahead in research increasing my enthusiasm more and more. I hope this work could reflect how much your encouragements were efficient.

I also thank my colleagues Dr. Elena Borra and Dr. Marzio Gerbella for all the moments we shared in the lab. Many thanks to you Marzio for helping me with statistic analysis.

Special thanks to my friend Dr. Benno Gesierich. Thank you for your help in my first journeys in Parma, above all for your availability to translate to me what people said when I spoke no word in Italian.

Finally, I wish to express my thanks to all my friends, colleagues and staff at the section of Fisiologia Umana-Parma. Many thanks to all of you for making life easier for me.

Bibliography

Alstermark B, Kummel H, Pinter MJ, Tantisira B (1990) Integration in descending motor pathways controlling the forelimb in the cat. 17. Axonal projection and termination of C3-C4 propriospinal neurones in the C6-Th1 segments. Exp Brain Res 81:447-461.

Alstermark B, Sasaki S (1985) Integration in descending motor pathways controlling the forelimb in the cat. 13. Corticospinal effects in shoulder, elbow, wrist, and digit motor-neurons. Exp Brain Res 59:353-364.

Arbib MA (1981) Perceptual structures and distributed motor control. In: Brooks, V.B. (Ed), Handbook of Physiology, section 1: The Nervous System, vol II: Motor Control. Williams and Wilkins, Baltimore, pp. 1449-1480.

Barbas H, Pandya DN (1987) Architecture and frontal cortical connections of the premotor cortex (area 6) in the rhesus monkey. J Comp Neurol 256: 211-228.

Belmalih A, Borra E, Gerbella M, Rozzi S, Luppino G (2007) Connections of architectonically distinct subdivisions of the ventral premotor area F5 of the macaque. Soc Neurosci Abstr Program No 636.5.

Bettio F, Demelio S, Gobbetti E, Luppino G, Matelli M (2001) Interactive 3-D reconstruction and visualization of primates cerebral cortex. Soc Neurosci Abstr Program No 728.724.

Bonin G von, Bailey P (1947) The neocortex of Macaca mulatta. University of Illinois Press, Urbana, Illinois

Borra E, Belmalih A, Gerbella M, Rozzi S, Luppino G (2007) Cortical connections of the macaque anterior intraparietal (AIP) area. Cereb Cortex. doi:10.1093/cercor/bhm146.

Brodmann K (1909) Vergleichende Lokalisationslehre der Großhirnrinde. Barth, Leipzig

Campbell MJ, Morrison JH (1989) Monoclonal antibody to neurofilament protein (SMI-32) labels a subpopulation of pyramidal neurons in the human and monkey neocortex. J Comp Neurol 282:191-205.

Carmichael ST, Price JL (1994) Architectonic subdivision of the orbital and medial prefrontal cortex in the macaque monkey. J Comp Neurol 346:366-402.

Carmichael ST, Price JL (1995) Sensory and premotor connections of the orbital and mesial prefrontal cortex of macaque monkeys. J Comp Neurol 363:642-664.

Cavada C, Goldman-Rakic PS (1989) Posterior parietal cortex in rhesus monkey: I. Parcellation of areas based on distinctive limbic and sensory corticocortical connections. J Comp Neurol 287:393-421.

Cerri G, Shimazu H, Maier MA, Lemon RN (2003) Facilitation from ventral premotor cortex of primary motor cortex outputs to macaque hand muscles. J Neurophysiol 90: 832-842.

Cippollloni PB, Pandya DN (1999) Cortical connections of the frontoparietal opercular areas in the rhesus monkey. J Comp Neurol 403:431-451.

Condé F (1987) Further studies on the use of the fluorescent tracers fast blue and diamidino yellow: effective uptake area and cellular storage sites. J. Neurosci Meth 21, 31-43.

Condé F, Lunnds JS, Jacobowitz DM, Baimbridge KG, Lewis DA (1994) Local circuit neurons immunoreactive for calretinin, calbindin D-28k or parvalbumin in monkey prefrontal cortex: distribution and morphology. J Comp Neurol 341:95-116.

Cusick CG, Seltzer B, Cola M, Griggs E (1995) Chemoarchitectonics and corticocortical terminations within the superior temporal sulcus of the rhesus monkey: evidence for subdivisions of superior temporal polysensory cortex. J Comp Neurol 360: 513-535.

Deacon TW (1992) Cortical connections of the inferior arcuate sulcus cortex in the macaque brain. Brain Res 573:8-26.

DeFelipe J, Hendry SH, Jones EG (1989) High-resolution light and electron microscopic immunohistochemistry of colocalized GABA and calbindin D-28k in somata of double bouquet cell axons of monkey somatosensory cortex. Eur J Neurosci 4: 46-60.

Di Pellegrino G, Fadiga L, Fogassi L, Gallese V, Rizzolatti G (1992) Understanding motor events: A neurophysiological study. Exp Brain Res 91:176-180.

Disbrow E, Litinas E, Recanzone GH, Padberg J, Krubitzer L (2003) Cortical connections of the second somatosensory area and the parietal ventral area in macaque monkeys. J Comp Neurol 462:382-399.

Dombrowski SM, Hilgetag CC, Barbas H (2001) Quantitative architecture distinguishes prefrontal cortical systems in the rhesus monkey. Cereb Cortex 11: 975-988.

Dum RP, Strick PL (1991) The origin of corticospinal projections from the premotor areas in the frontal lobe. J Neurosci 11: 667-689.

Dum RP, Strick PL (2005) Frontal lobe inputs to the digit representations of the motor areas on the lateral surface of the hemisphere. J Neurosci 25:1375-1386.

Fadiga L, Fogassi L, Gallese V, Rizzolatti G (2000) Visuomotor neurons: ambiguity of the discharge or 'motor' perception? Int J psychophysiol 35:165-77.

Fagg AH, Arbib MA (1998) Modeling parietal–premotor interactions in primate control of grasping. Neural Netw 11:1277-1303.

Felleman D, Van Essen DC (1991) Distributed hierarchical processing in primate cerebral cortex. Cereb Cortex 1:1-47.

Ferrari PF, Gallese V, Rizzolatti G, Fogassi L (2003a) Mirror neurons responding to observation of ingestive and communicative mouth actions in the monkey ventral premotor cortex. Eur J Neurosci 17: 1703-1714.

Ferrari PF, Gregoriou G, Rozzi S, Pagliata G, Rizzolatti G, Fogassi L (2003b) Functional organization of the inferior parietal lobule of the macaque monkey. Soc Neurosci Abstr Program No 919.7.

Fitzgerald PJ, Lane JW, Thakur PH, Hsiao SS (2004) Receptive field properties of the macaque second somatosensory cortex: evidence for multiple functional representations. J Neurosci 24:11193-11204.

Fogassi L, Ferrari PF, Gesierich B, Rozzi S, Chersi F, Rizzolatti G (2005) Parietal lobe: from action organization to intention understanding. Science. 308:662-667.

Fogassi L, Gallese V, Buccino G, Craighero L, Fadiga L, Rizzolatti G (2001) Cortical mechanism for the visual guidance of hand grasping movements in the monkey: a reversible inactivation study. Brain 124: 571-586.

Fogassi L, Gallese V, Fadiga L, Luppino G, Matelli M, Rizzolatti G (1996) Coding of peripersonal space in inferior premotor cortex (area F4). J Neurophysiol 76: 141-157.

Fulton JF (1935) A note on the definition of the “motor” and “premotor” areas. Brain 58: 311-316.

Gallese V, Fadiga L, Fogassi L, Rizzolatti G (1996) Action recognition in the premotor cortex. Brain 119:593-609.

Gallese V, Fogassi L, Fadiga L, Rizzolatti G (2002) Action representation and the inferior parietal lobule. In Attention & Performance XIX. Common mechanisms in perception and action, ed.W Prinz, B Hommel, pp. 247-66.

Gallese V, Murata A, Kaseda M, Niki N, Sakata H (1994) Deficit of hand preshaping after muscimol injection in monkey parietal cortex. Neuroreport 5:1525-1529.

Galletti C, Gamberini M, Kutz DF, Fattori P, Luppino G, Matelli M (2001) The cortical connections of area V6: an occipito-parietal network processing visual information. Eur J Neurosci 13:1572-1588.

Gallyas F (1979) Silver staining of myelin by means of physical development. Neurol Res 1:203-209.

Gentilucci M, Fogassi L, Luppino G, Matelli M, Camarda R, Rizzolatti G (1988) Functional organization of inferior area 6 in the macaque monkey. I. Somatotopy and the control of proximal movements. Exp Brain Res 71: 475-490.

Gentilucci M, Fogassi L, Luppino G, Matelli M, Camarda R, Rizzolatti G (1989) Somatotopic representation in inferior area 6 of the macaque monkey. Brain Behav Evol 33:118-21.

Gerbella M, Belmalih A, Borra E, Rozzi S, Luppino G (2007) Multimodal architectonic subdivision of the caudal ventrolateral prefrontal cortex of the macaque monkey. Brain Strut Funct 212: 269-301.

Geyer S, Matelli M, Luppino G, Zilles K (2000a) Functional neuroanatomy of the primate isocortical motor system. Anat Embryol 202: 443-474.

Geyer S, Zilles K, Luppino G, Matelli M (2000b) Neurofilament protein distribution in the macaque monkey dorsolateral premotor cortex. Eur J Neurosci 12:1554-1566.

Gosh S, Gattera R (1995) A comparison of the ipsilateral cortical projections to the dorsal and ventral subdivisions of the macaque premotor cortex. Somatosens Mot Res 12:359-78.

Godshalk M, Lemon RN, Kuypers HG, Ronday HK (1984) Cortical afferents and efferents of monkey postarcuate area: an anatomical and electrophysiological study. Exp Brain Res 56:410-424.

Graziano MS, Yap GS, Gross CG (1994) Coding of visual space by premotor neurons. Science 266:1054-7.

Gregoriou GG, Borra E, Matelli M, Luppino G (2006) Architectonic organization of the inferior parietal convexity of the macaque monkey. J Comp Neurol 496: 422-451.

He SQ, Dum RP, Strick PL (1993) Topographic organization of corticospinal projections from the frontal lobe: motor areas on the lateral surface of the hemisphere. J Neurosci 13: 952-980.

Hendry SH, Jones EG, Emson PC, Lawson DE, Heizmann CW, Streit P (1989) Two classes of cortical GABA neurons defined by differential calcium binding protein immunoreactivities. Exp Brain Res 76: 467-472.

Hepp-Reymond MC, Hüsler EJ, Maier MA, Qi HX (1994) Force related neuronal activity in two regions of the primate ventral premotor cortex. Can J Physiol Pharmacol 72: 571-579.

Hof PR, Glezer II, Conde F, Flagg RA, Rubin MB, Nimchinsky EA, Vogt Weisenhorn DM (1999) Cellular distribution of the calcium-binding proteins parvalbumin, calbindin, and calretinin in the neocortex of mammals: phylogenetic and developmental patterns. J Chem Neuroanat 16:77.

Hyvärinen J (1981) Regional distribution of functions in parietal association area 7 of the monkey. Brain Res 206:287-303.

Hyvarinen J (1982) Posterior parietal lobe of the primate brain. Physiol Rev 62:1060-129.

Jeannerod M, Arbib MA, Rizzolatti G, Sakata H (1995) Grasping Objects: the cortical mechanisms of visiomotor transformation. Trends Neurosci 18:314-20.

Jellema T, Baker CI, Oram MW, Perrett DI (2002) Cell populations in the banks of the superior temporal sulcus of the macaque monkey and imitation. See Meltzoff & Prinz 2002, pp. 267-90.

Jenny AB, Inukai J (1983) Principles of motor organization of the monkey cervical spinal cord. J Neurosci 3:567-75.

Kondo H, Tanaka K, Hashikawa T, Jones EG (1994) Neurochemical gradients along the monkey occipito-temporal cortical pathway Neuroreport 5: 613-616.

Kondo H, Tanaka K, Hashikawa T, Jones EG (1999) Neurochemical gradients along monkey sensory cortical pathways: calbindin-immunoreactive pyramidal neurons in layers II and III. Eur J Neurosci 11: 4197-4203.

Krubitzer L, Clarey J, Tweedale R, Elston G, Calford M (1995) A redefinition of somatosensory areas in the lateral sulcus of macaque monkeys. J Neurosci 15:3821-3839.

Kurata K, Tanji J (1986) Premotor cortex neurons in macaques: activity before distal and proximal forelimb movements. J Neurosci 6:403-411.

Kuypers HGJM, Huisman AM (1984) Fluorescent neuronal tracers. Adv. Cell Neurobiol 5:307-340.

Lewis JW, Van Essen DC (2000) Corticocortical connections of visual, sensorimotor, and multimodal processing areas in the parietal lobe of the macaque monkey. J Comp Neurol 428:112-137.

Lu M-T, Preston JB, Strick PL (1994) Interconnections between the prefrontal cortex and the premotor areas in the Frontal lobe. J Comp 341:375.

Luppino G, Belmalih A, Borra E, Gerbella M, Rozzi S (2005) Architectonics and cortical connections of the ventral premotor area F5 of the Macaque. Program No. 194.1.

Luppino G, Calzavara R, Rozzi S, Matelli M (2001) Projections from the superior temporal sulcus to the agranular frontal cortex in the macaque. Eur J Neurosci 14:1035-1040.

Luppino G, Matelli M, Camarda R, Rizzolatti G (1993) Cortical connections of area F3 (SMA-proper) and area F6 (Pre-SMA) in the macaque monkey. J Comp Neurol. 338:114-140.

Luppino G, Murata A, Govoni P, Matelli M (1999) Largely segregated parietofrontal connections linking rostral intraparietal cortex (areas AIP and VIP) and the ventral premotor cortex (areas F5 and F4). Exp Brain Res 128:181-187.

Luppino G, Rozzi S, Calzavara R, Matelli M (2003) Prefrontal and agranular cingulate projections to the dorsal premotor areas F2 and F7 in the macaque monkey. Eur J Neurosci 17:559-578.

Marconi B, Genovesio A, Battaglia-Mayer A, Ferraina S, Squatrito S, Molinari M, Lacquaniti F, Caminiti R (2001) Eye-hand coordination during reaching. I. Anatomical relationships between parietal and frontal cortex. Cereb Cortex 11:513-527.

Martino AM, Strick PL (1987) Corticospinal projections originate from the arcuate premotor area. Brain Res 404:307-12.

Matelli M, Camarda R, Glickstein M, Rizzolatti G (1986) Afferent and efferent projections of the inferior area 6 in the macaque monkey. J Comp Neurol 251:281-298.

Matelli M, Govoni P, Galletti C, Kutz DF, Luppino G (1998) Superior area 6 afferents from the superior parietal lobule in the macaque monkey. J Comp Neurol 402: 327-352.

Matelli M, Luppino G, Rizzolatti G (1985) Patterns of cytochrome oxidase activity in the frontal agranular cortex of macaque monkey. Behav Brain Res 18:125-137.

Mesulam MM (1982) Principles of horseradish peroxidase neurohistochemistry and their applications for tracing neural pathways. In: Tracing neural connections with horseradish peroxidase (Mesulam M-M, ed.), pp 1-152. Chichester: Wiley.

Murata A, Fadiga L, Fogassi L, Gallese V, Raos V, Rizzolatti G (1997) Object representation in the ventral premotor cortex (area F5) of the monkey. J Neurophysiol 78:2226-2230.

Murata A, Gallese V, Kaseda M, Sakata H (1996) Parietal neurons related to memory-guided hand manipulation. J Neurophysiol 75: 2180-2186.

Murata A, Gallese V, Luppino G, Kaseda M, Sakata H (2000) Selectivity for the shape, size, and orientation of objects for grasping in neurons of monkey parietal area AIP. J Neurophysiol 83:2580-2601.

Nelissen K, Luppino G, Vanduffel W, Rizzolatti G, Orban GA (2005) Observing others: multiple action representation in the frontal lobe. Science 310: 332-336.

Nimchinsky EA, Hof PR, Young WG, Morrison JH (1996) Neurochemical, morphologic, and laminar characterization of cortical projection neurons in the cingulate motor areas of the macaque monkey. J Comp Neurol 374: 136-160.

Okano K, Tanji J (1987) Neuronal activities in the primate motor fields of the agranular frontal cortex preceding visually triggered and self-paced movement. Exp Brain Res 66:155-66.

Pandya DN, Vignolo LA (1971) Intra- and Interhemispheric projections of the precentral, premotor and arcuate areas in the rhesus monkey. Brain res. 26:217-233.

Penfield W, Welch K (1951) The supplementary motor area of the cerebral cortex: a clinical and experimental study. Arch Neurol Psychiat 66: 289-317.

Perrett DI, Harries MH, Bevan R, Thomas S, Benson PJ (1989) Frameworks of analysis for the neural representation of animate objects and actions. J Exp Biol. 146:87-113.

Perrett DI, Mistlin AJ, Harries MH, Chitty AJ (1990) Understanding the visual appearance and consequence of hand actions. In Vision and Action: The Control of Grasping, ed.MA Goodale, pp. 163-342. Norwood, NJ: Ablex.

Petrides M, Cadoret G, Mackey S (2005) Orofacial somatomotor responses in the macaque monkey homologue of Broca's area. Nature 435:1235-1238.

Petrides M, Pandya DN (1984) Projections to the frontal cortex from the posterior parietal region in the rhesus monkey. J Comp Neurol 228(1):105-16.

Petrides M, Pandya DN (1994) Comparative architectonic analysis of the human and the macaque frontal cortex. In: Handbook of Neuropsychology (Boller F, Grafman J, eds.). Amsterdam: Elsevier pp 17-58.

Petrides M, Pandya DN (2002) Comparative cytoarchitectonic analysis of the human and the macaque ventrolateral prefrontal cortex and corticocortical connection patterns in the monkey. Eur J Neurosci 16: 291-310.

Preuss TM, Goldman-Rakic P (1989) Connections of the ventral granular frontal cortex of macaques with perisylvian premotor and somatosensory areas: anatomical evidence for somatic representation n primate frontal association cortex. J Comp Neurol 282:293-316.

Preuss TM, Goldman-Rakic PS (1991) Myelo- and cytoarchitecture of the granular frontal cortex and surrounding regions in the streptisine primate Galago and the anthropoid primate Macaca. J Comp Neurol 310:429-474.

Raos V, Franchi G, Gallese V, Fogassi L (2003) Somatotopic organization of the lateral part of area F2 (dorsal premotor cortex) of the macaque monkey. J Neurophysiol 89:1503-18.

Raos V, Umilta MA, Murata A, Fogassi L, Gallese V (2006) Functional properties of grasping-related neurons in the ventral premotor Area F5 of the macaque monkey. J Neurophysiol 95:709-729.

Rizzolatti G, Arbib MA (1998) Language within our grasp. Trends Neurosci 21:188-94.

Rizzolatti G, Camarda R, Fogassi L, Gentilucci M, Luppino G, Matelli M (1988) Functional organization of inferior area 6 in the macaque monkey. II. Area F5 and the control of distal movements. Exp Brain Res 71:491-507.

Rizzolatti G, Fadiga L (1998) Grasping objects and grasping action meanings: the dual role of monkey rostroventral premotor cortex (area F5). Novartis Found Symp 218:81-95.

Rizzolatti G, Fadiga L, Gallese V, Fogassi L (1996) Premotor cortex and the recognition of motor actions. Cognitive Brain Res 3:131-141.

Rizzolatti G, Gentilucci M (1988) Motor and visuomotor functions of the premotor cortex. In: Neurobiology of Neocortex, Dahlem Konferenzen der Freien Universita¨t Berlin, edited by Rakic P and Singer WS. Chichester,UK: John Wiley Ltd, p. 269-284.

Rizzolatti G, Graighero L (2004) The mirror-neuron system. Ann Rev Neurosci 27: 169-192.

Rizzolatti G, Luppino G (2000) The Organization of the Frontal Motor Cortex. News Physiol Sci 15:219-224.

Rizzolatti G, Luppino G (2001) The cortical motor system. Neuron 31:889-901.

Rizzolatti G, Luppino G, Matelli M (1998) The organization of the cortical motor system: new concept. Electroencephalog. Clin Neurophysiol 106:283-296.

Rizzolatti G, Scandolara C, Matelli M, Gentilucci M (1981) Afferent properties of periarcuate neurons in macaque monkeys. II. Visual responses. Behav Brain Res 2:147-163.

Roberts T, Akert K (1963) Insular and opercular cortex and its thalamic projections in Macaca mulatta. Sweiz Archiv Neurol Neurochir Psychiat 92: 1-43.

Rozzi S, Calzavara R, Belmalih A, Borra E, Gregoriou GG, Matelli M, Luppino G (2006) Cortical connections of the inferior parietal cortical convexity of the macaque monkey. Cereb Cortex. 16:1389-1417.

Sakata H, Taira M, Murata A, Mine S (1995) Neural mechanisms of visual guidance of hand action in the parietal cortex of the monkey. Cereb Cortex 5: 429-438.

Shimazu H, Maier MA, Cerri G, Kirkwood PA, Lemon RN (2004) Macaque ventral premotor cortex exerts powerful facilitation of motor cortex outputs to upper limb motoneurons. J Neurosci 24:1200-1211.

Taira M, Mine S, Georgopulos AP, Murata A, Sakata H (1990) Parietal cortex neurons of the monkey related to the visual guidance of hand movement. Exp Brain Res 83:29-36.

Tanne-Gariepy J, Rouiller EM, Boussaoud D (2002) Parietal inputs to dorsal versus ventral premotor areas in the macaque monkey: evidence for largely segregated visuomotor pathways. Exp Brain Res 145:91-103.

Tokuno H, Inase M (1994) Direct projections from the ventral premotor cortex to the hindlimb region of the supplementary motor area in the macaque monkey. Neurosci lett 171:159-62.

Umiltà MA, Brochier TG, Spinks RL, Lemon RN (2007) Simultaneous recording of macaque premotor and primary motor cortex neuronal populations reveals different functional contributions to visuomotor grasp. J Neurophysiol 98: 488-501.

Van Essen DC (1985) Functional organization of primate visual cortex. In: Jones EG, Peters A, editors. Cerebral cortex. New York: Plenum Press. p 259-329.

Vogt C, Vogt O (1919) Allgemeinere Ergebnisse unserer Hirnforschung. J Psychol Neurol 25:279-461.

Webster JS, Rapport LJ, Godlewski MC, Abadee PS (1994) Effect of attentional bias to right space on wheelchair mobility. J Clin Exp Neurosychol 16(1):129-37.

Wilson FA, Scalaidhe SP, Goldman Rakic PS (1993) Dissociation of object and spatial processing domains in primate prefrontal cortex. Science 260: 1955-1958.

Woolsey CN, Settlage PH, Meyer DR, Sencer W, Pinto HT, Travis AM (1952) Patterns of localisation in precentral and “supplementary” motor areas and their relation to the concept of a premotor area. Res Publ Assoc Res Nerv Ment Dis 30:238-264.